CONSTRUCTION AND OPERATION OF A HIGH TEMPERATURE SOLAR FURNACE: STUDIES OF ELEMENTAL BORON

by

FRED DEAN FISHER

A THESIS

submitted to

OREGON STATE COLLEGE

in partial fulfillment of
the requirements for the
degree of

DOCTOR OF PHILOSOPHY

June 1960

APPROVED:

Redacted for Privacy

Associate Professor of Chemical Engineering

In Charge of Major

Redacted for Privacy

Head of Chemical Engineering Department

Redacted for Privacy

Chairman of School Graduate Committee

Redacted for Privacy

Dean of Graduate School

Date thesis is presented May 2, 1960

Typed by Nadine McClelland

ACKNOWLEDGEMENT

The author wishes to express his gratitude to the U. S. Borax Research Corporation and the Dow Chemical Corporation for the financial assistance they contributed, and the U. S. Bureau of Mines, Albany, Oregon, for the experimental materials and x-ray analyses they provided.

The author also wants to thank the staff of the Chemical Engineering Department, Oregon State College, especially Dr. Charles E. Wicks, Professor Joseph Schulein, and Machinist Robert C. Mang, for their advice and assistance.

A special debt of gratitude is due my wife for her constant support and encouragement, without which this thesis would never have been written.

TABLE OF CONTENTS

	Page
Introduction	1
Advantages and Uses of Solar Furnaces . .	4
History of Solar Furnaces	6
Factors to be Considered in the Design of a Solar Furnace	18
Type of Furnace	18
Geometrical Configuration	19
Mounting and Tracking	26
Optical and Radiant Energy Considerations for a Solar Furnace	29
Solar Image formed by a Perfect Paraboloid	29
Derivation of Equation of Perfect Paraboloid Concentration Ratio . . .	36
Allowance for Furnace Transmission Losses	42
Maximum Temperatures Attainable with Solar Furnaces	48
Flux Distribution near the Focal Plane	56
Overall Design Considerations for the Oregon State College Solar Furnace	61
Design and Construction of Solar Furnace Components	66
Concentrator	66
Stationary Reflector	67
Heliostat	73

Photocell Tracking Controls 83

Sample Holder 91

Gas System 97

Electrical System 99

Housing of the Solar Furnace 106

Operation of the Solar Furnace 109

Alignment Adjustments of the Planar Mirrors 109

Operating Procedure with the Solar Furnace 110

Start Up Procedure 110

Shut Down Procedure 114

Trouble Shooting 114

Performance of the Oregon State College Solar Furnace 116

Studies of Elemental Boron 120

Description of U. S. Borax Elemental Boron 120

Studies of Amorphous Boron in the Solar Furnace 121

Studies with Arc Fused Boron 122

Discussion of Spectrometric Analyses 127

Discussion of Crystallographic Data. 128

Conclusions 129

Conclusions Relative to Solar Furnaces. . 129

Conclusions Relative to Elemental Boron 130

Recommendations 131

Bibliography 132

Appendix 138

Optical and Radiant Energy Calculations for the Oregon State College Solar Furnace 139

Stages of Development of the Oregon State College Solar Furnace 142

Heliostat and Stationary Reflectors 142

Azimuthal Tracking Photocell 145

FIGURES

Figure No.	Title	Page
1	Heliostat-Vertical Concentrator Furnace	21
2	Heliostat-Horizontal Concentrator Furnace	22
3	Heliostat-Stationary Reflector-Horizontal Concentrator Furnace	23
4	Cassegrainian Mounting	24
5	Straubel Two Step Mounting	24
6	Mounting of Lenses and Mirrors	25
7	Newtonian Mounting	25
8	Altazimuth Mounting	27
9	Equatorial Mounting	28
10	Image Formation in a Paraboloidal Concentrator	32
11	Relative Intensities in the Solar Image	33
12	Image Cast by a Differential Ring Area	38
13	Variation of Intensity of Radiation Across Solar Disc	41
14	Concentration Ratios for Various Furnace Factors and Rim Angles	49
15	Typical Measured Direct Sunshine Intensities	51
16	Maximum Temperatures Attainble in Solar Furnaces	54
17	Flux Distribution In and Near the Focal Plane	57

18 Target Parallel to Focal Plane . . . 58

19 Variation of Maximum Attainable Temperature with Distance from the Focal Plane. 60

20 Geometrical Configuration of the Oregon State College Solar Furnace. . 63

21 Concentrator Housing and Support Platform 68

22 Operator Stand and Vacuum Pump Shelf 69

23 Mirror Segments in Stationary Reflector with Important Sections Indicated by Oval Envelope 71

24 Mounting of Mirror Segments 74

25 Mirror Segments in Heliostat with Important Sections Indicated by Oval Envelope 77

26 Heliostat Basic Framework 79

27 Auxiliary Framework Mounted on Heliostat 80

28 Mirrors in Place on Heliostat 81

29 Altitude Control Photocell 84

30 Azimuth Control Photocell 88

31 Operation of the Azimuth Photocell. . 89

32 Sample Holder in Operating Position 92

33 Sample Holder Pylon and Rail 93

34 Sample Loading Jig 94

35 Gas Manifold System 98

36 Main Electrical Panel 100

37 Secondary Electrical Panel 101

38 Limit Switches. 102

39 Solar Furnace Building
from the Heliostat 107

40 Solar Furnace Building
and Walkways. 108

41 Sample in Focus Seen from
Paraboloid Vertex 118

42 Top View of Boron Sample 123

43 Side View of Boron Sample
Showing Surface Growth Stalagmites. . 124

44 Effect of Halving Non-planar
Mirror Segments 144

45 Early Azimuthal Control Patch 146

TABLES

Table Number	Title	Page
1	A Survey of Solar Furnace Installations in the United States .	8
2	Principal Symbols Used	30
3	Typical Transmissivity Factors for a Three-Mirror Paraboloidal Furnace.	48
4	X-Ray Spectrometric Analyses of Boron Samples	126
5	Crystallographic Data for Solar Furnace Melt and Surface Growths. .	128

CONSTRUCTION AND OPERATION OF A HIGH TEMPERATURE SOLAR FURNACE: STUDIES OF ELEMENTAL BORON

INTRODUCTION

In this day of abundance of conventional sources of energy, the direct utilization of solar radiation as such is economically attractive only under exceptional circumstances. However, as world supplies of fossil fuels are exhausted, the direct utilization of some of the tremendous quantities of energy which the sun supplies to the earth's surface will become more attractive. Even now, in cases of isolation from other energy sources, the utilization of direct solar radiant energy is finding application. Examples of such cases are to be found in such diverse places as earth satellites, remote scientific installations, life preserver solar water stills, and many more places all having in common a remoteness from more conventional energy sources.

An application of direct solar radiation having economic advantages, even in areas possessing adequate supplies of conventional energy sources, is the high temperature solar furnace. In such a solar furnace, the solar radiant energy impinging upon a relatively large area of the earth's surface is optically "compressed" or focused onto a much smaller surface. Any material placed at this focus is subjected to very strong heating. When one considers that the external temperature of the solar disc is about 6000°C, and that the radiant energy from this high-temperature source can be quite readily refocused to yield temperatures on the order of 3000°C in a readily controlled atmosphere, free from contaminants such as electrode fumes or furnace wall vapors, and also free from electrical or magnetic fields, then one realizes that a solar furnace has very attractive possibilities.

Important applications to which the advantages offered by the solar furnace appear especially desirable are high-temperature studies of extremely contaminant sensitive substances. An outstanding example of such a substance is elemental boron.

A research program of several years duration has been supported at Oregon State College by the U. S. Borax Research Corporation. Professor J. Schulein and his students over the years have developed a method for the commercial preparation of amorphous elemental boron and have sought since then for commercially applicable methods for the preparation of very pure crystalline material from this commercial grade, amorphous, elemental boron. A solar furnace with which to conduct high-temperature refining studies was constructed as part of this development program. Its use is, of course, not restricted solely to elemental boron studies; rather, it is available to anyone having a valid use for it, insofar as time limitations permit.

ADVANTAGES AND USES OF SOLAR FURNACES

Since temperatures far higher than the 4000°K theoretically attainable with solar furnaces are readily attained in arc discharge furnaces, solar furnaces appear to be of limited significance. The freedom from flame, electrode, and hot furnace wall contamination, the ease of atmospheric control, and the lack of electrical or magnetic fields, are advantages possessed by the solar furnace when contrasted to the more conventional ultra-high temperature sources. It is possible, by proper choice of furnace geometry, to cause a sample to contain its own melt; thus eliminating the necessity for high temperature crucibles and the attendant crucible introduced impurities. Visual observations of the sample can be made continuously during insolation.

Obviously, solar furnaces depend on sunlight; hence, they suffer from a restricted time of operation and a dependence upon atmospheric conditions. These disadvantages are offset to some extent by the "instant heating" characteristics of the solar furnace, i.e. no long heating up and cooling off periods are required.

Possible applications of solar furnaces are many and varied. A few of these are: studies of the high temperature chemistry and physics of metals, alloys, refractories, ceramics, and cermets; preparation of special materials for determination of their properties; high-temperature materials testing; thermal conductivity and emissivity studies (28:p.7); and, surprisingly, photochemical studies where the high photon flux permits large fractional conversions with short residence times (43:p.1335).

HISTORY OF SOLAR FURNACES

It is generally conceded that Archimedes, in 215 or 212 B.C., was the first to attain elevated temperatures by the reconcentration of solar radiation. He is reputed to have burned the Roman fleet blockading Syracuse by focusing the sun's rays on the ships (16:pp.157-158; 23:p.3). Similarly, Procus, in 614A.D., burned the fleet besieging Constantinople by the use of brass mirrors (16:p.158).

Another early record reports the use by the Athenians of solar radiation concentrated by polished golden mirrors to light the sacred fires of Vesta (16: p.158). In the 17th century, an optician, one Villete of Lyons, France, constructed several solar furnaces with polished iron mirrors. His furnaces were used in France, Denmark, Persia, and other countries (4:p.53). In 1695, Averani and Fargioni at Florence, Italy, used a large burning glass to cause a diamond, previously considered unalterable, to disappear (16:p.158). A great number of lenses and concave mirrors were constructed during this same period with which a large number of fusions and combustions were studied (16:p.158). Circa 1700, T. Schirnaus was able to melt slate, china, talc, and tile with a 0.97 meter diameter lens (16:p.158).

In the 18th century, Buffon, by superimposing the images reflected from a number of small flat mirrors, was able to melt metals and kindle wood (4:p.53). Lavoisier, in the 1770's was able to attain temperatures of about 3200°F by the use of two lenses in series. The lenses were reputed to be merely two pieces of glass filled with wine (4:p.64; 16:p.158).

The present era of solar furnace technology was ushered in with the construction, by Stack and Heyneman, circa 1900, of a small two-lens, adjustable mounting, enclosed sample furnace (16:p.158). In the twenties the Zeiss Company constructed several solar furnaces of various configurations (7:p.915). The California Institute of Technology in 1932 constructed a solar furnace using lenses and mirrors (7:p.915).

Since World War II several dozen solar furnaces have been constructed all over the world, but principally in France and the United States. France has at least 8 solar furnaces including one at Bouzareah, Algiers. Reference literature lists more than twenty solar furnaces in the United States (13:pp.115-116; 52:p.35; 53:p.55). Table 1 describes all the solar furnaces in the United States for which data are available.

TABLE 1

A SURVEY OF SOLAR FURNACE INSTALLATIONS IN THE UNITED STATES

Organization	A. D. Little, Inc.	Arizona State College
Furnace location	Cambridge, Mass.	Tempe, Arizona
Furnace description		
Main mirror		
Mounting	Altazimuth	Fixed; axis horiz.
Mirror material	Copper	Copper
Reflecting surface material	Stellite	Aluminum
Reflecting surface	Front	Front
Aperture	59.5 in.	60 in.
Focal length	25.6 in.	29.5 in.
Rim angle	60° 15'	65°
Theoretical image diameter	0.236 in.	0.238 in.
Auxiliary mirrors and lenses		
No. of aux. mirrors	None	One
No. of lenses	None	None
System		Heliostat
Tracking	Manual	Phototubes
Maximum temperature obtained		3300 K
Maximum flux measured		300 cal/cm^2/sec (est)
Ave. local solar const.	1.3 cal/cm^2/min	1.1 cal/cm^2/min
Reflectivity factor	75% (est.)	75% (heliostat)
Shadowing factor	96.4%	96%
Source of information	13	13

TABLE 1 (Continued)

Organization	B. F. Goodrich Co. Research Center	Bureau of Mines
Furnace location	Brecksville, Ohio	Morgantown, W. Va.
Furnace description		
Main mirror		
Mounting	Altazimuth	Altazimuth
Mirror material	Copper	Copper
Reflecting surface material	Rhodium	Rhodium
Reflecting surface	Front	Front
Aperture	60 in.	60 in.
Focal length	25.8 in.	26 in.
Rim angle	60°	
Theoretical image diameter	0.24 in.	
Auxiliary mirrors and lenses		
No. of aux. mirrors	None	None
No. of lenses	None	None
System		
Tracking	Phototubes	Manual
Maximum temperature obtained		2760 K
Maximum flux measured		
Ave. local solar const.		
Reflectivity factor	85% (est.)	
Shadowing factor	95% (est.)	85%
Source of information	53	13

TABLE 1 (Continued)

Organization	Calif. Inst. of Tech.	Convair
Furnace Location	Pasadena, Calif.	San Diego, Calif.
Furnace description		
Main mirror		
Mounting	Equatorial	Altazimuth
Mirror material		Copper
Reflecting surface material		Co-Ni alloy
Reflecting surface		Front
Aperture		60 in.
Focal length		25.5 in.
Rim angle		60°
Theoretical image diameter	0.50 in.	0.24 in.
Auxiliary mirrors and lenses		
No. of aux. mirrors	18	None
No. of lenses	38	None
System		
Tracking	Astron. control	Manual
Max. temperature obtained	3200 ± 100°C.	3050°C.
Maximum flux measured	170 cal/cm²/sec	629 cal/cm²/sec
Ave. local solar const.		1.3 cal/cm²/min
Reflectivity factor		85%
Shadowing factor		63%
Source of Information	13	13

TABLE 1 (Continued)

Organization	Convair	E. I. du Pont de Nemours & Co.	Fordham University
Furnace Location	Ft. Worth, Texas	Wilmington, Del.	New York, N.Y.
Furnace description			
Main mirror			
Mounting	Equatorial	Altazimuth	Altazimuth
Mirror material	Aluminum	Copper	Bronze
Reflecting surface material	Co-Ni alloy	Rhodium	Stellite
Reflecting surface	Front	Front	Front
Aperture	120 in.	60 in.	60 in.
Focal length	34.5 in.		25.5 in.
Rim angle	82°		60.8°
Theoretical image diameter	0.32 in.		0.238 in.
Auxiliary mirrors and lenses			
No. of aux. mirrors	None	None	None
No. of lenses	None		None
System			
Tracking	Astron. control	Manual	Phototubes
Maximum temperature obtained	2800°C.	3000°C.	3500°C.
Maximum flux measured	139 cal/cm^2/sec		
Ave. local solar const.			
Reflectivity factor			70% (meas.)
Shadowing factor			96% (meas.)
Source of information	13	13	13

TABLE 1 (Continued)

Organization	Kennecott Copper Corp.	Massachusetts Inst. of Tech.
Furnace location	Salt Lake City, Utah	Cambridge, Mass.
Furnace description		
Main mirror		
Mounting	Fixed; axis vert.	Special
Mirror material	Copper	Glass
Reflecting surface material	Rhodium	Silver
Reflecting surface	Front	Back
Aperture	60 in.	
Focal length	25.8 in.	
Rim angle	60°	
Theoretical image diameter	0.24 in.	3 in.
Auxiliary mirrors and lenses		
No. of aux. mirrors	2	One
No. of lenses	None	None
System	Heliostat	Special
Tracking	Phototubes	
Maximum temperature obtained	2800°C.	
Maximum flux measured		
Ave. local solar const.		1.5 $cal/cm^2/min$
Reflectivity factor	70% (est.)	60% (est.)
Shadowing factor	95% (app.)	
Source of information	13	13

TABLE 1 (Continued)

Organization	National Bureau of Standards	Oregon State College
Furnace location	Washington, D. C.	Corvallis, Ore.
Furnace description		
Main mirror		
Mounting	Fixed; axis horiz.	Fixed; axis vert.
Mirror material	Copper	Copper
Reflecting surface material	Rhodium	Rhodium
Reflecting surface	Front	Front
Aperture	60 in.	60 in.
Focal length	26 in.	26 in. (app.)
Rim angle	60^{o}	60^{o} (app.)
Theoretical image diameter	0.25 in.	0.242 in. (app.)
Auxiliary mirrors and lenses		
No. of mirrors	One	2
No. of lenses		None
System	Heliostat	Heliostat
Tracking	Phototubes	Photocells
Maximum temperature obtained	3300^{o}C.	
Maximum flux measured		
Ave. local solar const.	1.5 cal/cm^2/min	
Reflectivity factor		
Shadowing factor		
Source of information	13	

TABLE 1 (Continued)

Organization	Quartermaster R & D Command	Rocketdyne
Furnace location	Natick, Mass.	Canoga Park, Calif.
Furnace description		
Main mirror		
Mounting	Fixed; axis horiz.	Altazimuth
Mirror material	Glass	Glass
Reflecting surface material	Aluminum	
Reflecting surface	Front	Back
Aperture	28 ft. x 28 ft.	60 in.
Focal length	35.8 ft.	26 in.
Rim angle	32°	
Theoretical image diameter	4 in.	9/32 in.
Auxiliary mirrors and lenses		
No. of mirrors	One	None
No. of lenses		None
System	Heliostat	
Tracking	Phototubes	Phototubes
Max. temperature obtained		
Maximum flux measured		
Ave. local solar const.		
Reflectivity factor		
Shadowing factor		
Source of information	13	53

TABLE 1 (Continued)

Organization	University of Delaware	University of Minnesota
Furnace location	Newark, Del.	Minneapolis, Minn.
Furnace description		
Main Mirror		
Mounting	Altazimuth	Altazimuth
Mirror material	Copper	Copper
Reflecting surface material	Rhodium	Rhodium
Reflecting surface	Front	Front
Aperture	60 in.	60 in.
Focal length	26 in.	
Rim angle	60°	
Theoretical image diameter	0.25 in.	
Auxiliary mirrors and lenses		
No. of mirrors	None	None
No. of lenses	None	
System		
Tracking	Manual	Manual
Max. temperature obtained	3000°C (app.)	
Maximum flux measured		
Ave. local solar const.	1.35 cal/cm^2/min	
Reflectivity factor		
Shadowing factor		
Source of information	52	13

TABLE 1 (Continued)

Organization	Sandia Corporation	Stanford Research Inst.	University of Delaware
Furnace location	Albuquerque, N.M.	Menlo Park, Calif.	Newark, Del.
Furnace description			
Main mirror			
Mounting	Equatorial	Fixed; axis vert.	Altazimuth
Mirror material	Bronze	Copper	Glass
Reflecting surface material	Aluminized with SiO_2 overcoat	Rhodium	Silver
Reflecting surface	Front	Front	Back
Aperture	60 in.	60 in.	60 in.
Focal length	26.5 in.	26 in.	26 in.
Rim angle	60°		60°
Theoretical image diameter	0.231 in.	0.25 in.	0.24 in.
Auxiliary mirrors and lenses			
No. of mirrors	None	One	None
No. of lenses	None		None
System	Newtonian	Heliostat	
Tracking	Clock drive with phototube corrector	4 Phototubes	Phototubes
Max. temperature obtained			$3000^{\circ}C$
Maximum flux measured			
Ave. local solar const.	1.4 $cal/cm^2/min$		1.35 $cal/cm^2/min$
Reflectivity factor	82% (est.)		
Shadowing factor	92%		
Source of information	52	13	52

TABLE 1 (Continued)

Organization	University of Utah	WMC Prec. Works & RMF Steel Prod.
Furnace location	Salt Lake City, Utah	Kansas City, Mo.
Furnace description		
Main mirror		
Mounting	Stationary	Equatorial
Mirror material	Glass	Copper
Reflecting surface material	Silver	Rhodium
Reflecting surface	Back	Front
Aperture	60 in.	60 in.
Focal length	26 in. (app.)	26.3 in.
Rim angle		
Theoretical image diameter	0.24 in.	0.236 in.
Auxiliary mirrors and lenses		
No. of mirrors	One	
No. of lenses	None	
System	Heliostat	
Tracking	Phototubes	Phototubes
Maximum temperature obtained		3000°C.
Maximum flux measured		
Ave. local solar const.		
Reflectivity factor	80% (est.)	86%
Shadowing factor	99% (est.)	95%
Source of information	52	13

FACTORS TO BE CONSIDERED IN THE DESIGN OF A SOLAR FURNACE

The many factors which have to be considered in the design of a solar furnace can be classified into four general categories: 1) type of furnace, 2) geometrical configuration, 3) mounting and tracking, and 4) optical and radiant energy considerations.

Although all of the factors which are discussed under individual sub-headings should be considered when designing a solar furnace, it may be found, as it was in the case of the furnace which is the subject of this thesis, that few alternatives are possible if the furnace is to be used for a particular application in a particular geographical location.

TYPE OF FURNACE

The method by which the sun's rays are concentrated determines the type of the solar furnace. Such concentrators are of two general types: refracting lenses or reflecting paraboloidal mirrors.

Lens concentrator systems either can be simple, similar to a large reading glass, or quite complex, consisting of many lenses and plane mirrors. Lens systems enjoy little application at this time. The lens furnace at California Institute of Technology, built in 1932, is

The only large one now reported to be in existence (13: pp.115-116).

The overwhelming majority of solar furnaces employ paraboloidal reflecting concentrators of one piece construction. Some very large solar furnaces employ oriented flat or curved mirror segments to approximate a paraboloidal reflector surface. Curved mirror segments are formed by pressure loading a plane mirror at appropriate points, front and back, to cause the plane mirror to be deformed into an approximation of a portion of the surface of a large paraboloid. Most frequently these segments are mounted on frameworks to form a paraboloidal array. At least one furnace, however, has been proposed wherein flat or curved mirror segments are mounted in tiers and move individually so that the images of all the segments overlap on the target (5:p.7). Only reflecting concentrators will be further discussed in detail in this paper.

GEOMETRICAL CONFIGURATION

A great many geometrical configurations are possible for solar furnaces. Applied designs are described below.

The simplest possible configuration consists of a paraboloidal concentrator pointed directly at the solar disc. The control of the concentrator position relative to the sun is difficult in this system. Where solid-liquid transitions are to be studied, this system is undesirable since the melted sample will drip out of the focal "hot spot".

Where a plane reflector, called a heliostat, is used to direct the solar energy into the concentrator system, several configurations are possible. In Fig.1, a heliostat is used to direct the sun's rays into a vertically mounted paraboloidal concentrator. The largest solar furnaces now in use employ this system (4:p.56). This furnace still is not ideal for solid-liquid studies since the melt would again tend to drain away from the heated zone.

Fig. 2 shows a horizontally mounted paraboloidal mirror into which radiant energy is concentrated by a heliostat mounted directly below the concentrator. The separation between concentrator and heliostat must be so large that a tower is needed for mounting the concentrator if the concentrator is not to occlude sunlight from the heliostat. Two existing furnaces are reported to use this configuration for metallurgical studies, Table 1.

A third arrangement, which has the best features of the two previous examples, is shown in Fig. 3. The solar radiation is directed by the heliostat onto a diagonally mounted, stationary reflector,thence into the paraboloidal

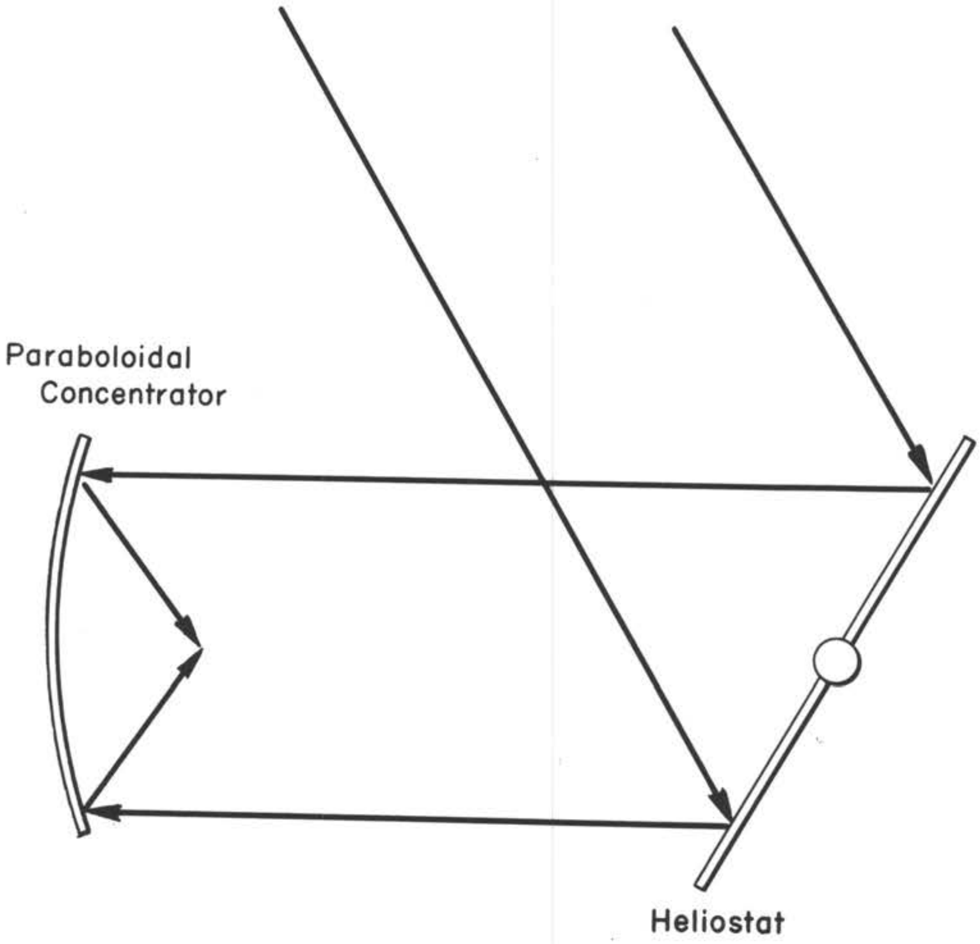

FIGURE I

HELIOSTAT - VERTICAL CONCENTRATOR FURNACE

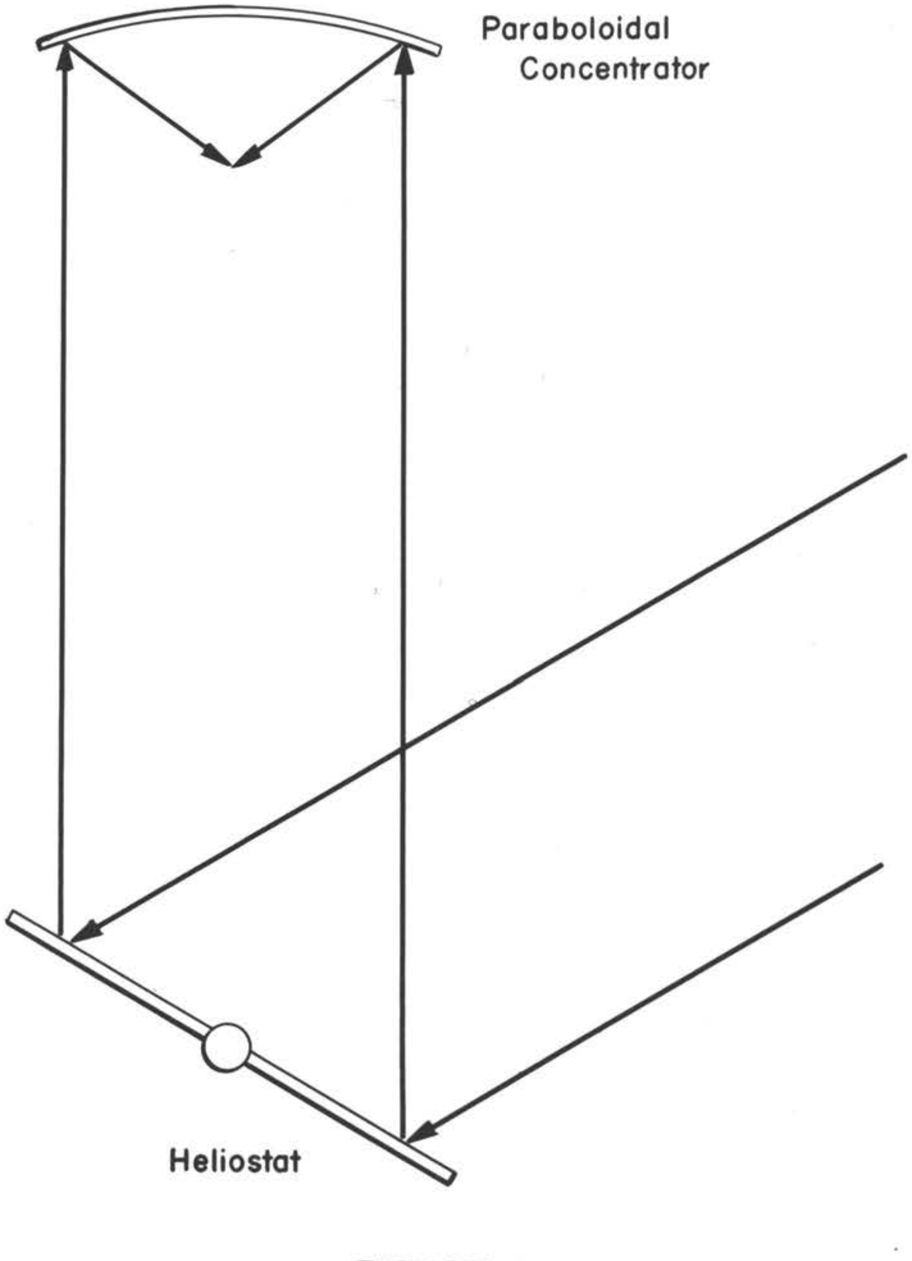

FIGURE 2

HELIOSTAT-HORIZONTAL CONCENTRATOR FURNACE

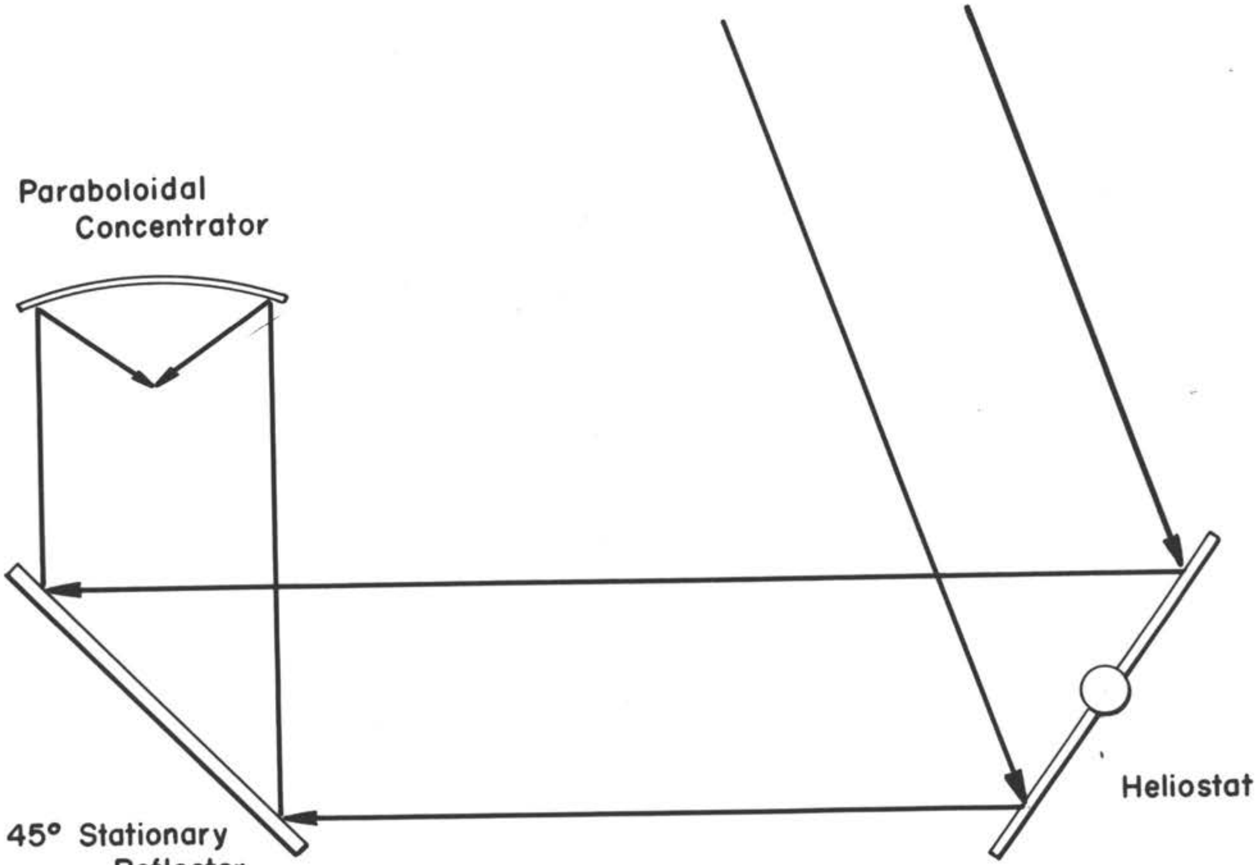

FIGURE 3

HELIOSTAT – STATIONARY REFLECTOR-HORIZONTAL CONCENTRATOR FURNACE

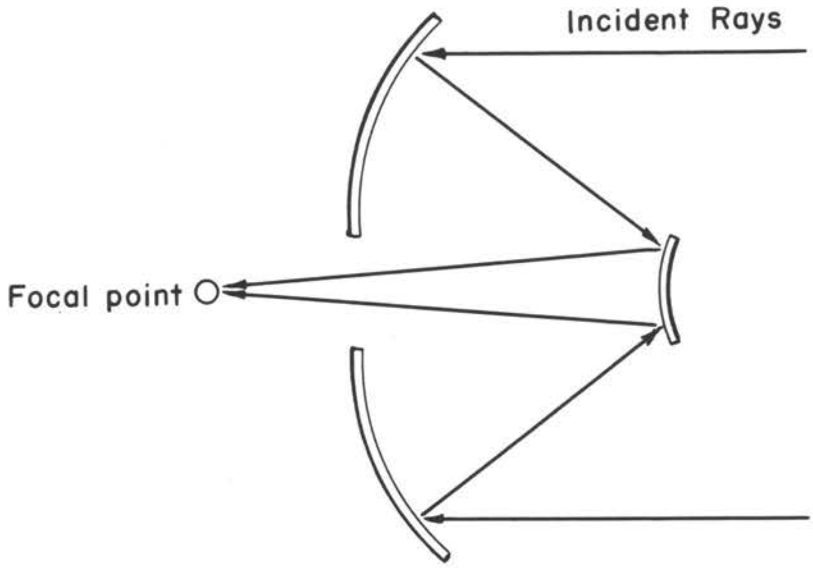

FIGURE 4
CASSEGRAINIAN MOUNTING

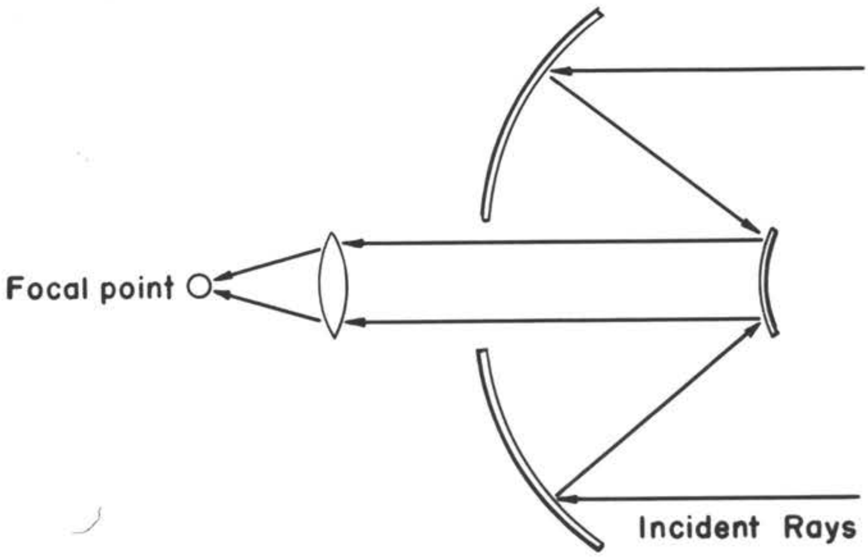

FIGURE 5
STRAUBEL TWO STEP MOUNTING

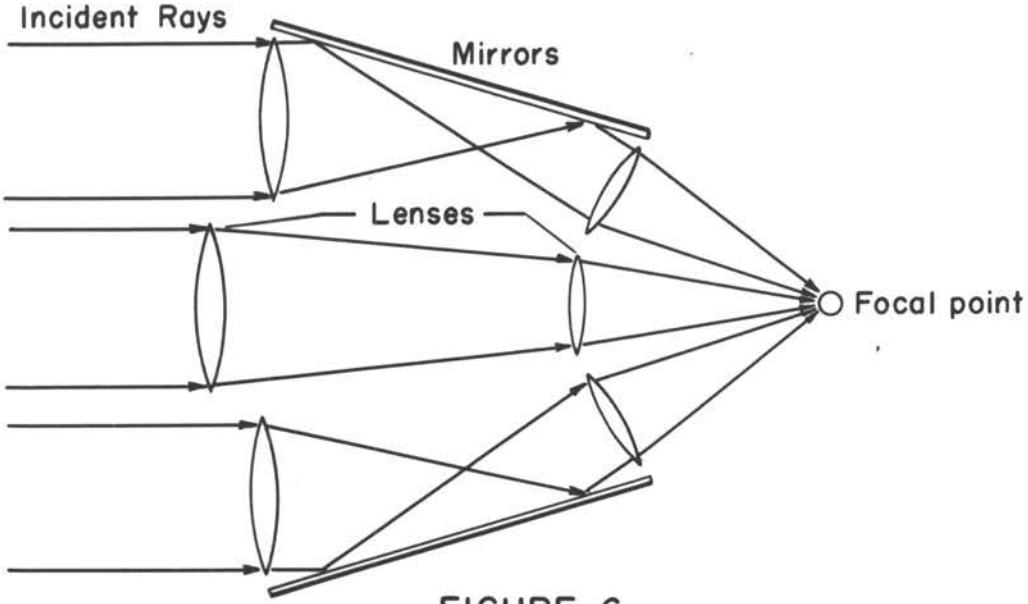

FIGURE 6

MOUNTING OF LENSES AND MIRRORS

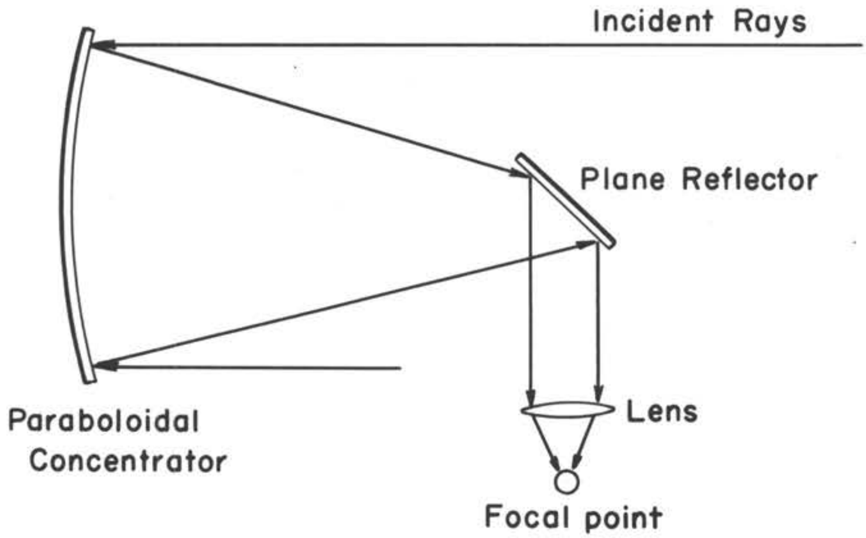

FIGURE 7

NEWTONIAN MOUNTING

concentrator. In this system the furnace components can all be mounted upon simple platforms and still have the sample irradiated upon its upper surface where a melt will remain and not tend to drain away.

Many more complex systems, mostly descended from telescopy, have been used. Some of these are presented schematically in Figs. 4, 5, 6, and 7.

MOUNTING AND TRACKING

The mounting and tracking of a solar furnace are interrelated terms whose specific application depend upon the geometrical configuration of the solar furnace. If the concentrator is continuously moved to always point at the sun, referred to as tracking, the mounting term then refers to the concentrator. If, however, a plane mirror, or heliostat, is used to track the sun and redirect the radiant energy into the stationary concentrator, then the mounting and tracking terms apply to the heliostat.

The most commonly used mounting system is the altazimuth, from altitude and azimuth. This is the standard type of mirror mounting used for searchlights. In Fig. 8 the altazimuth mounting is schematically represented. Changes of the mirror altitude are achieved by rotating it about a horizontal axis while azimuth changes

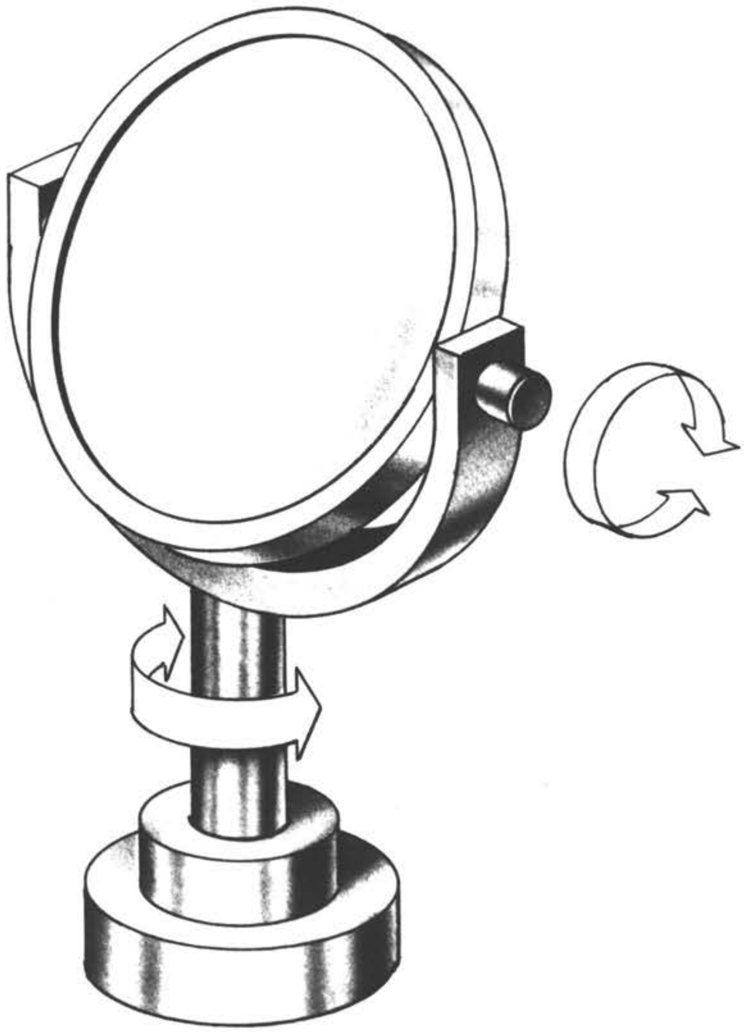

FIGURE 8

ALTAZIMUTH MOUNTING

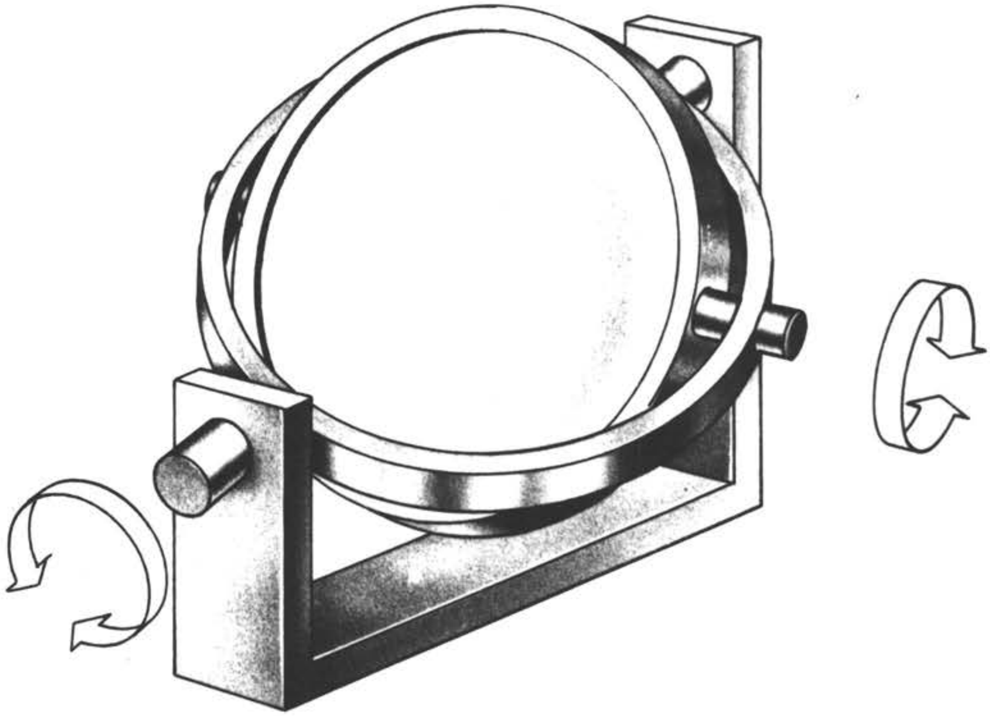

FIGURE 9

EQUATORIAL MOUNTING

are effected by rotation about a vertical axis in the same plane as the horizontal axis.

The other type of mounting, used only slightly for solar furnaces and more commonly for celestial telescopes, is the equatorial mounting. As shown in Fig. 9, the equatorial mounting has four pivot points all lying in the same inclined plane. This inclined plane is made parallel to the axis of rotation of the earth. Relative mechanical complexity, undoubtedly, is responsible for the widespread rejection of equatorial mounting in favor of the altazimuth type of mounting.

OPTICAL AND RADIANT ENERGY CONSIDERATIONS FOR A SOLAR FURNACE

The discussion of the optical design factors will deal primarily with the system employed in the Oregon State College solar furnace. This system includes a heliostat, a stationary reflector, and a horizontally mounted paraboloidal concentrator (Fig. 3).

Solar Image Formed By a Perfect Paraboloid:

A perfect paraboloid is defined as one whose surface is a geometrically true paraboloid and is perfectly reflective. If such a paraboloid is aimed directly at the center of the sun's disc, a circular composite image is formed at the focal plane by reflections from all parts of the paraboloid. This composite image consists of a circular center portion of maximum and uniform intensity, the "hot spot", which is surrounded by a fringe of radially decreasing intensity. (See Figs. 10 and 11.)

The meaning and dimensions of all principal symbols used in the drawings and in the following discussion are summarized in Table 2.

TABLE 2

PRINCIPAL SYMBOLS USED

A_e . . . Area of elliptical element.

A_f . . . Area of hot spot.

a . . . Paraboloid focal length, ft.

b_1 . . . Minor axis of elliptical element.

b_2 . . . Major axis of elliptical element.

C . . . Concentration ratio of a perfect paraboloid, dimensionless.

C_a . . . Concentration ratio of a solar furnace, dimensionless.

d . . . Hot spot diameter, ft.

E . . . Ratio A_f to A_e

F . . . Furnace factor, dimensionless.

f . . . Focal length

q_f . . . Solar radiation intensity upon hot spot, Btu/sq ft-hr

q_1 . . . Direct sunshine intensity at furnace site, Btu/sq ft-hr

q_s . . . Radiation intensity at surface of sun, Btu/sq ft-hr

T . . . Temperature, ^{o}R

y . . . Distance from paraboloid axis.

α . . . Angular diameter of sun's disc, radians.

α_r . . . Solar absorptivity of test sample, dimensionless.

ϵ . . . Emissivity of test sample, dimensionless.

δ . . . Distance from focal plane.

η . . . Furnace "transmissivity factors", dimensionless.

τ . . . Atmospheric transmissivity.

θ . . . Angle between paraboloid principal axis and paraboloid radius from focal point, degrees.

θ_1 . . . Rim angle of paraboloid, degrees.

ρ . . . Paraboloid radius from focal point, ft.

σ . . . Stefan-Boltzman constant, Btu/sq ft-hr (^{o}R).

Ω . . . Angular deviation of reflected light from a nearly planar mirror.

The diameter of the hot spot is given by:

$$d = a\alpha \qquad (1)$$

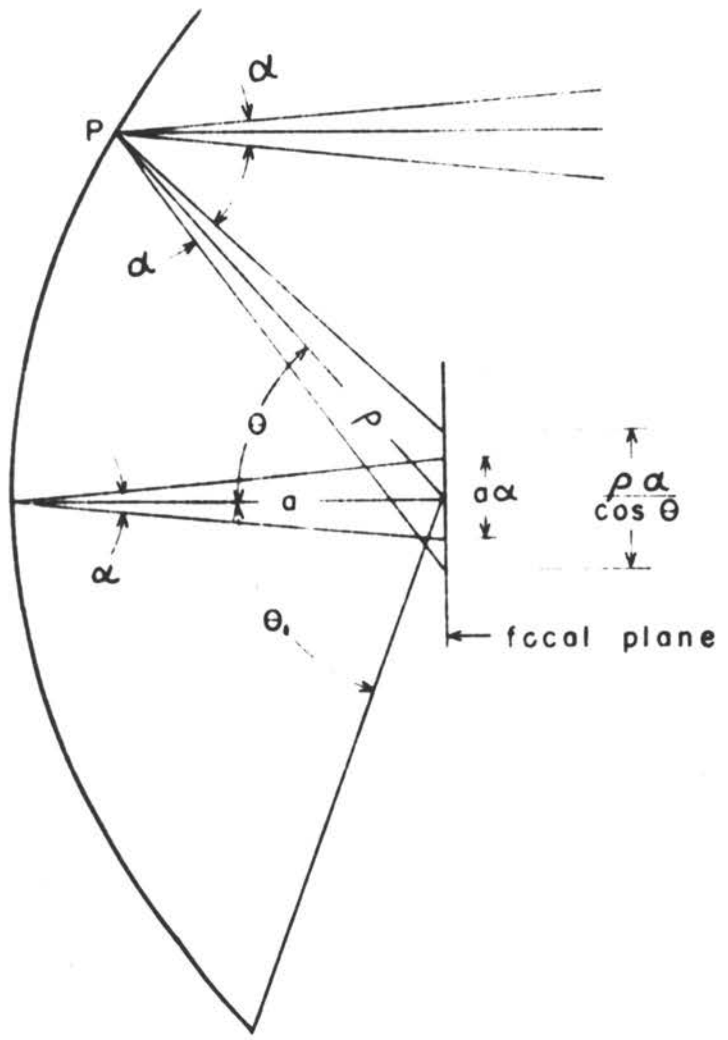

FIGURE 10

IMAGE FORMATION IN A PARABOLOIDAL CONCENTRATOR

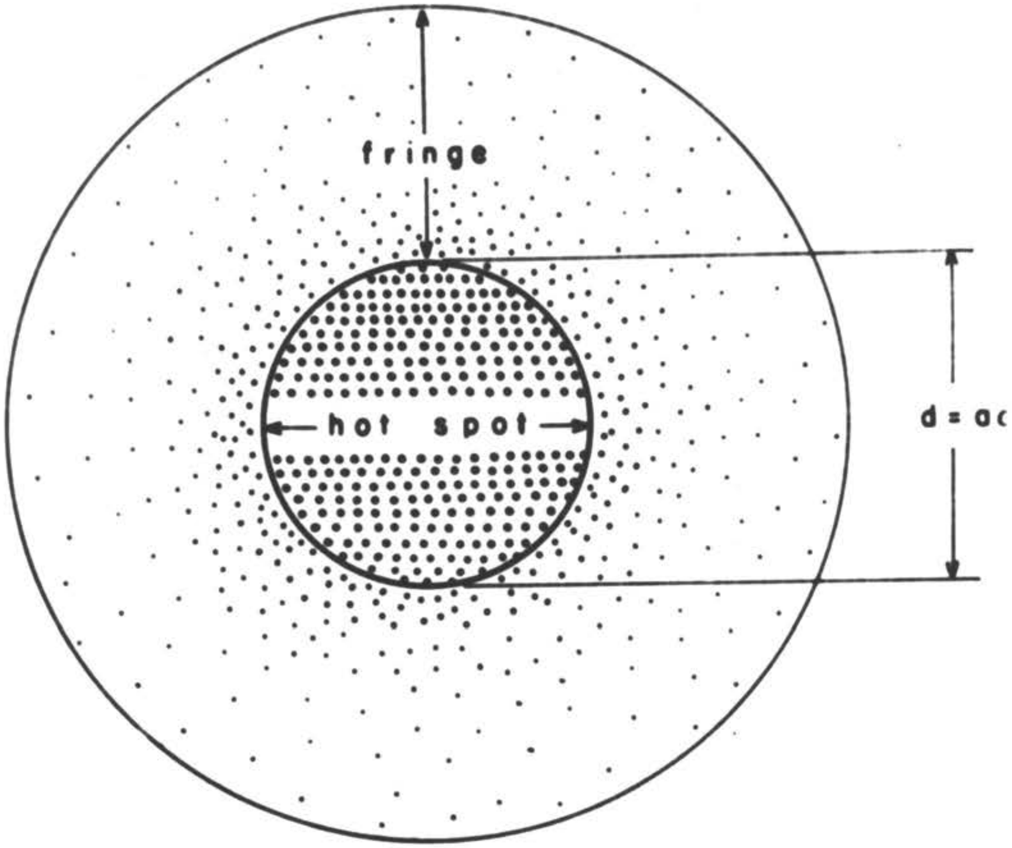

FIGURE II

RELATIVE INTENSITIES IN THE SOLAR IMAGE

The apparent angular diameter of the sun's disc, α, has an average value of 0.00931 radian. It varies from 0.00948 radian in January, when the earth is closest to the sun, to 0.00917 radian in July, when the earth is farthest from the sun (8:p.23). Hence, the hot spot diameter, d, will be slightly larger in January than in July.

The concentration ratio, C, produced at the hot spot is defined as the ratio between the theoretical solar radiation intensity upon the hot spot and the unconcentrated direct sunshine intensity at the furnace site:

$$C = \frac{q_f}{q_i} \qquad (2)$$

This ratio is calculated in detail in the next sub-section. To a close approximation, it is found to be a simple function of the paraboloid rim angle and the sun's angular diameter:

$$C = \frac{4}{\alpha^2} \sin^2 \theta_1 \qquad (3)$$

Hence, for a perfect paraboloid:

$$q_f = q_i \frac{4}{\alpha^2} \sin^2 \theta_1 \qquad (4)$$

The factor $4/\alpha^2$ appearing in the above equation has an average value of 46,200, ranging from a minimum of about

44,500 in January to a maximum of about 47,500 in July (8:p.24). This variation can usually be neglected in design of a furnace.

If the sun is assumed to be a uniform sphere whose surface radiation is q_s, and if the fractional reduction of direct sunshine in passing through the atmosphere is $(1 - \tau)$, it can be readily shown that:

$$q_i = \tau \frac{\alpha^2}{4} q_s \qquad (5)$$

Hence, equation (4) may be expressed as:

$$q_f = \tau \; q_s \sin^2 \theta_1 \qquad (6)$$

It will be noted from the above equation that, in the absence of atmospheric transmissivity losses, a perfect paraboloid of rim angle 90° would produce a radiation intensity upon the hot spot equal to the radiation intensity of the sun's surface. Also it will be noted that a given paraboloid within the earth's atmosphere will produce a radiation intensity upon the hot spot which is directly proportional to the atmospheric transmissivity factor, τ , and independent of the sun's distance. In many cases the factor, τ , can be expected to be slightly higher in summer than in winter, because of the shorter path length of sunshine through the atmosphere at higher angular solar altitudes.

Derivation of Equation of Perfect Paraboloid Concentration Ratio

The solar image formed at the focal plane by reflection from the vertex of the paraboloid is a circle, the "hot spot", of diameter, d, and area, A_f. From equation 1, $d = a\alpha$, then:

$$A_f = \frac{\pi a^2 \alpha^2}{4} \qquad (7)$$

Referring to Fig. 10, it is seen that the focal plane images formed by reflection from all other points on the paraboloid (within the range of solar furnace design) are ellipses. The ellipse formed at the focal plane by reflection from the point, P, has the approximate minor and major axis diameters:

$$b_1 = \rho\alpha \quad , \quad b_2 = \frac{\rho\alpha}{\cos\theta} \qquad (8)$$

The ratio E_θ between the hot spot area, A_f, and the ellipse area, A_e, is found to be:

$$E_\theta = \frac{A_f}{A_e} = \frac{a^2 \cos\theta}{\rho^2} \qquad (9)$$

Now if it is assumed that the elliptical image is of uniform intensity (as it very nearly is, except at extremely large values of θ), then the fraction E_θ of the total radiant energy reflected from P is directed to the hot spot.

The concentration ratio attained by a small ring-shaped portion of the paraboloid lying at an angle θ and bounded by the arc $d\theta$, (Fig. 12), is now considered. The total solar energy per unit time falling upon this ring-shaped portion of the paraboloid will be the product of the incident direct sunshine intensity and the projected area of the ring-shaped portion:

$$dq = q_1 dA \tag{10}$$

Inspection and consideration of Fig. 12 show that this projected area dA is:

$$dA = 2\pi\rho^2 \sin\theta \, d\theta \tag{11}$$

The fraction E_θ of the total energy dq is reflected to the hot spot. The resulting concentration ratio produced at the hot spot by the thin ring of the paraboloid is:

$$dC = \frac{dq_f}{q_1} = \frac{E_\theta \; q_1 \; dA}{A_f \; q_1} \tag{12}$$

Substituting from (7), (9), and (11) into the above yields:

$$dC \quad \frac{8}{\alpha^2} \sin\theta \; \cos\theta \; d\theta \tag{13}$$

Integrating from the center of the paraboloid to

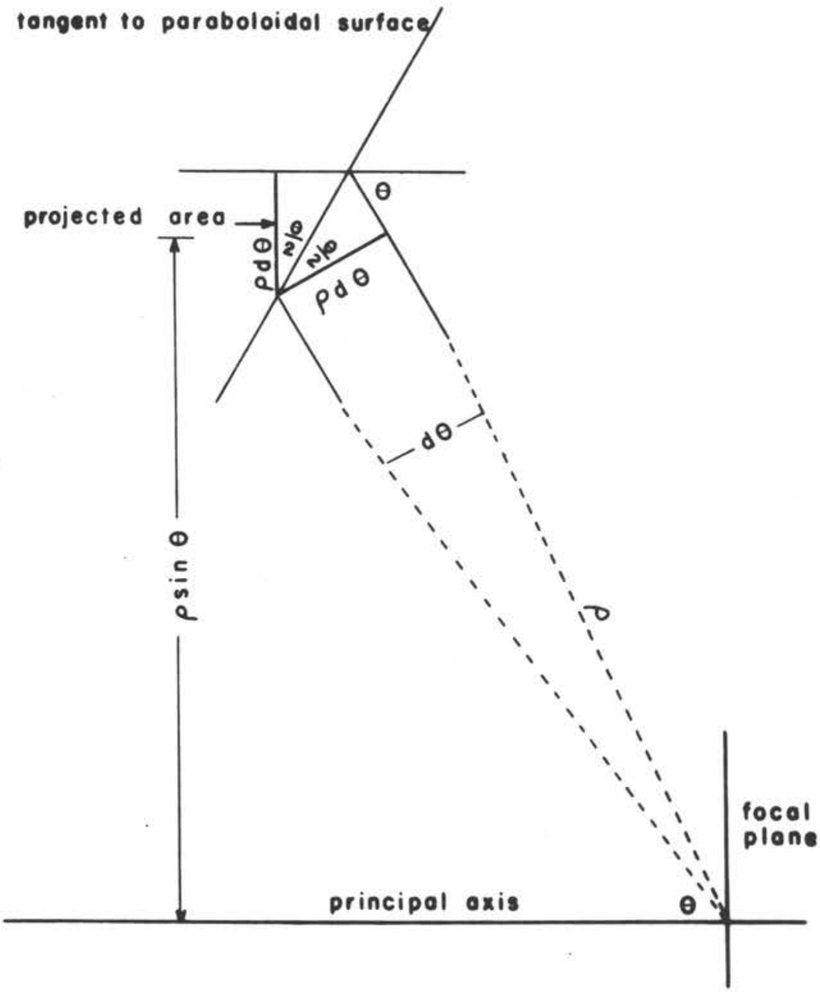

FIGURE 12

IMAGE CAST BY A DIFFERENTIAL RING AREA

rim angle θ_1 then gives the basic equation for the concentration ratio of a perfect paraboloid:

$$C = \frac{4}{\alpha^2} \sin^2 \theta_1 \tag{14}$$

The numerical results of this simple relation, but not the equation, have been worked out by Cabannes and Le Phat Vinh, (11:p.820). The equation itself is hidden in a complicated derivation by Farber and Davis, (24:p.220). Substantially the equation itself has been stated in recent papers by Duwez, (21:p.7), and by Benveniste and Hiester, (7:p.920). This equation is derived upon the following assumptions:

1. The exact elliptical image diameters are given by equation (8).
2. The intensity of a given elliptical image is uniform over its surface.
3. The sun's disc is of uniform intensity.

From the standpoint of the engineering accuracy of the basic concentration ratio equation (14), the inaccuracies contributed by assumptions (1) and (2) are of negligible importance even up to rim angles of 80° (8:p.28). This is a higher rim angle than would be practicable for a solar furnace. However, assumption (3), that the sun's disc is of uniform intensity, causes the basic concentration ratio to be slightly in error.

The sun's disc has a greater intensity at the center than at the edge. According to Abetti (1:p.317), its intensity varies with radius somewhat as shown in Fig. 13. Calculations from this curve indicate that the peak intensity at the center of the sun's disc is about 25 per cent greater than the average intensity of the disc (8:p.28). They also indicate that a perfect paraboloid of rim angle 60° should have a concentration ratio approximately 10 per cent greater than that given by the basic equation (14).

Insofar as an actual solar furnace is concerned, the effect of this limb-darkening is not necessarily in the direction of increasing the concentration ratio of the furnace over that which the furnace would have if the sun's disc were of uniform intensity. The limb-darkening phenomenon tends to increase any losses which may be present in the furnace as a result of geometrical imperfections of mirror surfaces. As a result, a solar furnace operating in actual (limb-darkened) sunshine may have either a slightly higher or a slightly lower concentration ratio than it would have if the sun's disc were of uniform intensity (8:p.28).

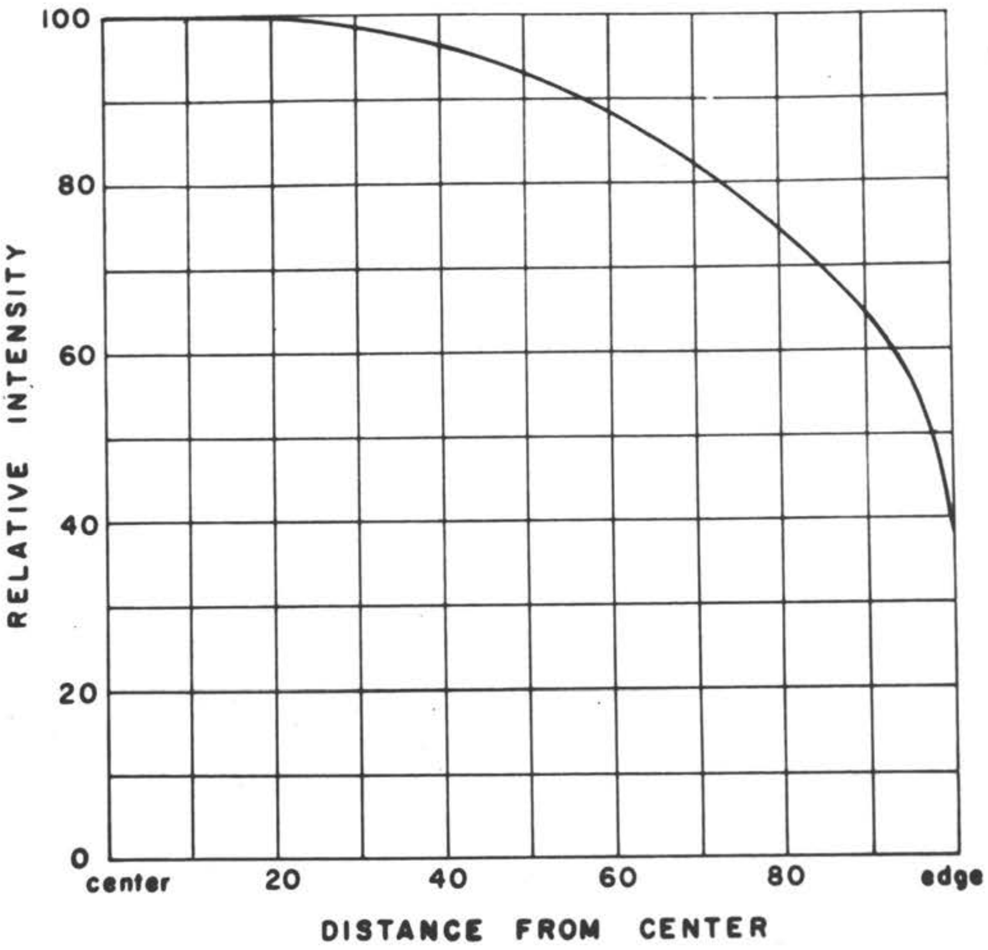

FIGURE 13

VARIATION OF INTENSITY OF
RADIATION ACROSS SOLAR DISC

Allowance For Furnace Transmission Losses

An actual paraboloidal solar furnace will have a hot spot of the same diameter as that of a perfect paraboloid, but the concentration ratio, C_a, of the actual furnace will be less than that of the perfect paraboloid by a suitable reduction factor, F, which is called the "furnace factor":

$$C_a = FC \tag{15}$$

Hence, the radiation intensity incident upon the hot spot of an actual solar furnace is

$$q_f = q_1 F \frac{4}{\alpha^2} \sin^2 \theta_1 \tag{16}$$

This furnace factor, F, is the catchall product of a series of transmissivity factors allowing for all solar energy losses in transit through the apparatus. The furnace factor may be expressed:

$$F = (\eta_1 \eta_2 \eta_3 \cdots \eta_n) \tag{17}$$

As an illustrative example of the meaning and approximate magnitudes of the various transmissivity factors, consider the case of a three-mirror paraboloidal furnace similar to the one constructed at Oregon State College. Assume that both the heliostat and the stationary reflector mirrors of the furnace are built up of many individual segments of back-silvered glass. Further, assume that the sample holder array at the hot spot is supported by some sort of tower. The resulting losses are briefly discussed and roughly evaluated in the paragraphs that follow.

Some solar energy will be lost by glass absorption. The sunshine must make four trips through the glass: in and out of the heliostat mirror and in and out of the stationary mirror. For clear glasses $\frac{1}{4}$ inch in thickness, of types which would be used in solar furnace design, values of the glass transmissivity factor, η_t, can be expected to range from about 0.94 to 0.98 per pass (8:p.24). The exact value, of course, depends upon the particular glass chosen. Glass transmissivities will decrease slightly with increasing incident angle of sunshine upon the mirror, a factor which must be allowed for in exact calculations.

A transmissivity factor, η_r, allows for the reflectivity of each silvered surface. This factor will vary with the quality of the silvering, the wave length distribution of the incident sunshine, and with incident angle of sunshine upon the surface. Reflectivity increases slightly with increasing incident angle. A reasonable assumption is that the surface reflectivity transmissivity factor will lie in the range of 0.91 - 0.95 for each silvered surface (8:p.24). The rhodium plated paraboloidal mirror has a reflecting, η_{r3}, of 0.90 to 0.95 (4:p.57).

A transmissivity factor, η_g, for each mirror is included to allow for the effect of geometrical imperfections of the mirror surfaces. The two heliostat mirror surfaces will not be truly plane and parallel, and likewise the stationary reflector and paraboloidal concentrator mirror surfaces will not be exactly true. The appropriate geometrical imperfection transmissivity factor will probably lie in the range of 0.90 - 0.96 per mirror (8:p.25).

The next transmissivity factor to be considered is the mirror frame shading transmissivity factor, η_f, of each mirror. Since in this type of furnace both the stationary reflector and the heliostat mirrors are built up of individual segments, there is a non-reflecting area associated with each mirror segment. For segments 10½ inches square having three exposed support bolt heads and washers, with a minimum possible separation, the non-reflecting area is about 5 per cent. This shading must be taken into account for both the heliostat and the stationary reflector. Reasonable values of the mirror frame shading transmissivity factor should range between

0.94 and 0.98 per mirror, depending upon the care and expense taken in construction details (8:p.25).

The sample holder apparatus at the hearth will contribute a shading loss. A reasonable estimate of the transmissivity factor, η_s, to allow for this loss should lie in the range of 0.85 to 0.95, depending, of course, on the design of the sample holder and its size relative to the entire paraboloid (8:p.25). It should be noted that shading produced near the center of the paraboloid will cause a greater percentage of concentration drop than the percentage of shading. This effect can be calculated, and it will be found that for a paraboloid of rim angle 60°, center shading of 1 per cent of the projected paraboloid area will produce nearly a 2 per cent drop in concentration (8:p.25). Similarly, a thin rod along a paraboloid radius -- to which a tower leg is roughly equivalent -- will produce a greater percentage concentration drop than the percentage of shading. In the case of the rod parallel to the radius and extending from center to rim of the paraboloid, it can be shown that, for a paraboloid of rim angle 60°, one per cent of shading by the rod will produce approximately a 1.25 per cent drop in concentration ratio (8:p.25). These effects must be allowed for in calculations. It is evident that a furnace should be designed to reduce all shading, and especially center shading, to an absolute minimum.

Finally, in what may seem a distressingly long listing of the losses to be expected from the furnace, the matter of mirror segment alignment should be considered. Both the heliostat and the stationary reflector are assumed to be built up of many small segments. These segments must be adjusted to proper alignment during construction, and they can be re-aligned only at intervals once the furnace is placed in operation. The question naturally arises: will they stay aligned? Probably, to some degree, they will not. Wind, weather, thermal strains, cleaning operations, and other causes can be expected to throw at least some of the mirror segments partially out of alignment. The designer must seek to minimize this factor, also to estimate or measure it, and to allow for it. A transmissivity factor, η_a, is assigned to allow for this effect, and its value is estimated as lying between 0.95 and 0.99 for a well-designed and carefully constructed furnace (8:p.25).

It now appears that all the depletion effects which will lower the performance of the hypothetical furnace as compared with a perfect paraboloid have been considered and roughly estimated. The various transmissivity factors which have been discussed are summarized in Table 3. For a three-mirror furnace of the type assumed, the furnace factor will be:

$$F = (\eta_{t1}^{2}\ \eta_{r1}\ \eta_{g1}\ \eta_{f1}\ \eta_{a}\ \eta_{t2}^{2}\ \eta_{r2}\ \eta_{g2}\ \eta_{f2}\ \eta_{r3}\ \eta_{g3}\ \eta_{s}) \qquad (18)$$

In the above equation the subscripts 1, 2, and 3, refer to the heliostat, the stationary mirror and the paraboloidal mirror respectively. No single loss is exorbitant, but the combination of all of them reduces the furnace performance very significantly below that of a perfect paraboloid. Combining all the low estimates of the various transmissivity factors results in a furnace factor of 0.32; combining all the high estimates results in a furnace factor of 0.62. A reasonably well designed three-mirror paraboloidal furnace should exhibit a furnace factor somewhere within this range, and with very careful design the values near the top of the range might be attained.

TABLE 3

TYPICAL TRANSMISSIVITY FACTORS FOR A THREE-MIRROR PARABOLOIDAL FURNACE

Symbol	Factor	Estimated Value Low	Estimated Value High
η_t	Glass transmissivity, per pass	.94	.98
η_{r1-2}	Surface reflectivity, per surface	.91	.95
η_{r3}	Rhodium reflectivity, per surface	.90	.95
η_g	Geometrical imperfection, per mirror	.90	.96
η_f	Mirror frame shading, per mirror	.94	.98
η_s	Tower shading	.85	.95
η_a	Alignment factor	.95	.99
	Overall furnace factor, F.	.32	.62

Fig. 14 presents the concentration ratios which can be attained with paraboloids of various rim angles and with furnace factors ranging from 0.30 to 0.60.

Maximum Temperatures Attainable With Solar Furnaces

The maximum temperatures which can be attained by a sample whose exposed face lies in the focal plane at the hot spot of a given furnace depends upon the direct sunshine intensity at the site, the concentration ratio of the furnace, and the relation between the solar absorptivity and emissivity of the sample.

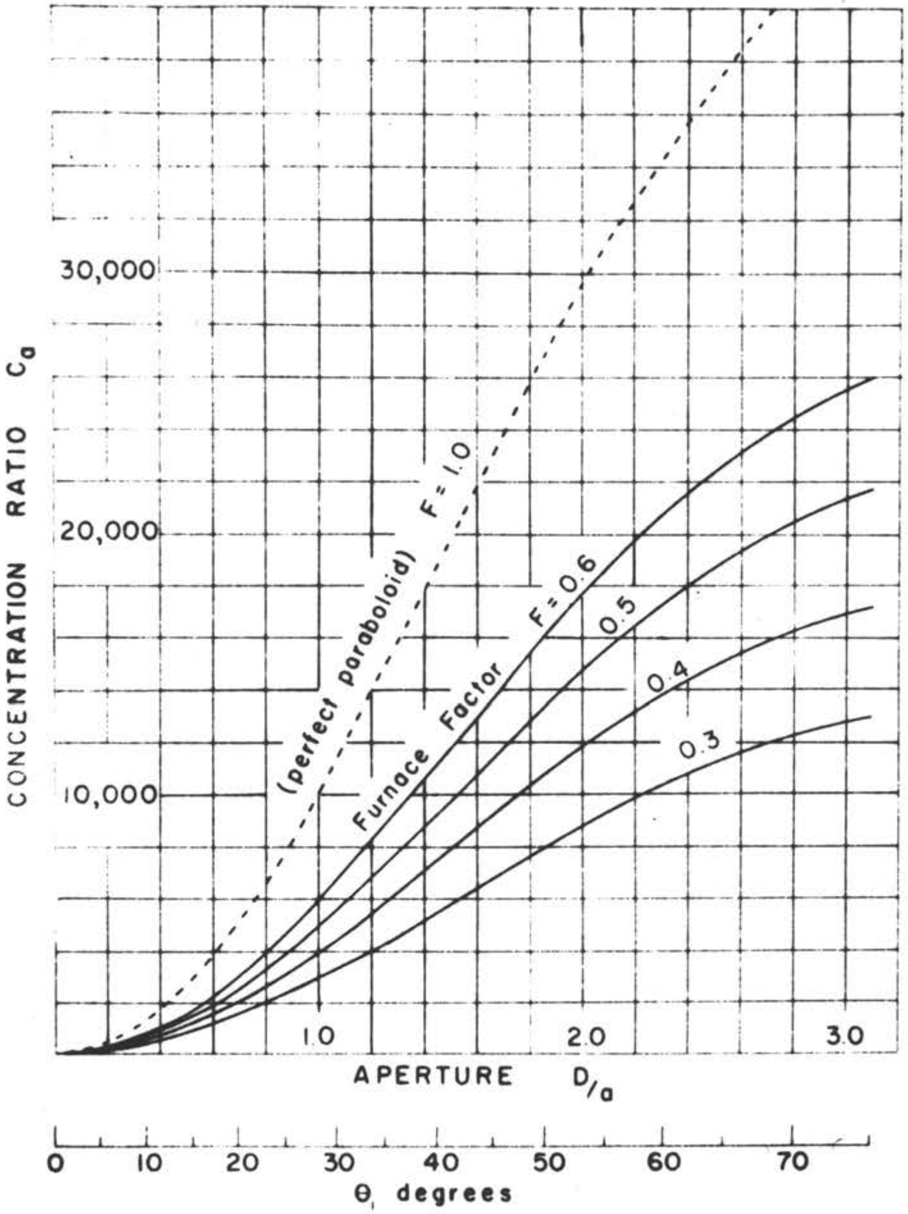

FIGURE 14

CONCENTRATION RATIOS FOR VARIOUS FURNACE FACTORS AND RIM ANGLES

The most logical solar furnace climatic area in the United States is somewhere in the Southwest (8:p.26). Within this area direct sunshine intensity measurements at present are made regularly at three stations: Table Mountain, California (about 60 miles northwest of San Bernardino); Albuquerque, New Mexico; and Tucson, Arizona. The records from the first two of these stations have been regularly published (8:p.26) for some time, and serve as a basis for engineering estimates for other locations. Typical values for 1955 are shown in Fig. 15. The Table Mountain station is located at an elevation of 7500 feet in a clear mountainous area. Direct sunshine intensities reported from this station can be taken as typical of those which might be expected at a furnace site chosen predominantly for high sunshine intensities. The Albuquerque pyrheliometric station is located at the city airport. Although the elevation is 5500 feet (which is favorable to obtaining relatively high solar intensities) the location is noticeably dusty and occasionally somewhat smoky. It is believed that sunshine intensities at least as high as those found at this station can be expected in most of the valley areas of the Southwest. In the clearer valley areas direct sunshine intensities

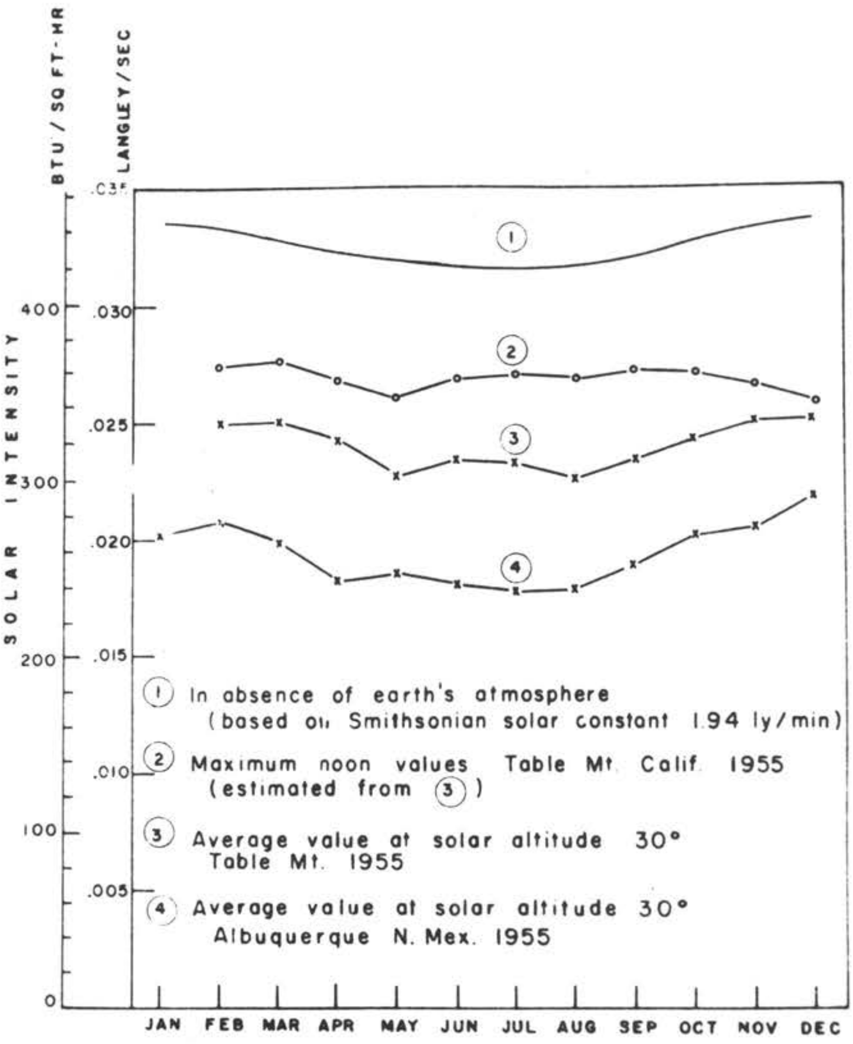

FIGURE 15

TYPICAL MEASURED DIRECT SUNSHINE INTENSITIES somewhat higher than those reported from Albuquerque can probably be expected fairly regularly.

Based on Fig. 15 and similar data, the following are considered to be reasonable engineering estimates of working values of direct sunshine intensities to be expected in the southwest (8:p.26):

High-elevation mountain-area locations chosen primarily for high solar intensities:

Occasional peak value . . . . 360 Btu/sq.ft-hr.

Working value which can be regularly expected . . . . 320 Btu/sq.ft-hr.

Average southwestern location:

Working value which can be regularly expected (and fairly often exceeded). . . . 260 Btu/sq.ft-hr.

Due to the unavailability of data pertaining specifically to Corvallis, Oregon, the solar radiation intensity of 260 Btu/sq.ft-hr. corresponding to average southwestern locations is assumed to apply fairly well for such a western Oregon location during favorable periods.

The "best" working location for a solar furnace is of course not necessarily simply the one with the highest intensity of direct sunshine. Conditions of cloudiness and convenient accessibility must also be considered.

In addition to estimating direct sunshine intensity at the site, it is necessary in estimating maximum attainable temperatures to consider the concentration ratio of the furnace, and the solar absorptivity and the emissivity of the sample under test.

In many cases it is reasonable to assume that the sample will lie within the hot spot at the focal plane and that by far the largest portion of the sample heat loss will be by radiation from the front (assumed plane) face of the sample. In such a case incoming sunshine heat gain may be equated to outgoing radiation loss:

$$\alpha_r \; C_a \, q_i = \epsilon \sigma \; T^4 \qquad (19)$$

or solving for T:

$$T = \left(\frac{\alpha_r \; C_a \; q_i}{\epsilon \sigma} \right)^{1/4} \qquad (20)$$

If the further assumption is made that the sample absorptivity is equal to its emissivity, the equation becomes:

$$T = \left(\frac{C_a \;\; q_i}{\sigma} \right)^{1/4} \qquad (21)$$

Fig. 16 is a plot of the above equation. It

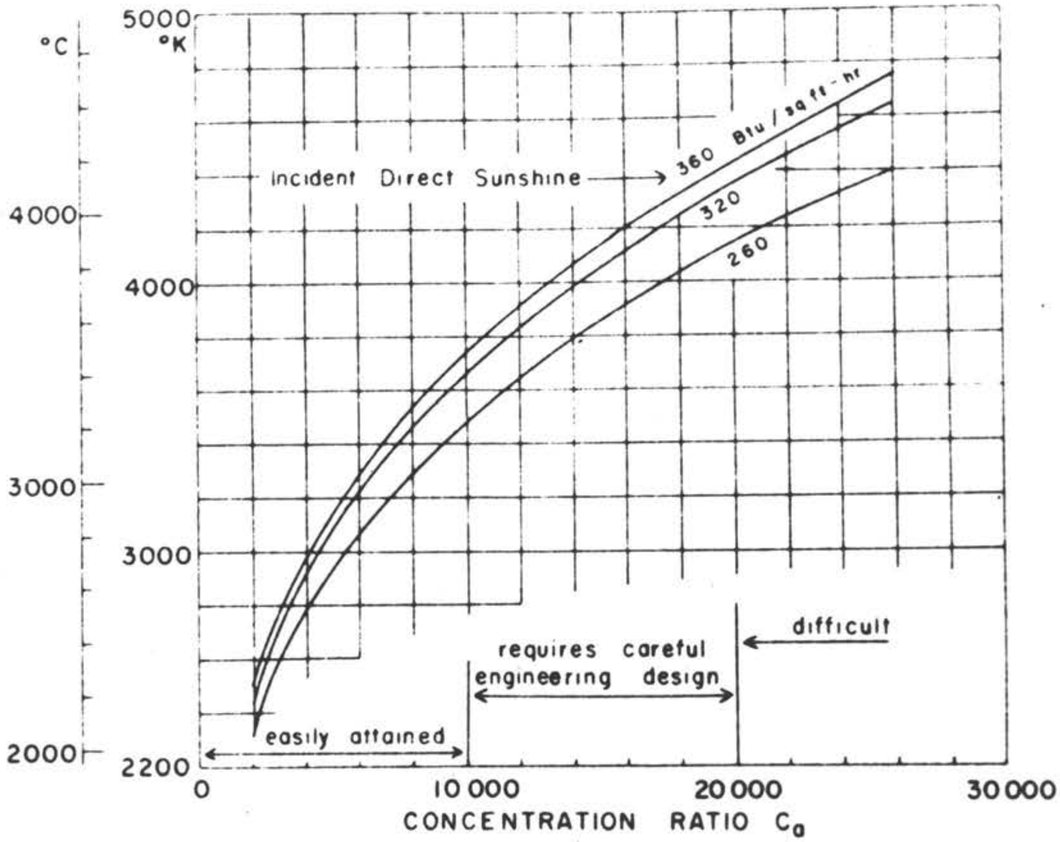

FIGURE 16

MAXIMUM TEMPERATURES ATTAINABLE IN SOLAR FURNACES

presents a good approximation to the maximum temperatures attainable by samples at the hot spot in the focal plane of a solar furnace.

The assumption that absorptivity is equal to emissivity is exactly true if the sample temperature is equal to the source temperature. It tends to be approximately true in case of solar furnace samples operating at a very high temperature, as such samples are approaching (very roughly) the apparent temperature of the sun. Also, in defense of the approximation involved in determining sample temperature through the assumption that absorptivity is equal to emissivity, it is to be noted that the fourth-power relationship in equation (20) is such that a given percentage error in the ratio α_r/ϵ will produce only about one-fourth as large a percentage error in the value of T (8:p.27). All in all, this equation gives an estimate of the maximum temperatures attainable both by many types of samples placed at the hot spot of a furnace and by blackbody cavities opening to the hot spot.

It will be noted from Fig. 14 that solar furnace concentration ratios of 20,000 or over appear practicably attainable, and from Fig. 16, it appears that such concentration ratios should produce maximum temperatures in excess of 4,000 C. Concentration ratios and temperatures of this magnitude have not been reported for any present solar furnace. Such temperatures might be attained with a solar furnace, provided that great care is taken in designing the furnace to the necessarily high furnace factor.

Flux Distribution Near The Focal Plane

An important consideration in the operation of a solar furnace is the required accuracy in positioning the sample into the exact focus of the paraboloidal concentrator in order to obtain maximum target temperatures. Another consideration is the possibility of purposely defocusing the sample to control the insolational intensity and, hence, the sample temperature. A knowledge of the heat flux near the focal plane enables one to evaluate these operational aspects of a solar furnace.

Fig. 17 (19:p.96) shows the flux distribution for planes parallel to and near the focal plane of a paraboloidal concentrator having a rim angle of 60°, where the distances, y, δ, and d, are defined in Fig. 18 and Table 3.

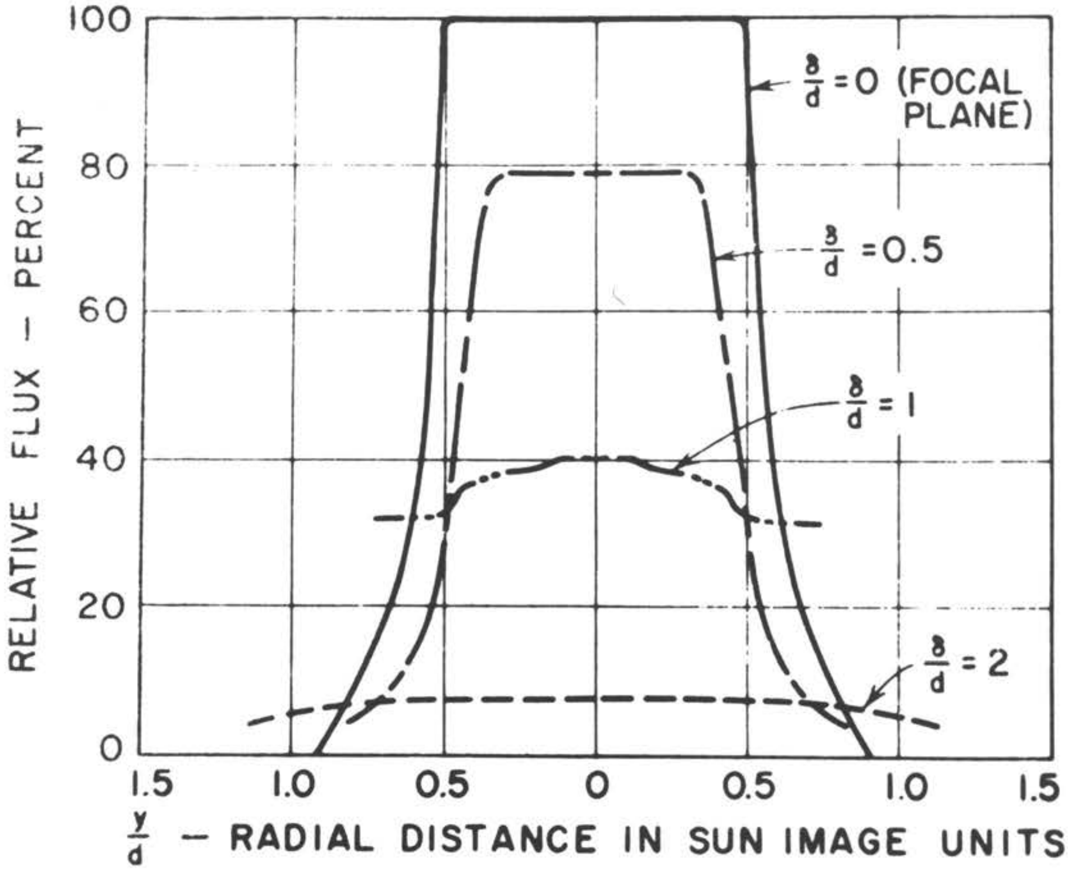

FIGURE 17

FLUX DISTRIBUTION IN AND NEAR THE FOCAL PLANE

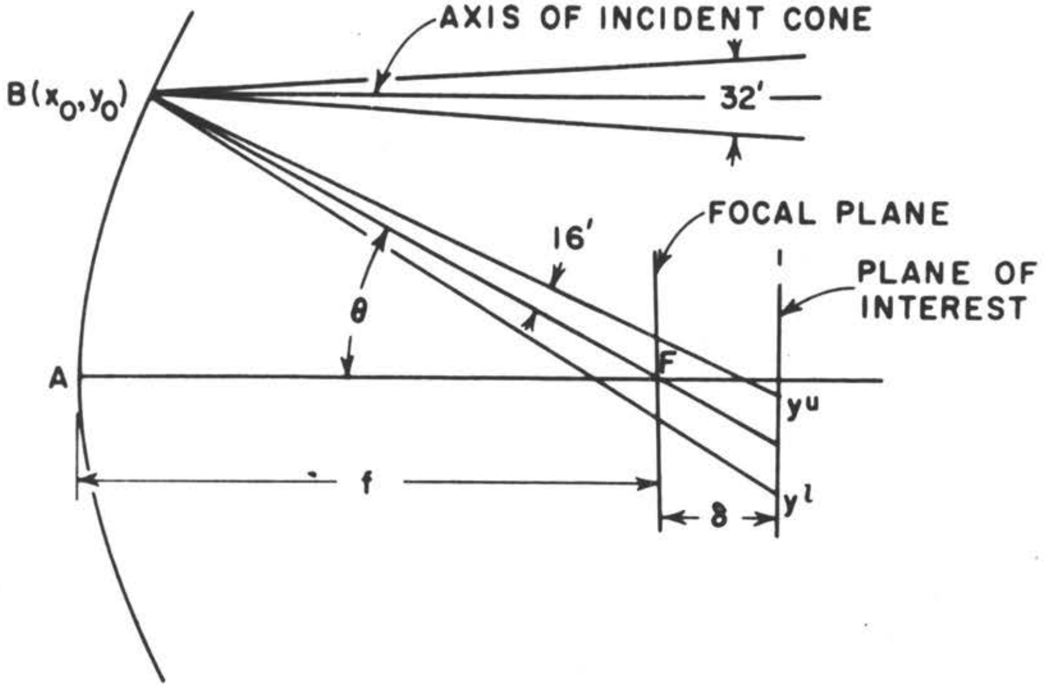

FIGURE 18

TARGET PARALLEL TO FOCAL PLANE

In Fig. 19, the equilibrium temperature attainable by a black body losing energy only by radiation from its face is depicted for furnace factors, F, of 1.00 and 0.51 (19:p.97).

A few remarks concerning Fig. 19 are in order. First, the rapid decrease of the temperature which a target can attain when it is moved from the focal plane by a distance of one sun image diameter should be noticed. Although this distance is only approximately 0.242 inches for a 60 inch, 60^{o} rim angle solar furnace, compared with a focal length for the furnace of 26 inches, the attainable target temperature decreases by about 1,000^{o}C when the target is moved this much off focus. Second, from the shape of the curve it can be seen that in order to obtain a temperature within 5 per cent of the maximum attainable temperature, the target must be placed within a distance of approximately one-half sun image diameter from the focal plane, which in this case is approximately 0.121 inches. It should be noted that the area of maximum heat flux decreases noticeably when the target is displaced even by this amount. Also, for furnaces of smaller sizes, the size of the sun image decreases, and therefore these distances decrease.

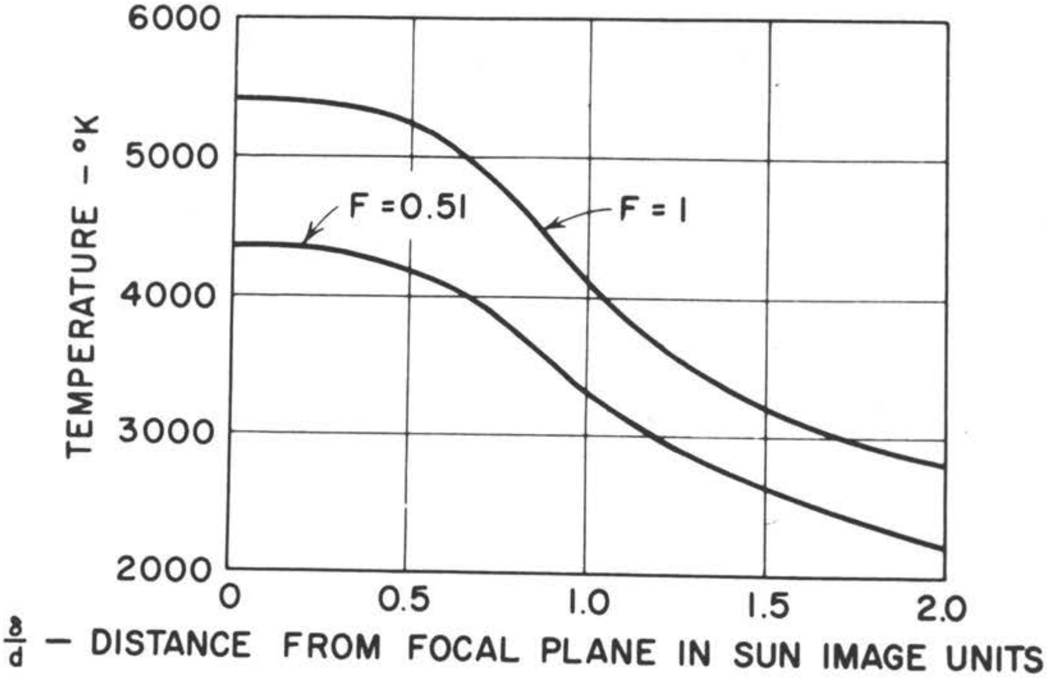

FIGURE 19

VARIATION OF MAXIMUM ATTAINABLE TEMPERATURES WITH DISTANCE FROM THE FOCAL PLANE

OVERALL DESIGN CONSIDERATIONS FOR THE OREGON STATE COLLEGE SOLAR FURNACE

The Oregon State College solar furnace project was initiated in an effort to obtain a source of high-temperature heat, free from the contaminants associated with more common high-temperature sources such as flames and electric arcs. This freedom from contamination was desired for high-temperature studies of systems which are very sensitive to the presence of contaminants.

In particular it was desired to be able to melt and attempt zone refining and growth of macro-sized crystals of elemental boron. A very inert environment is required for any high temperature studies of elemental boron since at elevated temperatures it combines readily with oxygen, nitrogen, carbon, and refractory metal vapors, etc. The solar furnace is able to provide such integrity of atmospheric environment through the use of a glass envelope around the sample. This envelope can be evacuated or filled with an inert gas as conditions warrant.

To insure that no contaminants are introduced into a sample being melted from the vessel containing the melt, the sample was made to provide its own melt containment. To achieve this end the paraboloidal concentrator mirror is mounted with its axis vertical, facing downward. The rays of radiant energy are thus directed to a spot on the upper face of a sample mounted at the focus as shown in Fig. 3. When the material at the focus is fused the melt is contained by the cooler, unfused material surrounding the focal "hot spot".

The sun's rays are directed up into the paraboloidal reflector by a diagonally inclined plane mirror placed beneath it. The sun's rays are directed onto the inclined plane mirror by a moveable plane mirror, the heliostat, as shown in Fig. 3.

This three-mirror design has the disadvantage of having greater reflective and transmissive radiant energy losses and, hence, lower maximum attainable temperatures than the more common one and two mirror furnaces. It was felt, however, that the ease of sample containment provided by this type of furnace when compared with such complexities as spinning "hohlraum" cavities (55:p.153), and pressed buttons mounted on refractory rods (41:p.27), which are inherent in any liquid phase studies using concentrators that do not converge downward onto the sample, more than compensates for this slight lowering of the maximum attainable temperature.

The geometric layout of the solar furnace is shown in Fig. 20. This furnace layout was inspired by that of the solar furnace built and operated by W. M. Tuddenham of the Kennecott Copper Co. in Salt Lake City, Utah. This

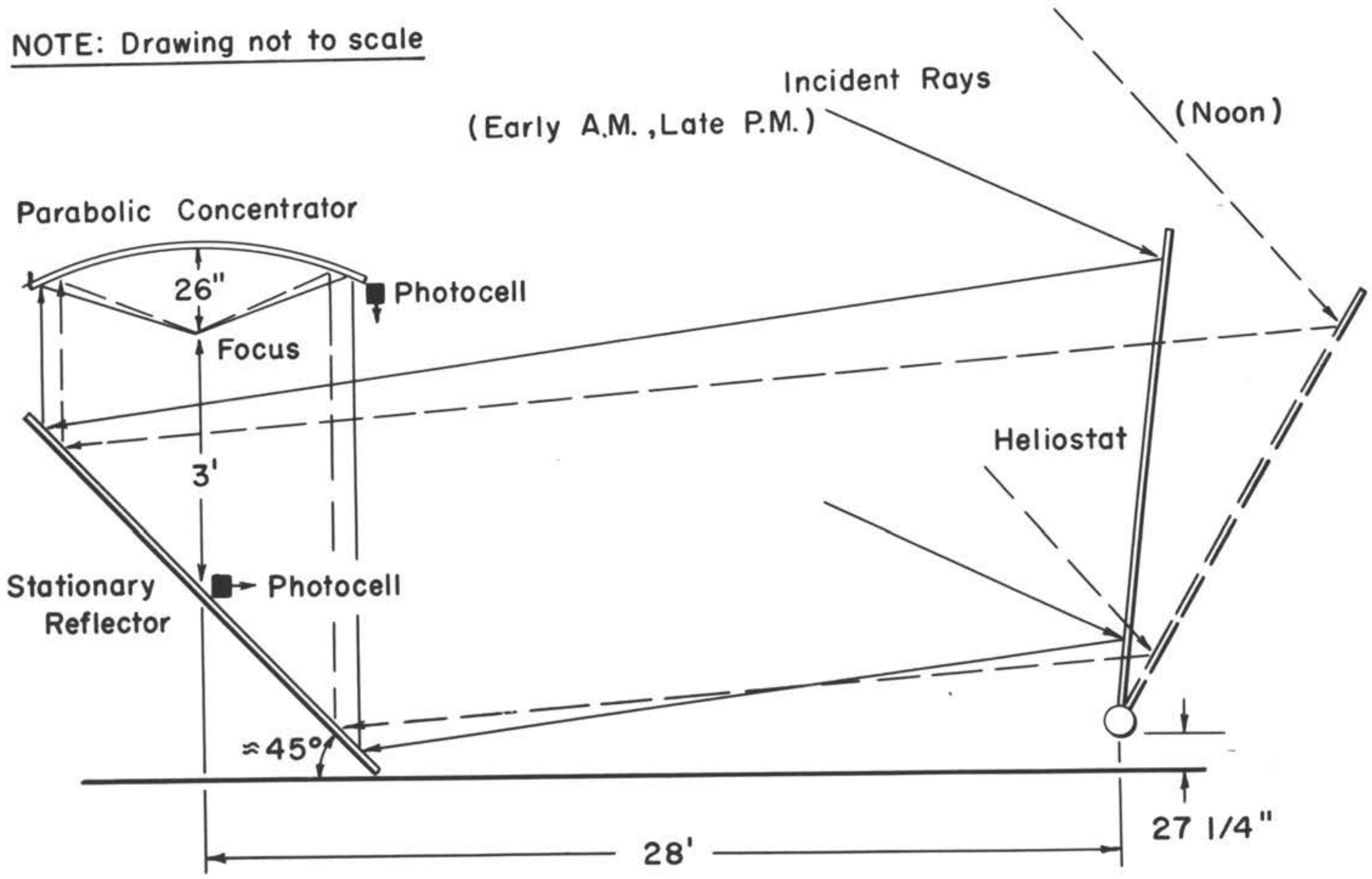

FIGURE 20

GEOMETRICAL CONFIGURATION OF THE OREGON STATE COLLEGE SOLAR FURNACE

furnace is not, however, a direct copy. The engineering of individual components is markedly different in most cases. This is due to several causes: an effort was made to improve shortcomings in the original as acknowledged by Tuddenham et al, wherever possible materials already possessed by the college were utilized, and, perhaps most importantly, an exact copy was not desirable since little design and development experience could be gained from such a project even if detailed plans had been available.

The use of only one plane mirror, a moveable heliostat, directing the solar rays up into a paraboloidal concentrator mounted horizontally on a tower as in Fig. 2 was rejected due to the safety hazard and the extensive construction required.

The solar furnace is located on the roof of the Oregon State College Chemical Engineering Building. This location was the only logical choice in that no other available space was suitable. In this location the sun's rays have unobstructed access to the solar furnace heliostat after mid-morning and until late afternoon in the spring, summer, and early fall. In the winter the heliostat would be partially shadowed by the penthouse and the solar furnace building except when very near zenith. In actual use, however, the sun's rays are always unobstructed during the times when solar intensities are great enough to achieve high temperatures, i.e. the four or five hours during the middle of clear spring, summer, and early fall days. Due to the western Oregon climate the solar furnace has not been operated during the late fall and winter months.

DESIGN AND CONSTRUCTION OF SOLAR FURNACE COMPONENTS

The Oregon State College solar furnace has as a nucleus a war surplus searchlight. The paraboloidal reflector of the searchlight serves as the basic construction element of the solar furnace, the concentrator. The yoke which supported the searchlight and provided freedom of rotation about horizontal and vertical axes now performs a similar function for the heliostat. The arc support pylon now supports the sample holder array. To these, other materials have been added to form the various components which make up the solar furnace. The function design and construction of each of these components are individually discussed in the ensuing sections.

CONCENTRATOR

The paraboloidal reflector of the searchlight which serves to focus the rays of the sun onto the sample is made of rhodium plated electroformed copper. It is 60 inches in diameter, has a focal length of 26 inches, a rim angle of 60° and is mounted in a cast aluminum housing. The optics of this paraboloidal mirror are discussed further in the appendix.

The cast aluminum mirror housing is mounted on a platform constructed of 4 inch boiler tubing uprights, 1 inch black iron pipe cross braces and 4 inch I-beam cross beams. All parts are joined by electric arc welds. The rim of the aluminum housing is thus supported about 6 feet off the floor. The mirror rim is about 18 inches above the rim of the housing or some 8.5 feet above the floor. A photograph taken during an early stage of construction is shown in Fig. 21.

The rectangular hole which can be seen in Fig. 21 was cut in the cast aluminum housing to provide operator access to the focal spot for sample loading and unloading purposes. A counter adjacent to this hole has been fabricated of plywood to provide a working area for preparation and loading of samples.

A stand which allows the operator easy access to the working area is shown in Fig. 22. This stand is about 3 feet high with 18 inch side boards to prevent dropped tools, etc. from bouncing onto the stationary mirror and to minimize the possibility of the operator inadvertently stepping off an end of the platform. It is constructed of plywood paneling mounted on a framework welded up of $1\frac{1}{2}$ inch angle iron. A shelf beneath the operators footboard supports the gas system vacuum pump.

STATIONARY REFLECTOR

The diagonally inclined stationary mirror redirects

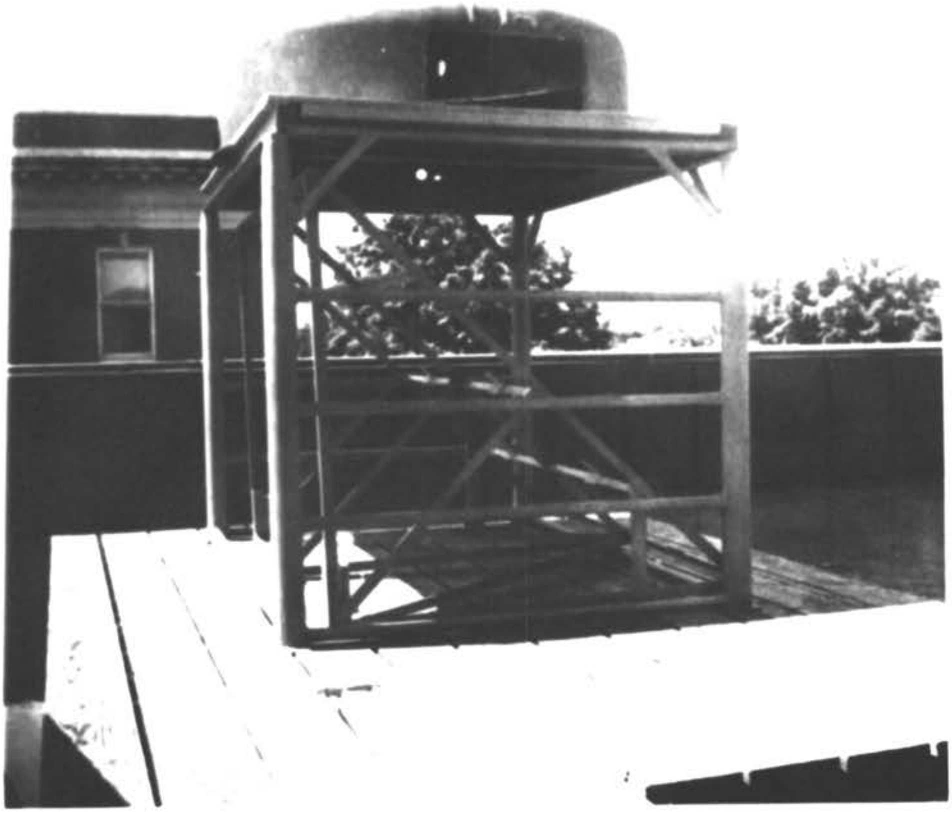

FIGURE 21

CONCENTRATOR HOUSING AND SUPPORT PLATFORM

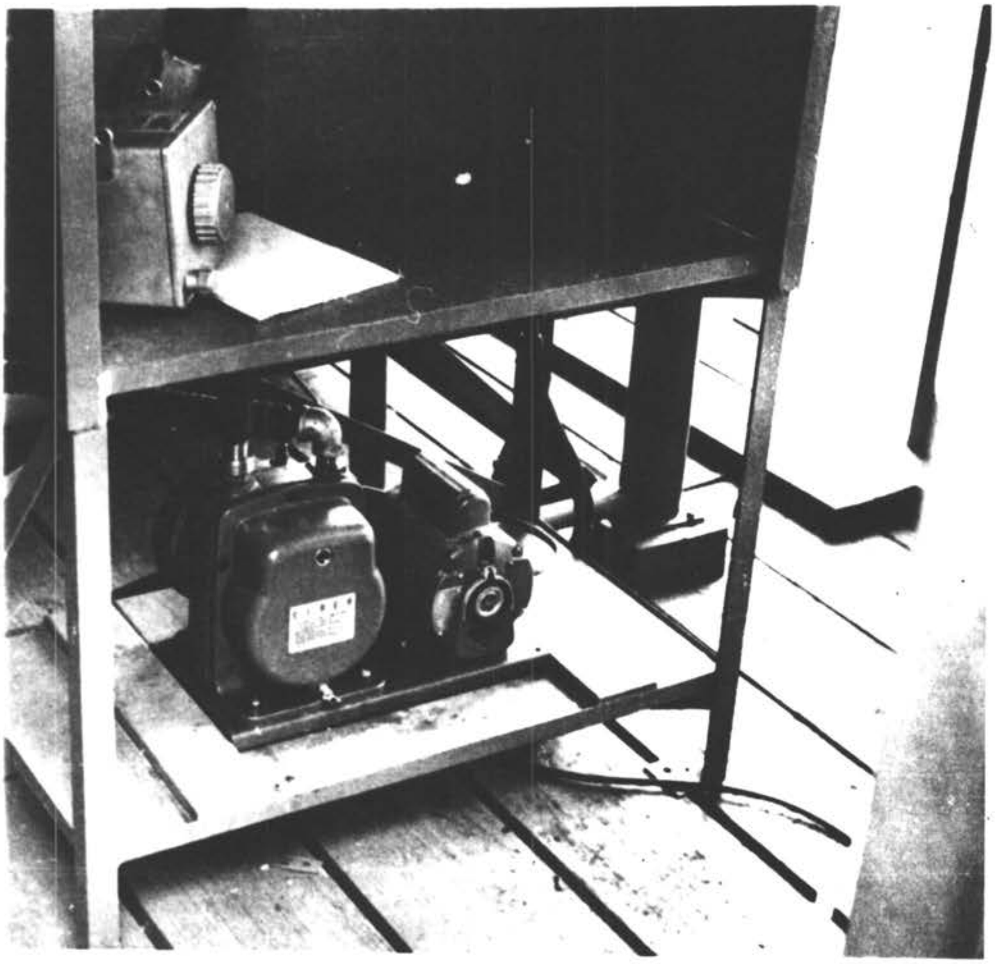

FIGURE 22

OPERATOR STAND AND VACUUM PUMP SHELF

the solar radiation being reflected to it from the heliostat up into the paraboloidal concentrator as shown in Fig. 20. It is diagonally inclined to the horizontal at an angle of about 45^o. If its base edge and that of the heliostat were on the same level, the angle of inclination would be 45^o. Since the heliostat base edge is the higher of the two, the angle of inclination required to reflect the sun's rays vertically is slightly less than 45^o. Adjustment of this angle of inclination is afforded by adjustable length legs formed of concentric pipes with locking bolts for fixing their relative positions.

The oval superimposed upon the schematic representation of the face of the stationary reflector in Fig. 23 represents the projection of the rim of the 5 feet diameter concentrator mirror upon the stationary reflector. The mirror segments which fall all or partly into this oval are thus the only ones which contribute to the reflection of radiant energy which ultimately arrives at the focus. The light reflected from peripheral positions of the paraboloidal reflector is less effective on a flat target than that reflected from near the center of the paraboloidal mirror due to the variations in flux distribution density in the focal plane as described in the section, Derivation of Equation of Perfect Paraboloid Concentration Ratio. Thus sections of the diagonal

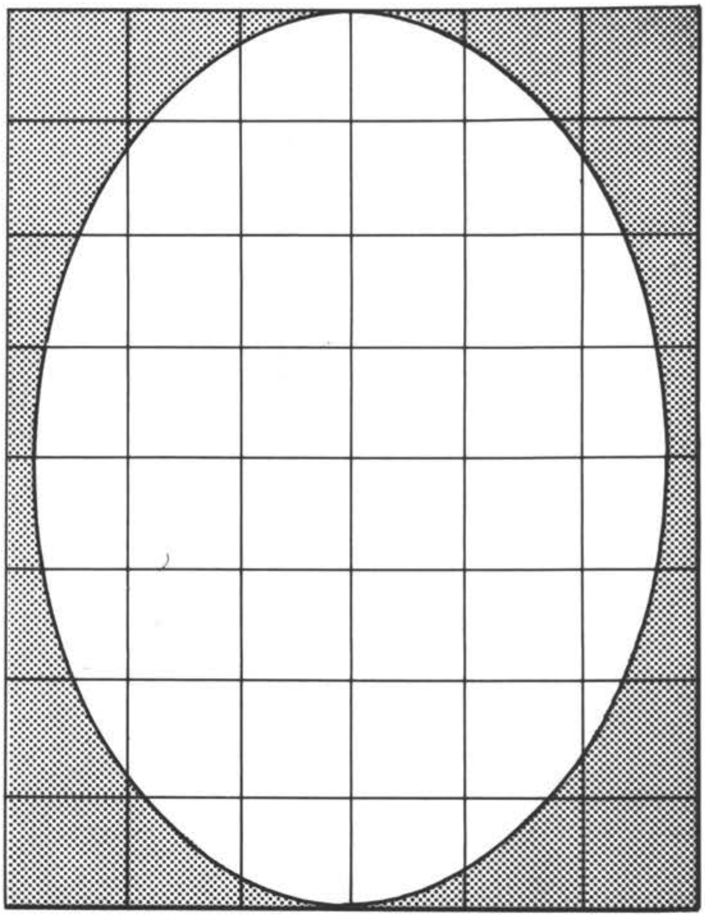

FIGURE 23

MIRROR SEGMENTS IN STATIONARY REFLECTOR WITH IMPORTANT SECTIONS INDICATED BY OVAL ENVELOPE reflector which correspond to peripheral portions of the paraboloidal reflector make lesser contributions to the concentration of radiant energy in the focal spot proper than do those sections corresponding to inner portions of the paraboloidal mirror. In order to optimize the performance obtainable with the considerably non-planar plate glass mirrors at hand, those having lesser deviations from planarity were placed in center positions, and those having progressively greater deviations from planarity were placed progressively farther from the center positions.

The present design of the stationary reflector as described here is quite different than the original design as regards the mirror segments and their mountings. The original design and an interim "pilot" stage of the present design are described in the Appendix.

The basic triangular truss framework of the mirror supporting structure can be seen in Fig. 21. It is constructed of all welded $1\frac{1}{2}$ inch angle iron. To this basic framework an auxiliary flat, flexible framework of $\frac{1}{2}$ inch by $1\frac{1}{2}$ inch channel iron is fastened with counter sunk stove bolts at frequent intervals. The basic framework provides rigid support to the light auxiliary framework which is made approximately planar by the use of shims under the attachment stove bolts.

The slight remaining deviations from planarity are within the adjustment range of the mirror mounting bolts.

The mirror segments are mounted at three points as shown in Fig. 24. The stainless steel mounting bolts and springs and their geometry are also illustrated in Fig. 24. The three tapered helical springs supporting each mirror segment allow ready adjustment of height and angles of the mirror segment relative to the framework by turning of the mounting bolts within the threaded mounting holes in the auxiliary framework. The final adjustment to co-planarity of the mirror segments is discussed further in the section Alignment Adjustments of the Planar Mirrors. The mirrors of both this reflector and the heliostat are Double O parallel ground plate glass, back silvered, $\frac{1}{4}$ inch thick.

HELIOSTAT

A heliostat of the altazimuth type which is to reflect the solar rays onto the stationary reflector and hence into the paraboloidal concentrator must continuously vary its angle to the horizontal, or altitude angle, and to the north-south plane, or azimuth angle, as the sun traverses the sky. A

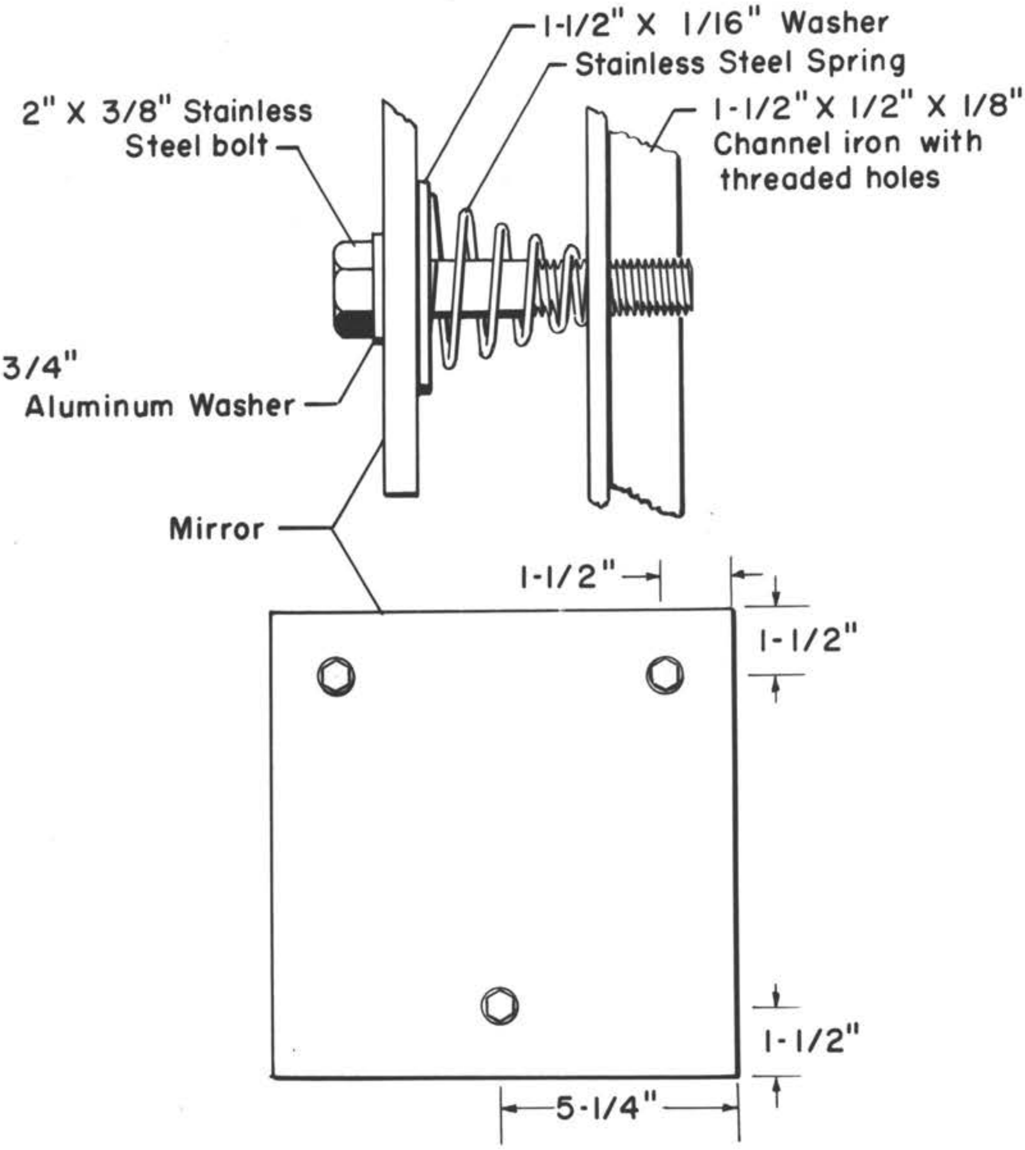

FIGURE 24

MOUNTING OF MIRROR SEGMENTS

discussion of this altazimuth mounting as contrasted to the equatorial type is given in the section, Geometrical Configuration. This continual variation of altitude and azimuthal angles, generally referred to as tracking, is approximated in the Oregon State College solar furnace by changing these angles in small increments throughout the period of furnace operation.

Two electric motors, controlled independently by two photocell radiant energy sensors, drive the heliostat through these small incremental changes of altitude and azimuth angles when they are periodically energized by the photocell relay circuits. In this manner the directions of the solar rays reflected from the heliostat are held approximately constant and, hence, the position of the focal spot remains essentially stationary during extended periods of operation.

The solar disc achieves a minimum declination of 18 °at the Corvallis latitude at zenith on June 21, as can be readily ascertained from any standard navigational tables. In order to direct the solar rays onto the diagonally inclined mirror the heliostat must at that time be tilted to an angle of 54° from the horizontal. When the sun is near the horizon the heliostat must be in a near vertical position in order to direct the solar radiation into the solar furnace proper. All other times will require altitude angles between 54° and 90°.

The heliostat, therefore, has been made capable of being depressed to altitude angles of less than 54° and elevated to somewhat over 90°. The heliostat can be rotated from azimuth angles of 90° (due east) through 180° (due south) to 270° (due west). In actual use, however, the heliostat is never operated more than 45° either side of due south and only rarely is it necessary to orient the heliostat more than about 20° either side of due south. This is due to the fact that the sun's apparent horizontal position is never north of due east or north of due west of the solar furnace. Further, during the hours when solar intensities are at useable levels, the sun's apparent horizontal position is usually within 45° of either side of south requiring only 22½° azimuth angles either side of south in order to direct the solar radiation onto the diagonally inclined plane mirror.

The distorted oval envelope superimposed on the schematic diagram of the face of the heliostat mirror, Fig. 25, encloses the areas which reflect ultimately into the paraboloidal concentrator mirror for maximum azimuth angles of 22½° east and west of due south and

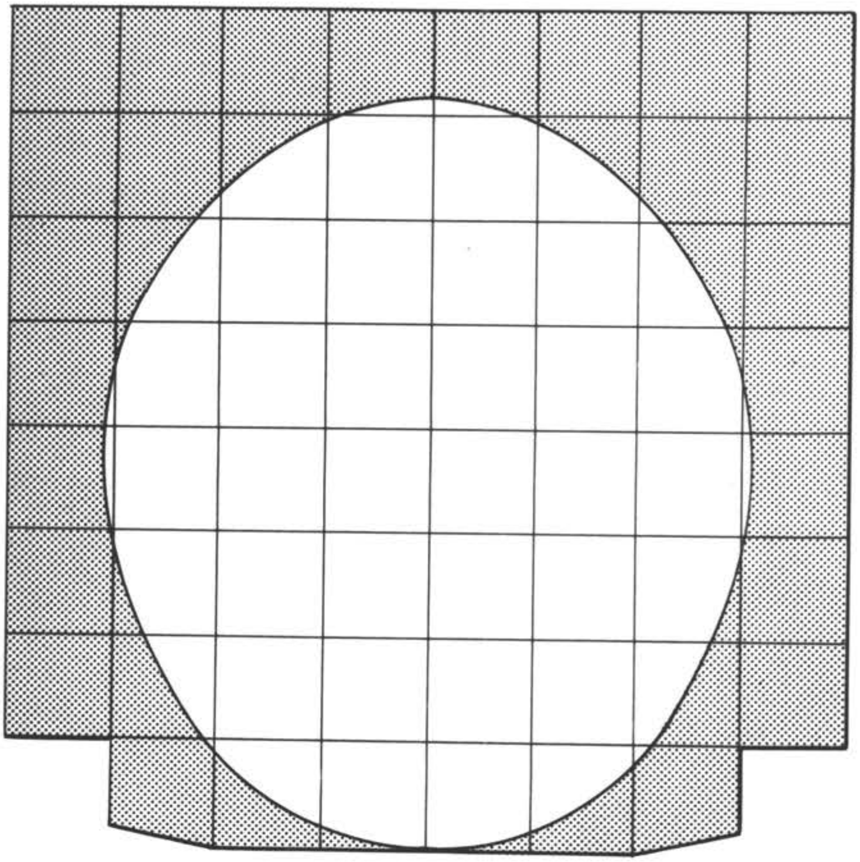

FIGURE 25

MIRROR SEGMENTS IN HELIOSTAT
WITH IMPORTANT SECTIONS INDICATED BY
OVAL ENVELOPE

for altitude angles of 54° to 90°. Here, as in the stationary reflector, the mirrors have been graded with the best mirrors placed near the center and with increasingly non-planar mirrors placed progressively nearer the periphery of the envelope.

The heliostat framework is like that of the stationary mirror in that it consists of two units, a rigid supporting framework to which is attached a lighter leveling framework. The rigid framework is shown in Fig. 26. It is welded up of $1\frac{1}{2}$ inch angle iron with 1 inch strap iron tension braces. The auxiliary framework is welded up of $1\frac{1}{2}$ inch by $\frac{1}{2}$ inch channel iron, it is attached to the rigid framework, and the mirrors are attached to it just as they are in the stationary reflector. These are shown in Fig. 27 and 28.

The heliostat pivots about an axis drawn vertically through the center of the bottom edge of the face and about an axis drawn horizontally through the bottom edge of the mirror face. The rotating base of the searchlight provides the vertical axis. To this base a 6 inch I-beam is affixed with 6 inch risers at its ends supporting the axis pivots. These pivots are from the searchlight and were originally mounted on the ends of the yoke arms and into the cast aluminum mirror housing.

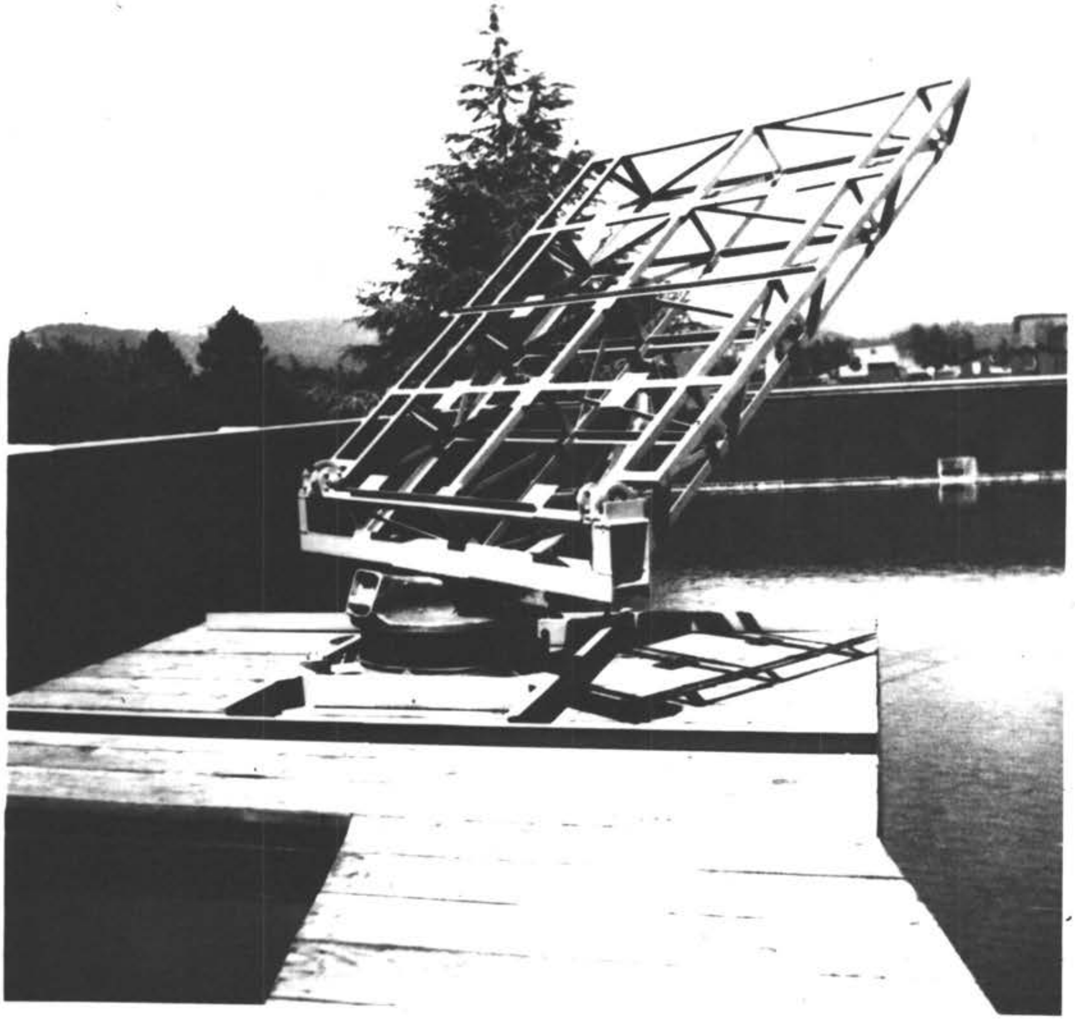

FIGURE 26

HELIOSTAT BASIC FRAMEWORK

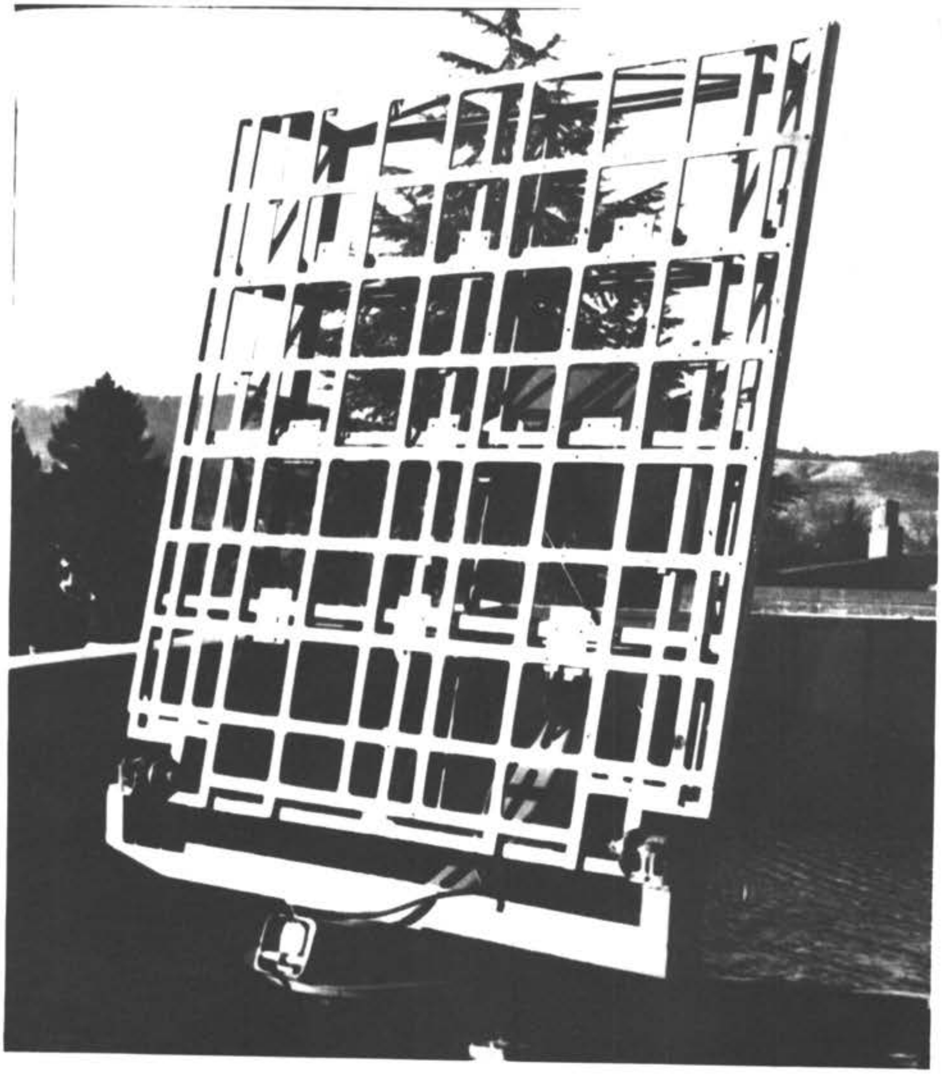

FIGURE 27

AUXILIARY FRAMEWORK MOUNTED ON HELIOSTAT

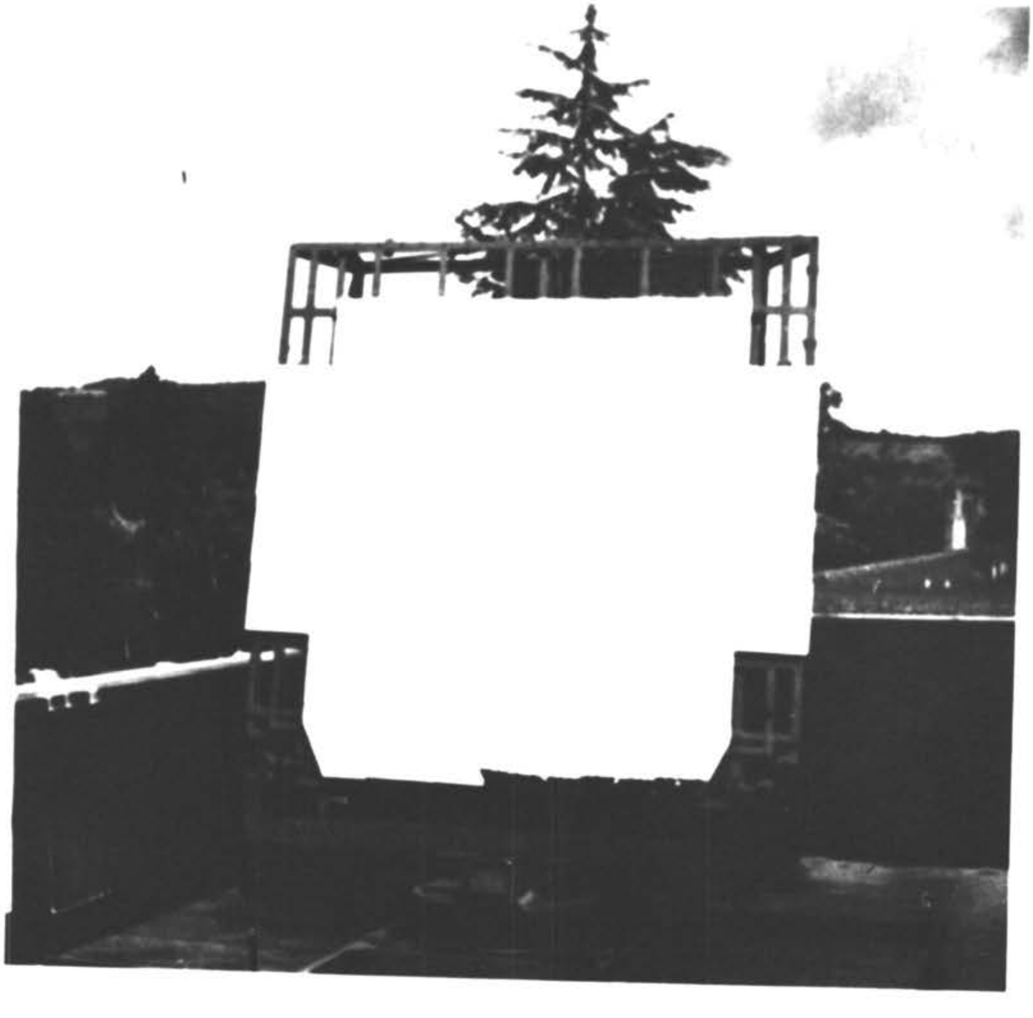

FIGURE 28

MIRRORS IN PLACE ON HELIOSTAT

The heliostat is supported at various altitude angles by a bronze screw affixed with pivots to the center back of the heliostat framework and turning in a pivoted nut. The pivots for the nut are affixed to one of the arms of the original yoke which has been shortened somewhat to allow the heliostat to be depressed sufficiently. The other yoke arm has been cut off near the platform. The bronze screw is turned by a gear reducer, sprocket-chain, and V-belt drive mechanism driven by a 1/3 HP electric motor which is remotely reversible. Azimuthal movement is provided by a $\frac{1}{4}$ HP non-reversing electric motor and gear reducer driving the mirror about the vertical axis from east to west through the original worm gear drive of the searchlight.

A reversing motor is required for the altitude drive since the sun travels two directions in the vertical plane during the course of a day's operation. During the AM while the sun is ascending, the altitude angle must decrease, and in the PM when the sun is descending, the altitude angle must increase in order to reflect the sun's rays in a near horizontal plane. However, the azimuthal drive is always from east to west during operation; so no remote reversing of this drive is necessary. At the beginning of a run, the operator can position the heliostat in an eastward setting by manually disengaging the drive gear, turning the heliostat, and re-engaging the drive gear. These drive motors are discussed further from an electric circuitry point of view in subsequent sub-sections.

PHOTOCELL TRACKING CONTROLS

The two photocells which are used as radiant energy sensors for controlling the altazimuth drive motors are inexpensive units normally used for switching on household lights as darkness descends and turning them off again at sunrise. The units are of the model, Fisher-Pierce Nightlighter. They have a switching capacity of 300 watts and sell for only $10.94. Since 300 watts is inadequate to start the drive motors, the photoswitches (photocell driven relays) are used to trip heavier power relays which actually do the switching of the drive motor circuits.

The altitude angle controlling photoswitch is mounted in the front of the cast aluminum paraboloidal mirror housing as shown in Fig. 29. From this position the sensitive element "sees" the bottom edge of the heliostat. In operation the photoswitch is opened when the edge of the beam of sunlight coming from the heliostat strikes the photo-sensitive element and is closed

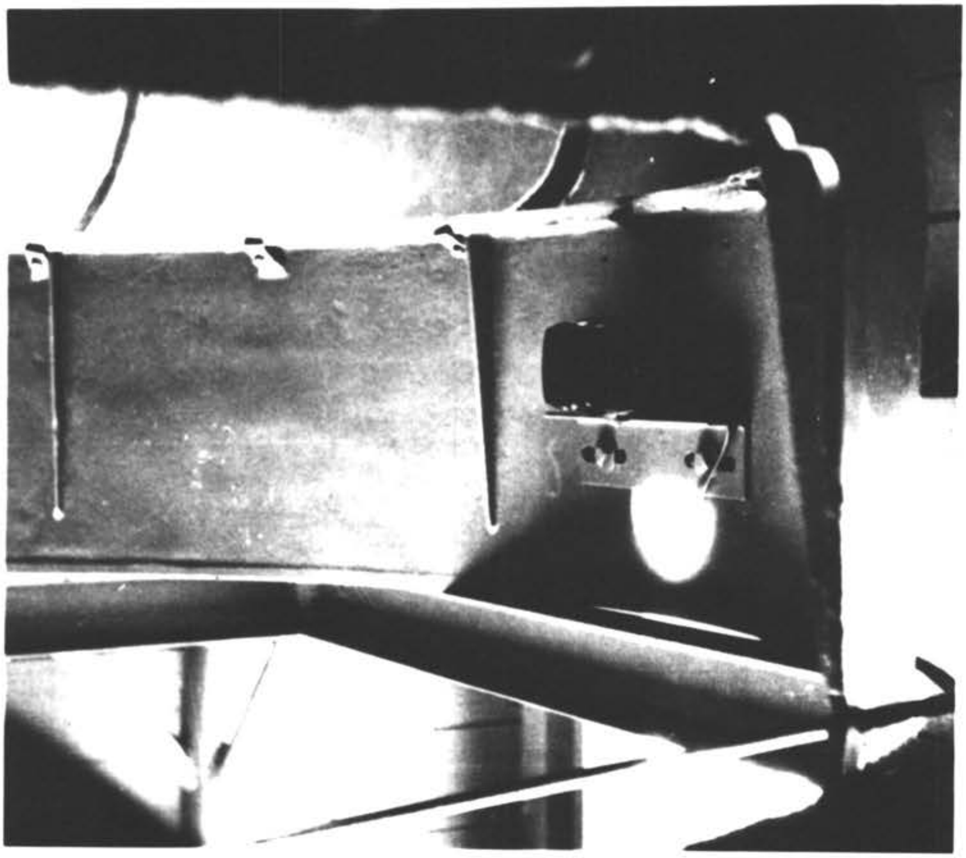

FIGURE 29
ALTITUDE CONTROL PHOTOCELL

when the edge of the beam is not impinging upon the photo-sensitive element.

In order that the photocell be sensitive to the presence or absence of direct insolation, its aperture must be reduced to only a very narrow slit since the unit as manufactured is normally open even in daylight shadow. This reduction of aperture is accomplished by means of black electrical tape. This tape allows ready adjustment of the aperture as needed to fit the needs of the day. For very bright clear days, a minimum aperture is used; whereas, if operation is desired on hazy days or near the end of clear days, then the aperture must be increased.

In the morning as the sun is ascending, its angle relative to the face of the heliostat is decreasing. This causes the bottom edge of the reflected beam to be lowered. This lowering of the beam edge appears ultimately at the photocell as a displacement of the beam edge across the sensing element. As this beam edge strikes the aperture slit, which is parallel to it, the photoswitch is caused to open. This opening of the photoswitch allows a normally closed power relay to actuate the drive motor which lowers the heliostat.

As the heliostat is lowered at a rate such as to raise the bottom edge of the reflected beam of sunlight several times more rapidly than the apparent motion of the solar disc causes it to be lowered, the edge of the beam is caused to retrace its path back across the photocell face and back onto the rim of the paraboloidal concentrator. When the beam edge no longer impinges upon the photocell aperture slit, the photocell is deactivated; the photoswitch is caused to close; the power relay then is opened and the lowering of the heliostat ceases. The heliostat remains at the new altitude angle until the motion of the sun causes the photocell to be once again actuated. The period of a complete electrical cycle is usually about 1 minute, varying somewhat with the time of day and aperture slit width. Of this period about 1/3 is devoted to drive on operation and 2/3 to drive off operation. No vibration of the heliostat is apparent at the focus when the altitude drive motor is running.

For afternoon operation the sequence used in the morning must be reversed. Switches at the control panel, see Operating Procedure with the Solar Furnace, are provided for performing this reversal. As the sun descends, the lower edge of the reflected beam is raised and after reflection by the stationary planer mirror is displaced away from the photocell aperture slit towards the center of the paraboloidal concentrator mirror. As the beam edge ceases to impinge upon the aperture slit, the photoswitch closes and completes a circuit through the coil of a normally open power relay which is thereby caused to close. The drive motor then begins to raise the heliostat to a higher altitude angle which causes the edge of the reflected light beam to re-impinge upon the photocell aperture slit and thus to stop the upward movement of the heliostat until the sun's apparent motion initiates a repetition of the whole process. The exact point at which the switch over from AM to PM operation is performed is not critical since the apparent rate of vertical displacement of the solar disc when very near zenith is extremely slight.

The azimuth angle controlling circuitry is much less complex than that of the altitude control since movement in only one direction, east to west, is necessary by remote control. At the end of a day's operation the operator manually returns the heliostat to any desired position by disengaging the drive pinion, turning the heliostat, and re-engaging the drive pinion by means of a lever in the base of the heliostat near the azimuth drive motor.

The azimuth angle controlling photocell is shown in Fig. 30. A schematic drawing of its operation is shown in Fig. 31. Here, as with the altitude angle controlling

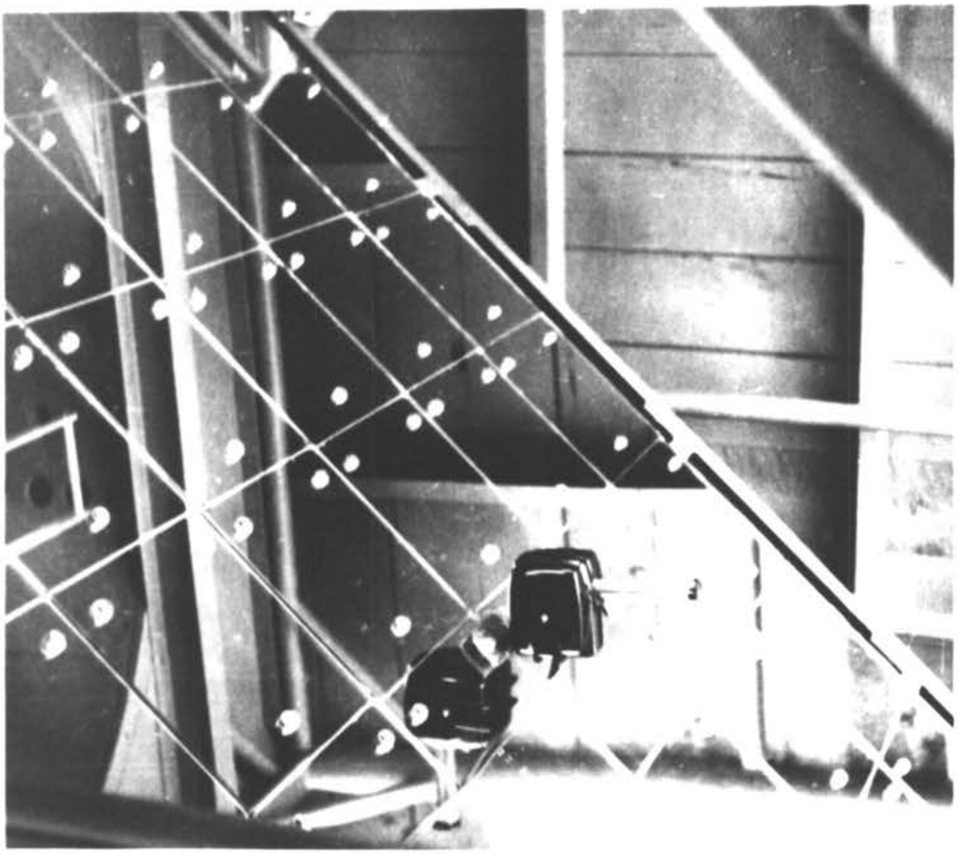

FIGURE 30

AZIMUTH CONTROL PHOTOCELL

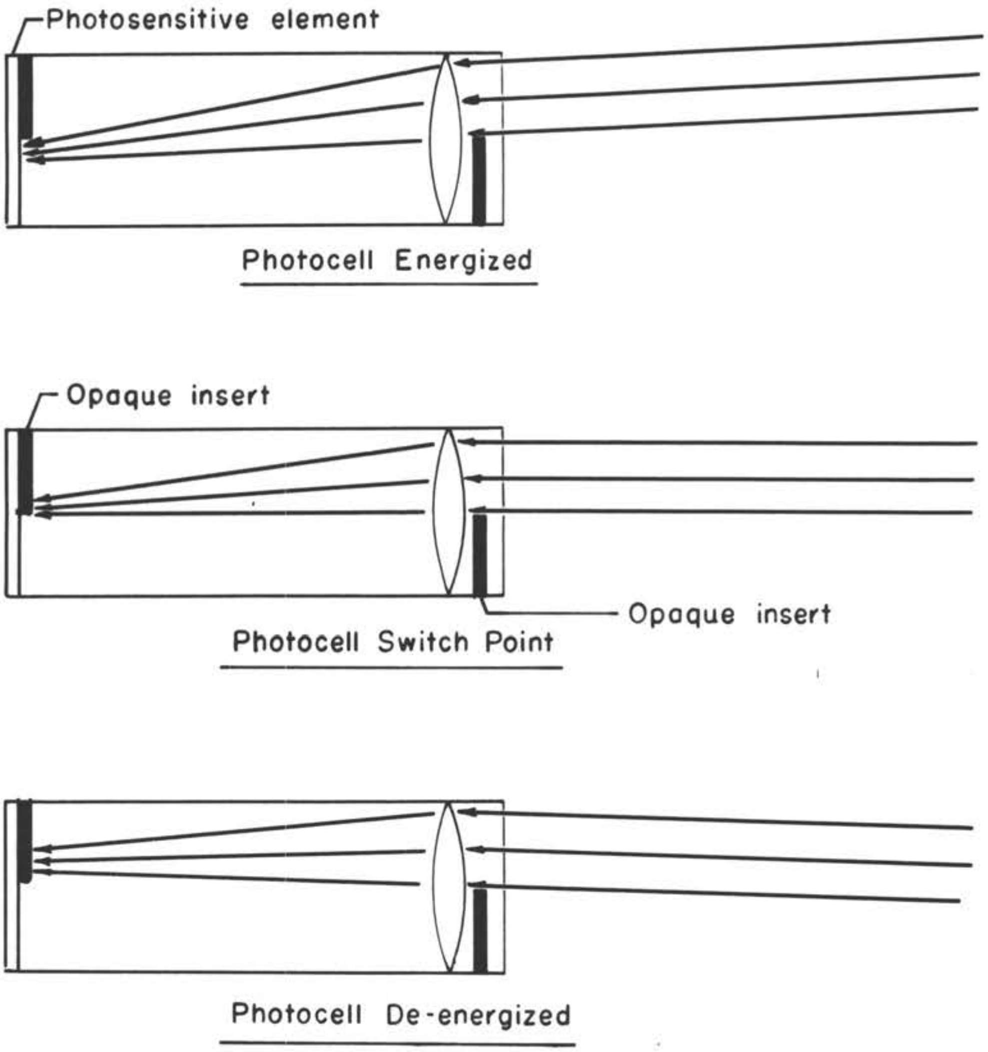

FIGURE 31

OPERATION OF AZIMUTH PHOTOCELL

photocell, sensitivity adjustments are made by varying the slit width or effective aperture. This present system represents an improvement in reliability and efficiency over an earlier system which is described in the Appendix. The azimuth angle photocell controls a power relay which in turn controls a $\frac{1}{4}$ HP motor. This motor drives the original searchlight ring gear and pinion-worm gear azimuthal drive mechanism through a V-belt gear reducer system. The gear reducer is attached to the original drive pin with a rubber star coupling.

During operation the sensitivity of the azimuthal control is such that the focal spot moves somewhat less than one third of the focal diameter, i.e. about 2 mm., during each energization of the drive motor. At least part of this movement is caused by excessive play in the original searchlight pinion gear which allows lagging and backlashing while moving the heliostat. Correction of this condition would necessitate such formidable difficulties that it was tolerated for this present study. The deleteriousness of this excessive sideways movement was not apparent although more sensitive future studies may necessitate improving the azimuthal "resolution" of the solar furnace. The "resolution" of the photocell can be made as great as desired by increasing the focal length of the objective lens and the corresponding length of the lens barrel.

SAMPLE HOLDER

The sample holder must provide freedom from atmospheric contamination for the sample as well as freedom of movement of the sample in three dimensions relative to the focal "hot spot" of the solar furnace. Of course, the sample holder must also have some provision for supporting the samples.

In the Oregon State College solar furnace the freedom from atmospheric contamination is provided by a cylindrical glass envelope which can be seen in Figs. 32, 34, and 35. This envelope is simply an 18 inch by 6 inch cylindrical pyrex jar obtained from chemical stores. This jar is closed by an aluminum plate which is attached by draw bolts to a similar plate at the base of the jar. A seal is effected by means of a rubber gasket placed between the aluminum plate and the jar lip. A rubber pad between the base of the jar and the corresponding aluminum plate provides a shock bumpering action. Inlet and exhaust pipes are provided in the aluminum sealing plate. These pipes are connected with flexible hoses to a gas system which shall be discussed separately under the heading Gas System, immediately following this present section.

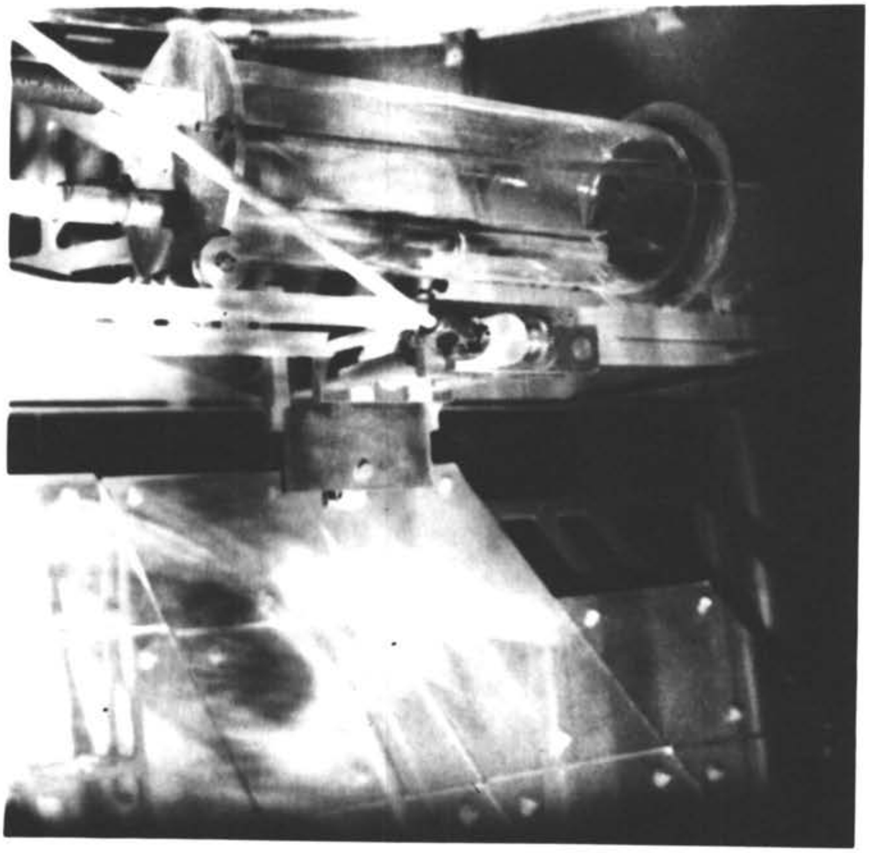

FIGURE 32

SAMPLE HOLDER IN OPERATING POSITION

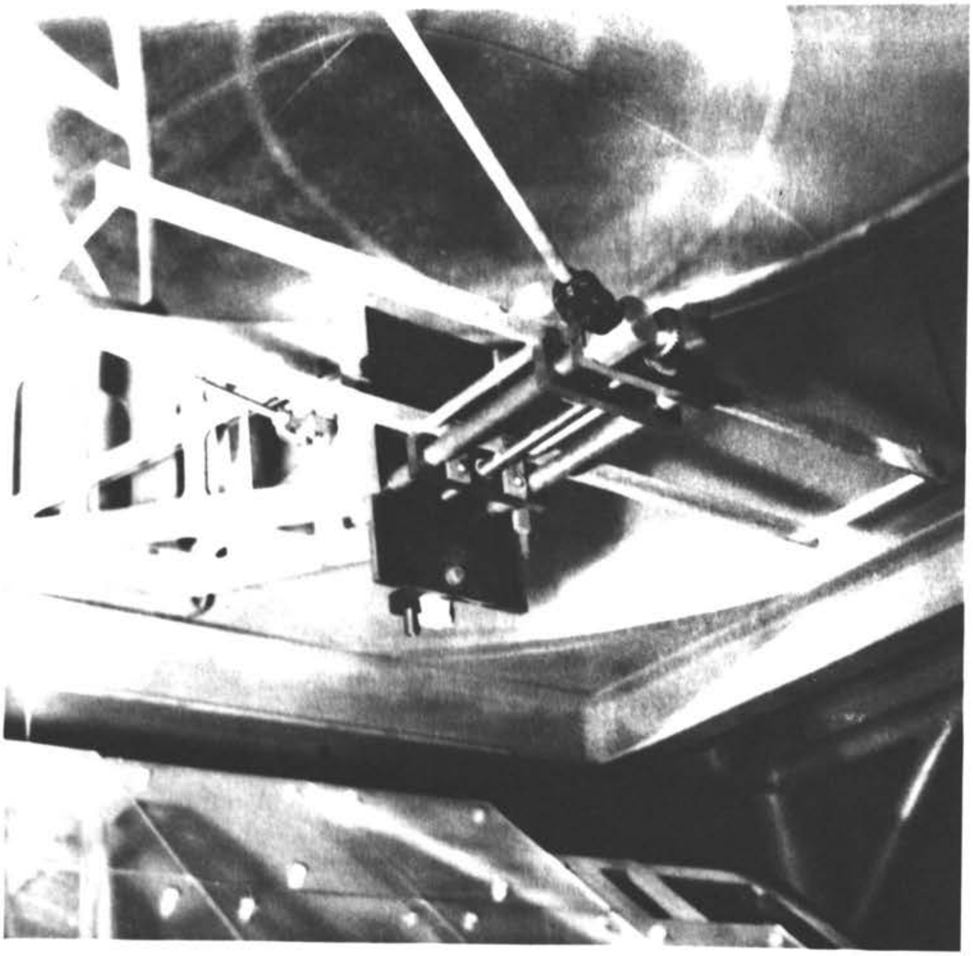

FIGURE 33

SAMPLE HOLDER PYLON AND RAIL

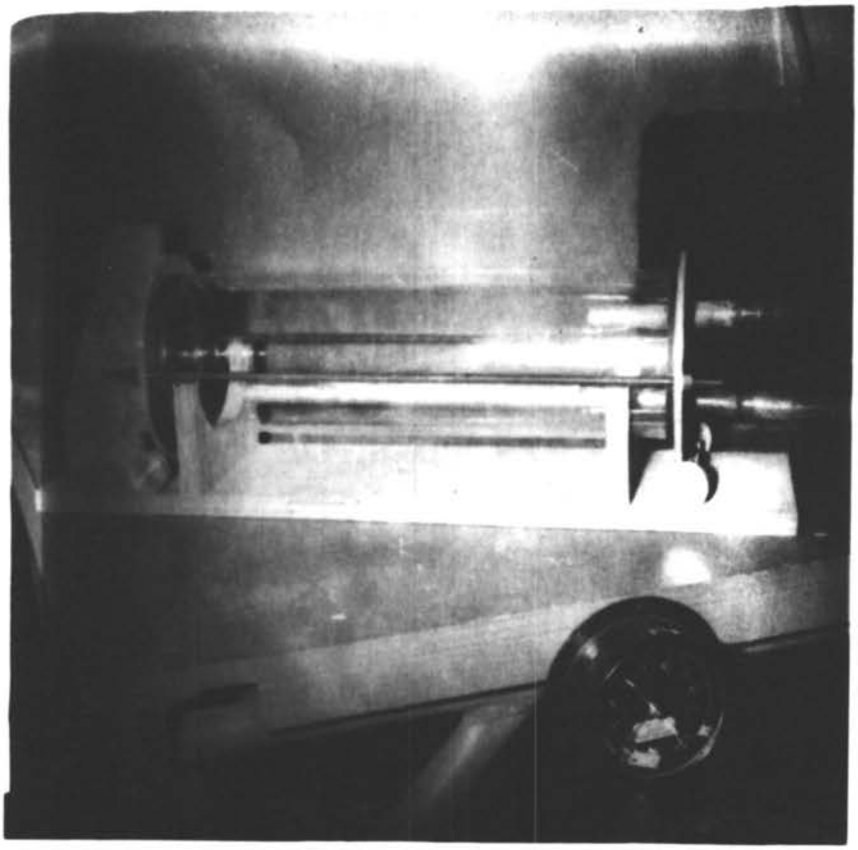

FIGURE 34

SAMPLE LOADING JIG

Adjustment in the vertical plane is provided by a follower nut attached to the sample holder base plate and driven by a threaded shaft. This base plate slides up and down in milled grooves in the original arc-support pylon of the searchlight as shown in Fig. 33. The threaded vertical driver shaft can be remotely turned through bevel gearing by a handwheel. A similar arrangement provides for adjustment in the concentrator-stationary reflector-heliostat plane. Adjustment of the sample holder position in the focal spot-operator plane is accomplished by moving the glass container along aluminum rails using flanged wheels mounted to the two aluminum end plates. The hoses of the gas system provide handles by which the position of the sample containing envelope can be varied along the length of the aluminum rails. A more elaborate motor driven mechanism can be easily added if steady movement of the sample through the focus is desired as might be the case for zone refining studies.

The sample holder envelope can be removed from the furnace for the changing of samples by simply lifting it from the transverse rails and withdrawing it through the operator's access hole in the side of the furnace. A plywood jig as seen in Fig. 34 facilitates alignment of the aluminum end plates, draw bolts, and flanged wheels.

Exact alignment is not necessary since one axle is pivoted about its center to allow all four wheels to continuously touch the guide rails without wobbling.

A shelf inside the glass envelope and rigidly mounted to the extended inlet gas pipe provides support for the samples in the sample holder array. Samples are usually mounted upon an insulating medium, about an inch in thickness, to put them approximately at the axial center of the cylindrical envelope.

Since all the radiant energy must go through the glass wall of the envelope and since the portion absorbed in this transit is essentially independent of the diameter of the envelope, the criteria of selection of a safe envelope size are those of mechanical strength and maximum allowable wall temperature. In this case, a diameter of 6 inches was chosen to allow sufficient room in the envelope for operator access, samples, gas pipes, etc. At this diameter the wall thickness of the cylindrical jar used was more than adequate to withstand the vacuum and internal pressures of up to two atmospheres which were encountered in this study. Heating of the glass envelope presented no thermal shock problems when care was taken to never allow the glass wall to coincide with the focal "hot spot".

GAS SYSTEM

The glass envelope can be evacuated through a rubber hose connected to the envelope by means of a gas ballast vacuum pump shown in Fig. 22. The use of a gas ballast vacuum pump allows the pumping of some condensable vapors in the gas without resorting to cold traps. These vapors were thought likely to occur due to the strong chemisorption of water upon finely divided elemental boron which would be released upon heating. A throttling and positive cutoff valve in the exhaust line provides control of the pumping rate. A fibreglass packed filter removes particulate matter in the exhausting gases.

Inert gas is supplied, if desired, from a high pressure cylinder to the glass envelope through a gas manifold system containing a pressure regulator, a flow meter, and a vacuum-pressure gauge, as shown in Fig. 35. By adjustment of the exhaust line throttling valve and the inert gas pressure regulator, desired pressures and flows of the inert gas, from about two atmospheres to moderately hard vacuum, and zero to several liters per minute, can be maintained in the glass envelope. Two atmospheres internal gas pressure is attainable only if extreme care is exercised in making the hose attachments and pressure regulator adjustments.

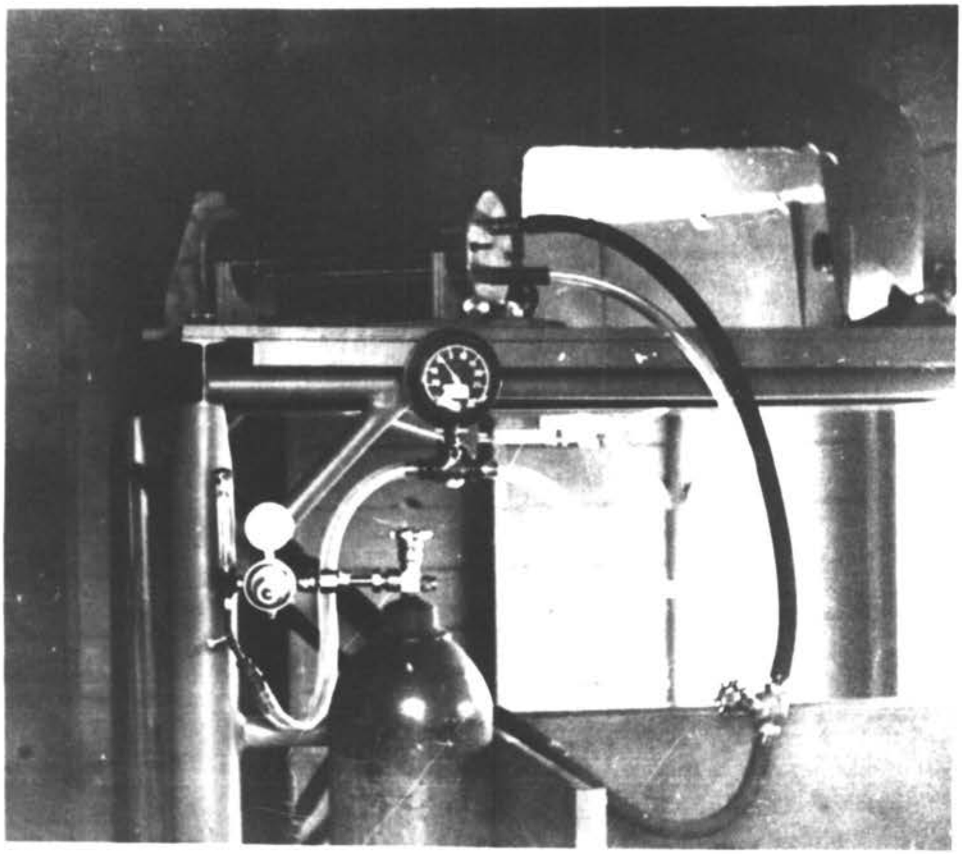

FIGURE 35

GAS MANIFOLD SYSTEM

ELECTRICAL SYSTEM

The solar furnace laboratory is supplied with 110 volts, 60 cycle, single phase current, at a fuse box. All electrical power circuits originate in this fuse box. Figs. 36, 37, and 38 show the electrical components used in the solar furnace laboratory. A detailed description of these components as shown in Figs. 36, 37, and 38 follows.

FB The fuse box and main breaker switch controls all electrical power to the solar furnace laboratory.

S-1 A double pole double throw switch which connects the proper power relay for AM or PM operation into the photocell circuit. Switch S-1 is up for PM and down for AM operation.

S-2, S-3 & S-4 Double pole double throw switches which reverse the direction of the vertical drive motor. All three are always moved together. All are in the up position for PM operation and all are in the down position for AM operation.

CAUTION: Switch S-5 must be off when reversing the settings of switches S-2, S-3,

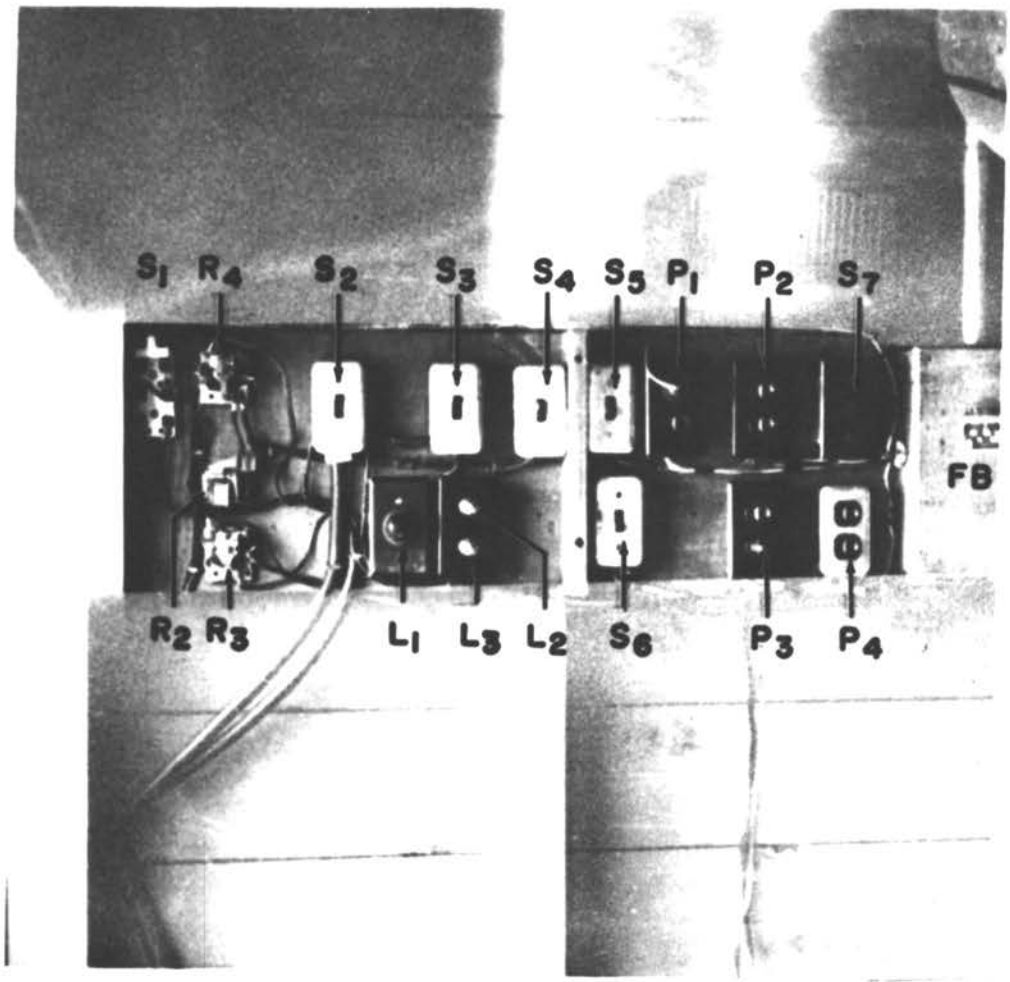

FIGURE 36

MAIN ELECTRICAL PANEL

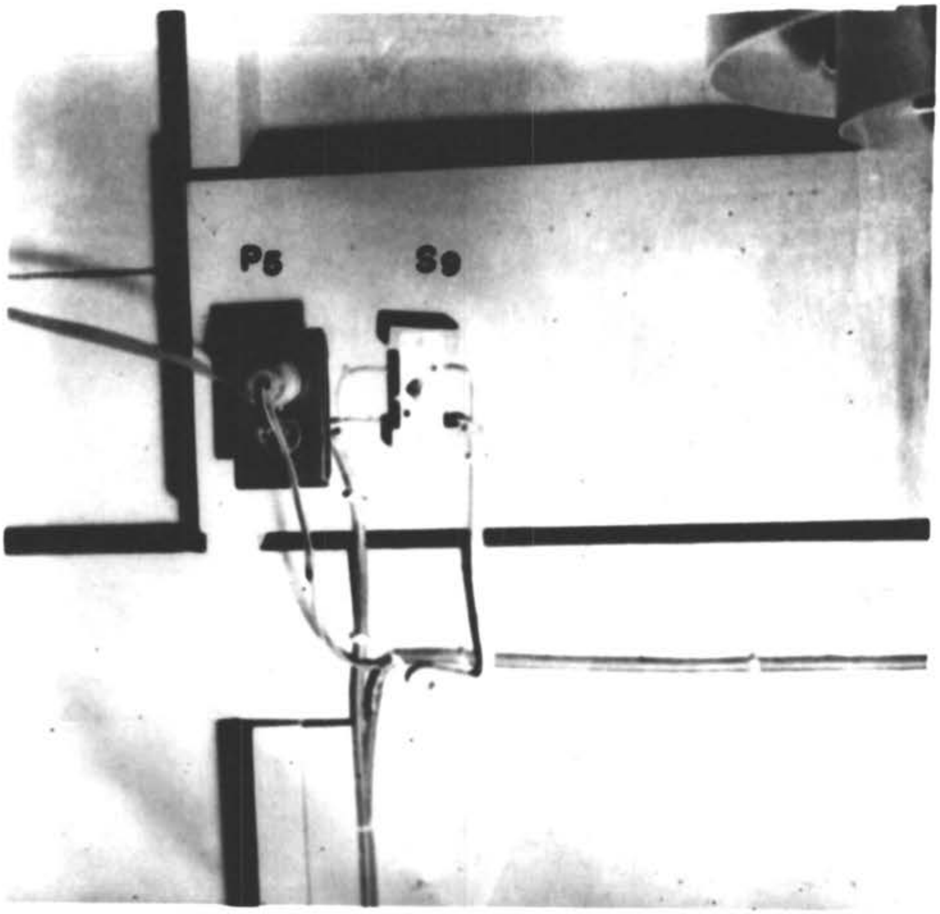

FIGURE 37

SECONDARY ELECTRICAL PANEL

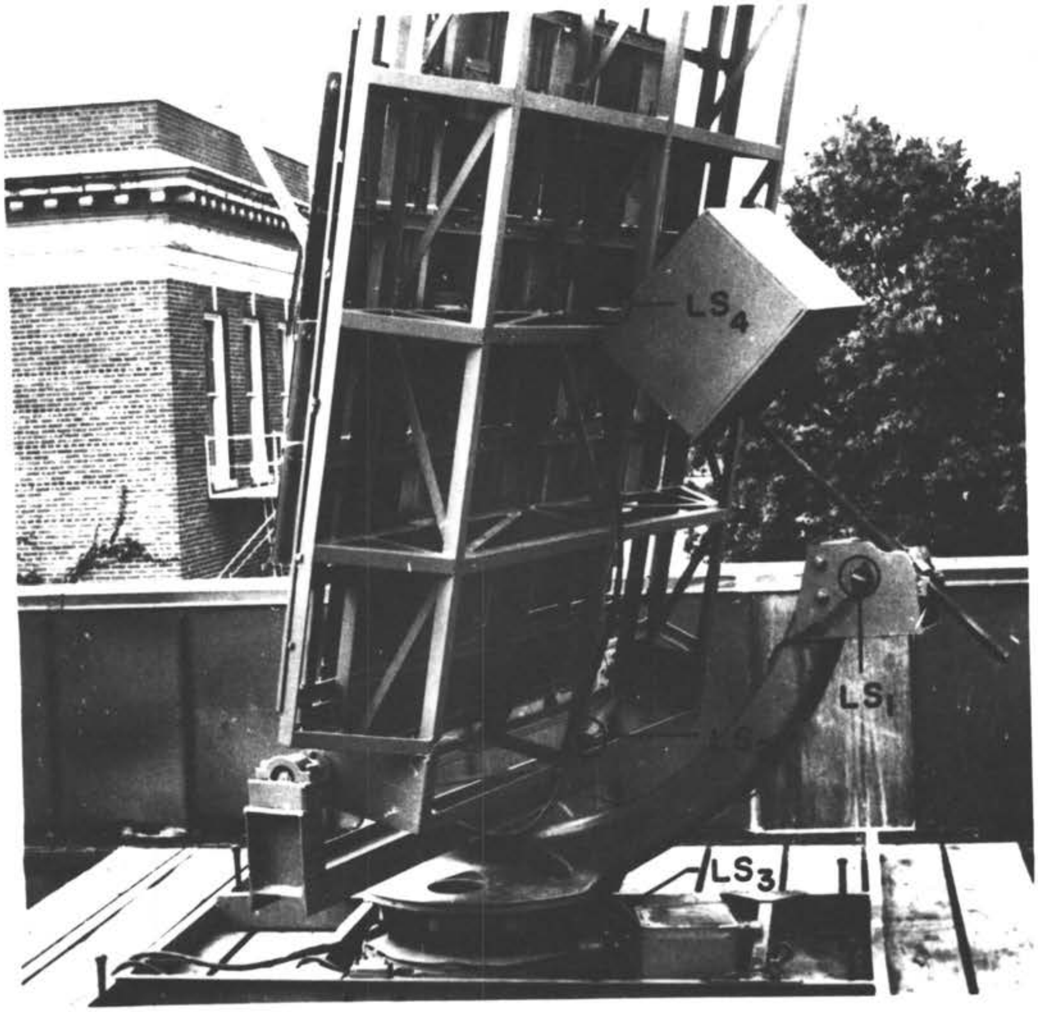

FIGURE 38

LIMIT SWITCHES

and S-4; otherwise a short circuit may result and a fuse will be blown.

S-5 Heliostat vertical drive power switch.

S-6 Heliostat azimuthal drive power switch. Reversing circuitry is not needed in the azimuthal drive since the drive gear can be disengaged, the heliostat returned manually to an eastward facing position, and the drive gear then re-engaged.

S-7 A power switch which controls plug receptacles P-1 and P-2. The light fixture is usually plugged into one of these.

S-8 Vacuum pump power switch, immediately to right of FB.

S-9 Photocell power supply switch.

R-1 A normally open power relay, controls vertical drive motor for PM operation.

R-2 A normally closed power relay, controls vertical drive motor for AM operation.

R-3 A normally open power relay, controls the azimuthal drive motor.

P-1,

P-2 Plug receptacle boxes controlled by switch S-7.

P-3,

P-4 Plug receptacle boxes controlled only by main power switch, FB.

P-5 Plug receptacle box into which the vertical drive photocell is plugged.

P-6 A rubber single plug receptacle located at the base of the 45 degree plane reflector which provides power for the azimuthal drive photocell.

CAUTION: If the prongs of either the photocell male plug or those of the power relay circuit which insert into the photocell female plug receptacle should become reversed, a short circuit will ensue and a fuse will be blown.

L-1 A red light which when lighted indicates that the azimuthal drive motor is running.

L-2, L-3 Red lights which when singly lighted* indicate that the vertical drive motor is running and the heliostat is being raised, L2, or lowered, L3.

* Should lights L-2 and L-3 both be lighted then either limit switch LS-1 and/or LS-2 have been tripped and must be reset before normal operation can recommence.

LS-1 Limit switch for vertical depression. This switch is actuated by the edge of the steel motor mounting bracket.

LS-2 Limit switch for vertical elevation. This switch is actuated by a steel cable attached to the heliostat base.

LS-3 Limit switch for azimuthal drive. This switch is actuated by the head on one of the bolts which attach the drive gear to the heliostat frame. The switch is tripped when the heliostat is facing almost due west.

CAUTION: Manual, i.e. non-electrical, actuation can damage or move this switch. Use care when manually moving the heliostat to extreme westward facing positions.

LS-4 A switch which bypasses or short circuits the two vertical drive limit switches. This switch is normally off. Due to the positive mechanical displacement character of the vertical drive mechanism, this switch is necessary to allow operation in the opposite direction from a tripped limit switch sufficient to allow resetting of the tripped limit switch.

CAUTION: Always check that switch LS-4 is indeed in the off position; otherwise, limit switches LS-1 and LS-2 cannot perform their functions and extensive damage to the heliostat may possibly ensue.

HOUSING OF THE SOLAR FURNACE

The solar furnace is enclosed in a shed which affords protection of the furnace and ancillary equipment from inclement weather. This shed also protects the operator and the tracking photocells from the effect of too much sunshine during operation. A large door in the shed admits the solar rays from the heliostat into the shed and onto the diagonal plane mirror. This is shown in Fig. 39. Two personnel doors are provided for access to the solar furnace and from the solar furnace to the heliostat. These doors open onto walkways as shown in Fig. 40.

The heliostat drive motors are protected by rain deflecting covers. During the winter months the mirrors are removed from the heliostat for indoor storage.

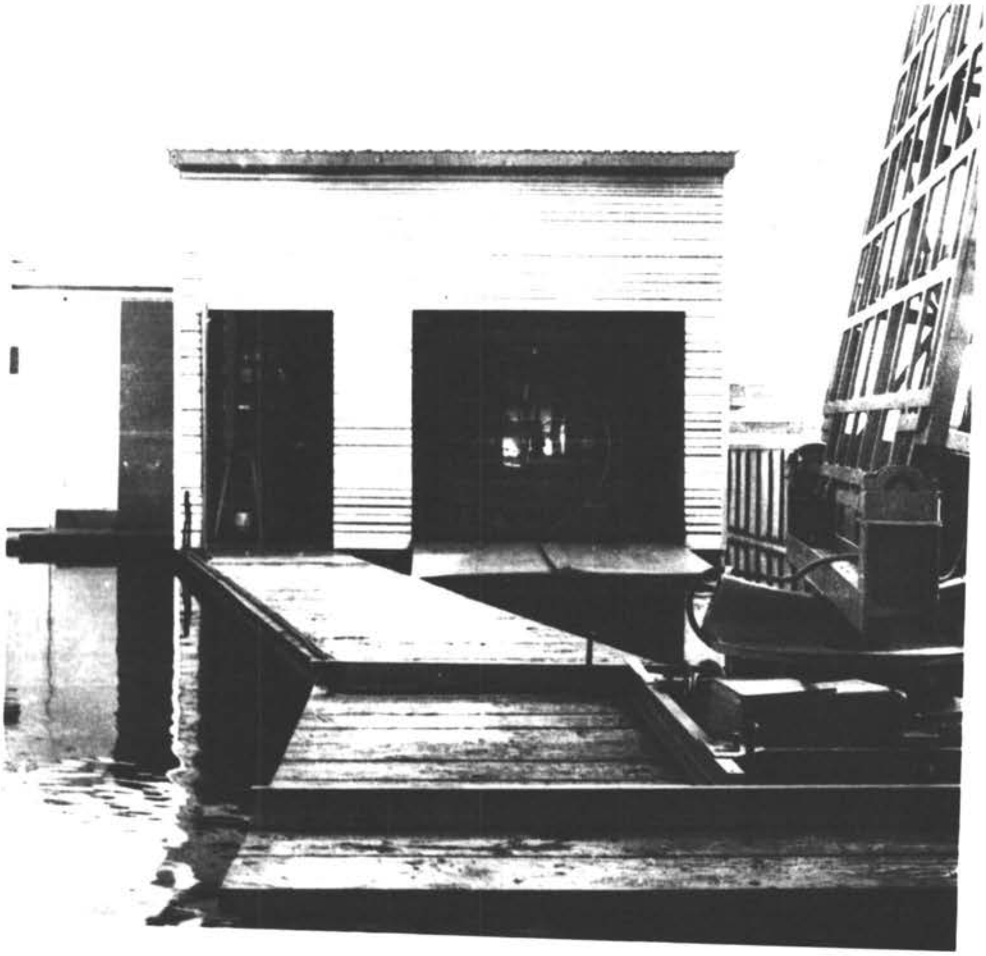

FIGURE 39

SOLAR FURNACE BUILDING FROM THE HELIOSTAT

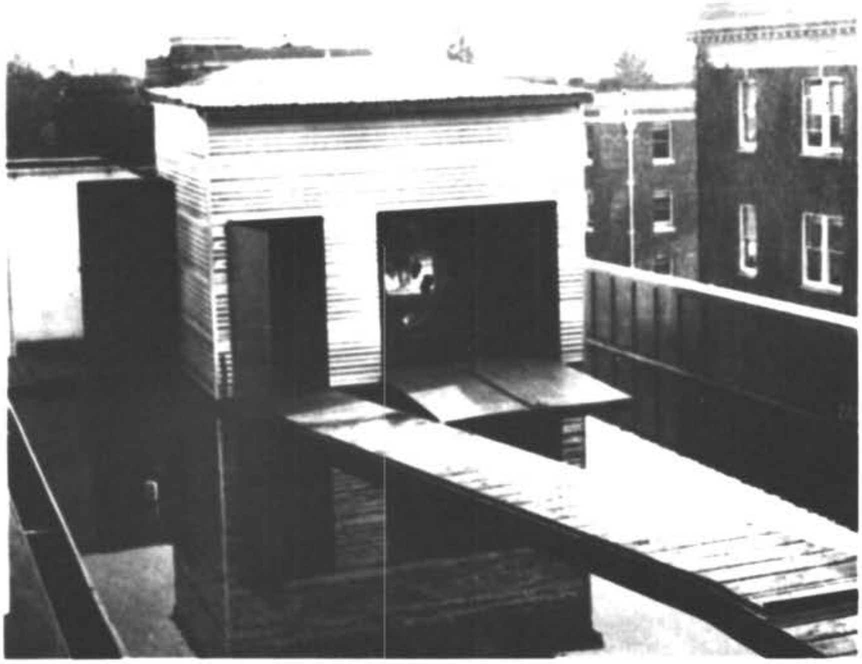

FIGURE 40

SOLAR FURNACE BUILDING AND WALKWAYS

OPERATION OF THE SOLAR FURNACE

The operation of the solar furnace falls into two stages: adjustment to co-planarity of the individual mirror segments in the heliostat and the stationary reflector mirrors, and actual irradiation operations with the solar furnace.

ALIGNMENT ADJUSTMENTS OF THE PLANAR MIRRORS

The adjustment techniques used for co-planarizing or aligning the mirror segments in the heliostat vary somewhat from those used for the alignment of the stationary reflector mirror segments.

The heliostat mirror segments are adjusted by means of the three mounting bolts until the image reflected by each mirror segment upon the face of the solar furnace building falls into its proper position relative to the images of its immediate neighbors. Very fine alignments can be made in this fashion by continuing the adjustment until the dark spaces between two images caused by an obtuse setting of the two corresponding adjacent mirrors and the bright spaces corresponding to an acute setting of two adjacent mirror segments are eliminated or at least minimized.

The stationary mirror is aligned by an analogous procedure except that parallel incident light rays are provided by a small bulb placed at the focus of the paraboloidal concentrator. The images of each of the mirror segments are then cast upon a drape placed over the closed door facing the heliostat. Adjustments of the individual segments are, from this point on, analogous to those of the heliostat.

OPERATING PROCEDURE WITH THE SOLAR FURNACE

The operating procedure followed for investigations of the behavior of substances at high thermal fluxes in the solar furnace are detailed below in chronological order. Cross references are constantly made to components of the electrical system as described in the sub-section, Electrical System, and Figs. 36, 37, and 38.

Start Up Procedure:

1 Turn on main power switch at fuse box, FB.

2 Remove sample holder from furnace and place in plywood holder. Make sure that nothing which can be damaged by heat is in the focal plane of the furnace. Upon starting up, the focal spot can move around appreciably due to misalignment of the heliostat and may damage objects left near the focus area.

3 Open main door.

4 Wash mirrors if necessary.

CAUTION: Use care when removing and replacing photocell. Plastic dovetail joint is very fragile.

5 Manually set heliostat in approximately correct azimuthal setting by disengaging drive gear, turning heliostat, and re-engaging drive gear.

6 Adjust vertical position of heliostat. If image is too high, heliostat is too low and must be raised. Place switches S-1, S-2, S-3, and S-4 in up positions. Turn switches S-5 and S-9 to ON positions. At this time light L-2 will come on, and when the control position is reached light L-2 will go off. If image is too low, heliostat is too high, and must be raised. To do this place switches S-1, S-2, S-3, and S-4 in down positions. Turn switches S-5 and S-9 to ON positions. At this time light L-3 will go off.

When the heliostat is properly positioned vertically, the direction in which it is to move for Tracking the sun, up for AM, down for PM, is determined by switching S-5 to OFF position, placing switches S-1, S-2, S-3, and S-4 to up position for PM or to down positions for AM operation. Then turn switch S-5 to the ON position.

CAUTION: When moving switches S-2, S-3, and S-4, switch S-5 must be off, otherwise, a short circuit may ensue, and a fuse will be blown.

7 Start azimuthal drive to tracking. Turn switch S-6 to ON position. Disengage drive gear and move heliostat so that the image slowly moves from the west past the center position to the east. Slightly east of the center the azimuthal drive motor should come on. Hold the heliostat steady and allow the azimuthal drive motor to run until the drive gear can be smoothly re-engaged. Should the center or control point need to be changed, it can be accomplished by bending the photocell mounting bracket. CAUTION: Plastic dovetail slip joint is very fragile. Apply bending force solely to the mounting bracket and not to the photocell case proper.

8 Make sure the limit switch bypass switch, LS-4 is in the OFF position. When the drive motors are running, manually trip the limit switches LS-1, LS-2, and LS-4 momentarily to check operation.

9 Insert the sample to be irradiated into the sample holder and tighten the two tension nuts using the plywood assembly jig for proper positioning of the end plates.

CAUTION: The rubber gasket must have the notch fitted over the bottom hose fitting.

Turn on the vacuum pump switch, S-8, and open the globe valve in the vacuum line. Open the argon tank valve, and by adjusting the regulator valve introduce a moderate flow of argon into the sample container. When the sample container has had enough time to become freed of air, grasp the two hose nipples and insert the entire holder into the furnace and onto the support rails.

CAUTION: Have hoses free of entanglements before attempting to lift the sample holder into the furnace.

10 Adjust the position of the sample in relation to the focus by manipulating the vertical adjustment wheel with the left hand, the right-left adjustment wheel with the right hand, and the in-out adjustment by pulling or pushing on the vacuum hose. This latter adjustment can be maintained in the desired position by weighting the hose with the lead brick provided for this purpose.

11 When heating is finished, remove the sample holder from the furnace and replace in plywood assembly jig. Close the vacuum globe valve and allow the container to become filled with argon to one atmosphere pressure, reverse naturally, for pressurized operation.

CAUTION: The Tygon hose will blow off if pressure exceeds zero gauge by a few pounds per square inch. When pressure is equalized and sample is sufficiently cooled, the sample holder can be opened, and the sample removed. The endplate can be conveniently held for a short time when changing samples by inserting the end of the argon inlet tube beneath the vertical adjustment drive wheel. Wash sample holder in preparation for next run.

12 For subsequent samples repeat steps 9 through 11.

Shut Down Procedure:

1 Turn off switches S-5, S-6, S-8, and S-9.

2 Either close large door or turn heliostat away from opening to the east. The cause for this is explained in step 2 of start up procedure.

3 Turn off main power switch before leaving laboratory.

4 When closing down for the day, close and lock all doors. Make sure main power switch, FB, is off.

Trouble Shooting:

1 If a relay fails to trip at the usual control point, it usually is necessary to vary the aperture or the photocell involved. If the photocell fails to de-energize its associated power relay when light strikes it, the aperture must be increased. If the photocell does not energize its relay when light does not strike the sensitive element, then its aperture must be decreased. Extremely bright or unusually dim

days may occasion tracking system failures of this type. Also, by varying the aperture of the azimuthal drive, an optimum aperture can be arrived at which gives azimuthal control with a minimum "drift" or movement of focal spot from side to side. Vertical drift is not apparent and seems to present no need for improvement.

PERFORMANCE OF THE OREGON STATE COLLEGE SOLAR FURNACE

When performance characteristics for the solar furnace are calculated by the methods presented earlier, (see Optical and Radiant Energy Consideration for a Solar Furnace), very optimistic estimates are obtained. Deviations between predicted performance levels and observed performance levels are probably due to two sources: 1) The assumption of a black body sample losing energy only by radiation from its face. 2) Uncertainties in estimated transmissivity factors and solar intensities.

Whereas, the calculated maximum attainable temperatures for the solar furnace range from a low estimated value of 3300°C to a high of 3950°C, (see Appendix), the actual maximum observed temperature involved the melting of a 3 mil thick tantalum foil, M.P. 2996°C (30:p.629). The effect of conductivity of the sample is illustrated by the observation that while tantalum foil was melted, a compacted mass of niobium turnings, M.P. 2415°C (30:p.629), was only partially melted, and a hafnium ingot, M.P. 2130°C (30:p.629), was not melted at all. Massive pieces of less conductive boron, M.P. 2100°C (30:p.629), and alumina, M.P. 2050°C (34:p.447), were readily fused locally, wherever subjected to the focal "hot spot" of the solar furnace.

In the case of a thin tantalum foil, M.P. 2996°C, the conductive losses radially from the heated zone would be low; however, radiative loss from the back side would be virtually as large as from the face. When this back side loss is taken into account, a concentration ratio, C, of 16,000 is obtained (see Appendix). This is in contrast to a concentration ratio of 8,000 which is the calculated value for a non-conductive, non-convective, black body at the temperature of 2996°C (Fig. 16). The furnace factor, F, corresponding to C 16,000, is 0.46 (Fig. 14). This compares favorably with the estimated values for F of 0.32 to 0.69, Table 3. General feelings of persons acquainted with this project are that temperatures higher than 2996°C would be attainable under favorable atmospheric conditions, since the tantalum foil was melted on a hazy, fall day.

The definition of the focal hot spot still leaves something to be desired. The focal spot is not a bright disc surrounded by a fringe as shown in Fig. 13; rather, it is a disc surrounded by "feathers" or "wings" (Fig. 41). One surmises that the deviations apparent in the fringe area are also present to some degree in the central disc, and that this would lower the heat flux

FIGURE 41

SAMPLE IN FOCUS SEEN FROM PARABOLOID VERTEX attainable in this disc. The alignments of the two planar mirrors have been made as good as economically possible using commercial grade glass; hence, any readily achieved improvements must be made in the paraboloidal concentrator mirror. From observations of the distorted images formed by light emitted from a filament placed at the focus, optical imperfections of the mirror were noted. Inspection of the mirror surface revealed a great number of "dimples" and tool marks, as well as extensive pitting which would also detract from the furnace performance. A new, unused paraboloidal concentrator has been obtained for future use of the solar furnace.

STUDIES OF ELEMENTAL BORON

In its original conception, the solar furnace was to be a flexible tool with which to attempt high temperature refining of elemental boron as supplied by the U. S. Borax Research Corporation. With the uncontaminated high-temperature heat supplied by the solar furnace it was hoped that elemental boron could be melted and upgraded by recrystallization from the melt. The possibility of growing macrocrystals of elemental boron for future solid state studies was considered as a desirable adjunct to the refining study.

DESCRIPTION OF U. S. BORAX ELEMENTAL BORON

Elemental boron is produced by U. S. Borax Corporation in three grades: amorphous, 92-95% purity; amorphous, 95-97% purity; and crystalline, 99+% purity. The 92-95% purity amorphous form is produced by magnesium reduction of boric oxide. The 95-97% purity amorphous form is produced by refinement of the 92-95% purity product in an undisclosed process. The crystalline form is prepared by fusion of 95-97% purity amorphous boron in a vacuum furnace. This simple fusion up-grades the 95-97% material to 99+% purity; unfortunately, an undesirable tungsten impurity is introduced from an incandescent tungsten electrode.

The amorphous forms are very finely divided, sub-micron, powders. The crystalline material may be obtained in sizes ranging from about ½ inch chunks to -200 mesh. Elemental boron is very hard, 9.6 on Moh's scale, and care must be taken to avoid extensive galling of dies which are used for pressing compacted furnace samples from the finely divided amorphous boron. This information was obtained upon a personal visit to the U. S. Borax Research Corporation, Anaheim, California.

STUDIES OF AMORPHOUS BORON IN THE SOLAR FURNACE

Little success was obtained in attempts to fuse compacted powders in the solar furnace. The tremendous thermal expansions of adsorbed and entrapped gases caused compacted boron or lanthanum oxide powders to virtually explode when subjected to strong heating. Even very compact samples of boron prepared by "baking out" pressed cakes in a vacuum furnace were extremely difficult to melt in the solar furnace. The upper layer of powder was rapidly "blasted off" with the result that holes were formed under the focus and no melts were formed. Only by pressurizing the sample holder to two atmospheres with argon could even small melts be obtained.

Continued difficulty with powdered, amorphous elemental boron led to the abandonment of plans to melt and zone refine long samples prepared from compacted powders.

STUDIES WITH ARC FUSED BORON

Arc fused elemental boron prepared from U. S. Borax amorphous boron by the U. S. Bureau of Mines, Albany, Oregon, was selected for additional investigations of high temperature refining of elemental boron. This material was contaminated with tungsten from the arc electrode; consequently, the solar furnace irradiated samples also contained tungsten. Other impurities in the original amorphous boron also appear in subsequent preparations.

When samples were held for long periods of time at high temperatures, fused zones of about 2 mm. thickness surrounded by "whisker" or stalagmites were formed, Figs. 42 and 43. These phenomena occur as a consequence of the short liquid range of boron. Estimates of this liquid range vary from essentially zero (46:p.335) to 450°C (30:p.77). When boron is placed at the focus of the solar furnace, melting occurs at the surface and thence downward until the temperature drop across the melt

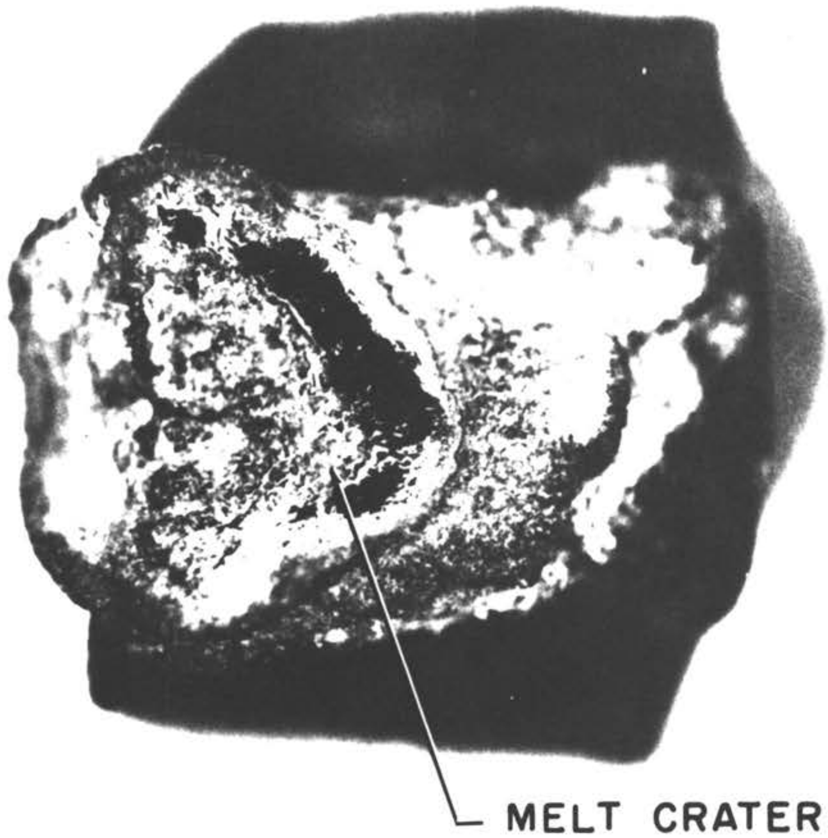

FIGURE 42

TOP VIEW OF BORON SAMPLE

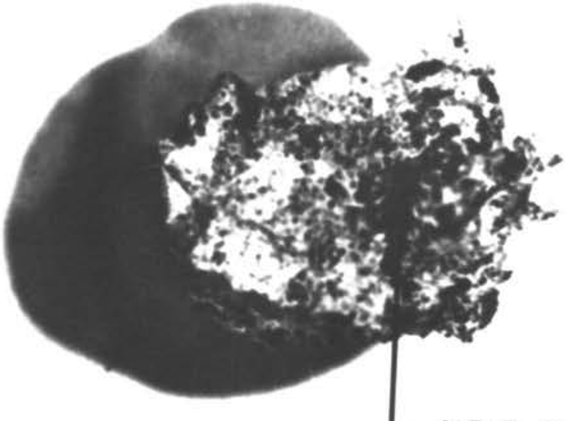

FIGURE 43

SIDE VIEW OF BORON SAMPLE SHOWING SURFACE GROWTH OF STALAGMITES equals the liquid temperature range of boron. At that time, boiling of the surface begins and further penetration of the melt into the massive substrate occurs only as material is vaporized from the surface. This vaporized boron condenses and crystallizes in "whiskers" around the edge of the melt crater. Variation of the pressures of argon gas from a fore pump vacuum to two atmospheres did not appreciably effect the maximum melt thickness. Most experimental runs were made at low pressures in order to minimize "smoking" of the glass envelope directly above the sample with the fluidized particles of boron and impurities cooked off of the sample.

X-ray spectrometric analyses of the amorphous boron, arc fused boron, the surface melt boron, and the "whiskers" or surface growth boron are presented in Table 4.

TABLE 4

X-RAY SPECTROMETRIC ANALYSES OF BORON SAMPLES

	Al	B	Ca	Cr	Cu	Fe	Mg	Mn	Ni	P	Pb	Si	Ti	W	Na	Li	V
Amorphous	D	A	E	E	F	C	F	E	F	C	E	D	-	-	D	D	-
Arc Fused	F*	A	D	E	D	C	F	E	E	-	-	D	F	C	-	-	F
Solar Furnace Surface Melt	E*	A	E	E	E	C	G	E	F	-	-	C	-	E	-	-	-
Solar Furnace Surface Growth	D*	A	D	D**	E	C	F	F	F	-	-	D	F	D	-	-	-

*Samples prepared in an alumina mortar

** Probably should have been E

Letters indicate estimates from qualitative analysis:

A	over 10%	E	0.01 to 0.1%
B	5 to 10%	F	0.001 to 0.01%
C	1 to 5%	G	under 0.001%
D	0.1 to 1%	-	not detected

Discussion of Spectrometric Analyses:

An examination of the Table 4 reveals that in nearly every case a difference in composition occurs between arc melted boron and the same material after subsequent remelting in the solar furnace. In the case of iron, the concentrations are high in every case. In such high concentrations, 1-5%, small changes in concentrations might be easily undetected in this type of analysis. In those cases where no apparent concentration changes occur between substrate and melt, a concentration change occurs between the melt and the vaporized material, with the exception of iron. Iron is introduced by grinding operations at U. S. Borax Corporation, and it is generally felt that this iron content can be greatly reduced by leaching with acid.

X-ray crystallographic analyses were also obtained for surface melt and surface growth samples prepared in the solar furnace. These analyses are given in Table 5.

TABLE 5

CRYSTALLOGRAPHIC DATA FOR SOLAR FURNACE MELT AND SURFACE GROWTHS

Type of Sample	Major Constituent	Minor Constituent
Surface melt	Boron carbide B_4C*	Rhombohedral boron with traces of WB_{12}
Surface growth	Tungsten boride probably WB_{12}	Rhombohedral boron

*Sample prepared by grinding in boron carbide crucible

Discussion of Crystallographic Data:

The presence of rhombohedral boron is the most noteworthy feature of these analyses. That rhombohedral boron is always formed by equilibrium recrystallization formed by equilibrium from the melt is becoming increasingly apparent as more such samples are prepared and analyzed, (33:pp.70-76). When this study was begun tetragonal boron as prepared by the method of Laubengayer, et al (32:p.9), was generally assumed to be the stable form of high temperature boron. In the last two years several studies, (33:pp.70-76) mostly of U. S. Borax Research Corporation 99% crystalline boron, have shown the existence of a rhombohedral high temperature stable form of boron.

CONCLUSIONS

The conclusions reached in this study fall into two divisons, those relative to the utility of solar furnaces for high temperature research and those relative to elemental boron.

CONCLUSIONS RELATIVE TO SOLAR FURNACES

When this project was initiated, the participants were subjected to many pessimistic comments concerning the feasibility of such project in a western Oregon location. While the temperatures attained by the furnace were not as high as those predicted by the optimistic theoretical calculations, the design objective of melting boron, M.P. 2100°C, was achieved and surpassed.

The solar furnace has real utility for high-temperature studies of contaminant sensitive materials. Its use as such, however, requires ingenuity in the design of the experiments if its limitations, e.g. small sample size, limited exposure times, high thermal stresses, etc., are to be circumvented sufficiently to allow the fullest utilization of the advantageous features of the solar furnace.

CONCLUSIONS RELATIVE TO ELEMENTAL BORON

From the studies of elemental boron it may be concluded that:

1) Since the one stage refining revealed an improvement in purity of elemental boron, zone refining, i.e. the repetitive melting, partial vaporizing and subsequent refreezing of a sample in a countercurrent fashion, would be expected to effect marked increases in the purity of commercial grade boron.

2) These studies reconfirm that a high temperature stable rhombohedral boron does exist.

3) Treatments of powdered samples in the solar furnace require the development of special techniques.

RECOMMENDATIONS

In a recent publication (58:p.40) the preparation of adherent, thermally stable, sticks of elemental boron from powdered amorphous boron is described. This preparation involves the use of boron oxide to cement the boron particles together. When the sample is heated above 1500 C, the boron oxide vaporizes leaving a fairly strong compact sample of elemental boron. Such a technique could well eliminate the difficulties with compacted boron powders encountered in this study.

Where a sample is not to be traversed through the focus, as in zone refining studies, the substitution of a spherical sample holder for the cylindrical one now used could materially reduce the critically important center shading loss in the solar furnace.

BIBLIOGRAPHY

1. Abetti, Giorgio. The sun. New York, Van Nostrand, 1938. 493 p.

2. Adney, et al. Solar furnace support studies. vol. 2. Holloman Air Force Base, U. S. Air Force Missile Development Center, 1959. 300 p. (U. S. Armed Services Technical Information Agency. no. AD 213260)

3. Allison, Fred and Gordon Hughes. Suggested methods of aligning the planes of the solar furnace heliostat mirrors into parallelism. Journal of Solar Energy Science and Engineering 2:46-48. July-Oct. 1958.

4. Association for Applied Solar Energy. Proceedings of the world symposium on applied solar energy, Phoenix, Arizona. Menlo Park, Stanford Research Institute, 1956. 304 p.

5. Baum, V. A., R. R. Aparasi and B. A. Garf. High-power solar installations. Journal of Solar Energy Science and Engineering 1:6-12. Jan. 1957.

6. Bean, K. E., R. J. Starks and W. E. Medcalf. Study of the physical chemistry and metallurgy of semiconducting materials. Third Quarterly Report for period of March 15, 1958 to June 15, 1958. 24 p. (U. S. Army Signal Corp. PR&C No. 58-ELS/R-3901)

7. Benveniste, Guy and Nevin K. Hiester. The solar furnace--new tool for high-temperature work. Mechanical Engineering 78:915-920. 1956.

8. Bliss, Raymond W. Notes on performance design of parabolic solar furnaces. Journal of Solar Energy Science and Engineering 1:22-29. Jan. 1957.

9. Bliss, Raymond W. Designing solar furnaces for specific performance. Journal of Solar Energy Science and Engineering 1:55-62. April-July 1957.

10. Byron, Brenden B., Herbert W. Newkirk, Jr. and Sydney H. Woodcock. A study of temperature measurement in a solar furnace. Journal of Solar Energy Science and Engineering 2:13-17. Jan. 1958.

11. Cabannes, F. and A. Le Phat Vinh. Calcul de la repartition de l'energie solaire reflechis par un miroir parabolique. Journal de Physique et le Radium 15:817-820. 1954.

12. Campbell, I. E. High-temperature technology. New York, Wiley, 1956. 526 p.

13. Cohen, Raymond K. and Nevin K. Hiester. A survey of solar furnace installations in the United States. Journal of Solar Energy Science and Engineering 1:115-116. April-July 1957.

14. Conn, William M. Recent progress in solar furnaces for high-temperature research and development work. Journal of the Franklin Institute 257:1-12. 1954.

15. Conn, William M. A review of the production of molten zirconia in the solar furnace. Journal of Solar Energy Science and Engineering 3:39-42. Oct. 1959.

16. Daniels, Farrington and John A. Duffie. Solar energy research. Madison, University of Wisconsin, 1955. 290 p.

17. Davies, John M. and Eugene S. Cotton. Design of the quartermaster solar furnace. Journal of Solar Energy Science and Engineering 1:23-27. April-July 1957.

18. De La Rue, R. E., Jr., T. E. Tietz and N. K. Hiester. Economics and design study of solar furnaces. Stanford, Calif., 1956. 15 p. (Stanford Research Institute Report TN-56-382)

19. De La Rue, R. E., Jr. <u>et al</u>. Flux distribution near the focal plane. Journal of Solar Energy Science and Engineering 1:94-98. April-July 1957.

20. Dietz, A. G. H. Space heating with solar energy. Cambridge, Massachusetts Institute of Technology, 1954. 45 p.

21. Duwez, Pol. Utilization of solar furnaces in high-temperature research. American Society of Mechanical Engineers. Transactions 79:1019-1023. 1957.

22. Edlin, Frank E. Industrial considerations of solar furnaces. Journal of Solar Energy Science and Engineering 1:52-54. April-July 1957.

23. Elliot, J. Richard, Jr. Tapping the sun. Barron's, Dec. 22, 1958, p.3, 16-18.

24. Farber, J. and B. I. Davis. Analysis of large aperture parabolic mirrors for solar furnaces. Journal of the Optical Society of America 4:216-20. Mar. 1957.

25. Forsythe, W. E. Smithsonian physical tables. 9th ed. Washington, 1954. 827 p. (Smithsonian Miscellaneous Collections. vol. 120)

26. Gardon, Robert. A segmented-mirror solar furnace for high-intensity thermal radiation studies. Review of Scientific Instruments 25:459-463. 1954.

27. Glaser, Peter E. A solar furnace for use in applied research. Journal of Solar Energy Science and Engineering 1:78-83. April-July 1957.

28. Glaser, Peter E. Engineering research with a solar furnace. Journal of Solar Energy Science and Engineering 2:7-10. April 1958.

29. Glaser, Peter E. The status of solar furnace research. Journal of Solar Energy Science and Engineering 3:47. Oct. 1959.

30. Hampel, Clifford A. Rare metals handbook. New York, Reinhold, 1954. 657 p.

31. Hiester, Nevin K., Thomas E. Tietz and Robert De La Rue, Jr. Economic factors in furnace design. Journal of Solar Energy Science and Engineering 1:28-43. April-July 1957.

32. Hoard, J. L. Structures of fluorocarbons, elementary boron, and boron compounds. 1955. 18p. (U. S. Atomic Energy Commission. NYO-7214)

33. Hoard, J. L. and Arthur E. Newkirk. An analysis of polymorphism in boron based upon x-ray diffraction results. Journal of the American Chemical Society 82:70-76. 1960.

34. Hodgmen, Charles D. (ed.) Handbook of chemistry and physics. 32d. ed. Cleveland, Chemical Rubber Publishing Company, 1950. 2879 p.

35. Hukuo, Nobuhei and Hisao Mii. Design problems of a solar furnace. Journal of Solar Energy Science and Engineering 1:108-114. April-July 1957.

36. Jose, Paul D. The design of the heliostat mirror for a solar furnace. Journal of Solar Energy Science and Engineering 1:23-27. April-July 1957.

37. Kassander, A. Richard, Jr. Fuel for solar furnaces. Journal of Solar Energy Science and Engineering 1:44-47. April-July 1957.

38. Lange, Luise. Deriving the equations of the sections of a cone. American Mathematical Monthly 63:488-491. 1956.

39. Laszlo, Tibor. Temperature and flux vs. geometrical perfection. Journal of Solar Energy Science and Engineering 1:78-83. April-July 1957.

40. Laszlo, Tibor. Solar furnaces for high temperature research. Journal of Solar Energy Science and Engineering 3:43-46. Oct. 1959.

41. Littke, Walter. Thermische dissoziation und schmelzpunkt von TiO_2. Thesis. Freiburg im Breisgau, University of Freiburg, 1957. 56 numb. leaves.

42. Loh, E. et al. Theoretical considerations on performance characteristic of solar furnaces. Stanford, Calif., 1956. 27 p. (Stanford Research Institute Report TN-56-69)

43. Marcus, R. J. and H. C. Wohlers. Solar heat, photochemistry. Industrial and Engineering Chemistry 51:1335-1340.

44. Noguchi, Tetsuo. Solar furnace research in Japan. Journal of Solar Energy Science and Engineering 3:44-47. Oct. 1959.

45. Parmelee, G. V. The transmission of solar energy radiation through flat glass under summer conditions. Transactions of the American Society of Heating and Ventilating Engineers 51:317-344. 1945.

46. Sidgwick, N. V. The chemical elements and their compounds. Oxford, Clarendon Press, 1950. 2 vols.

47. Shaw, W. C., D. E. Hudson and G. C. Danielson. Electrical properties of crystalline boron. 1953. 152 p. (U. S. Atomic Energy Commission. ISC-380)

48. Simon, Alfred W. Calculation of energy at points outside the focal spot of a parabolic condenser. Journal of Solar Energy Science and Engineering 2:22-24. April 1958.

49. Simon, Alfred W. Calculation of the concentration of the solar radiation through the focal spot of a parabolic mirror. Journal of Solar Energy Science and Engineering 2:25-29. April 1958.

50. Simon, Alfred W. The loss of energy by absorption and reflection in the heliostat and parabolic condenser of a solar furnace. Journal of Solar Energy Science and Engineering 2:30-33. April 1958.

51. Stimson, Thomas E., Jr. The sun is really in business. Popular Mechanics 110:57-62, 220. Aug. 1950.

52. Survey of solar furnace installations in the United States, supplement. Journal of Solar Energy Science and Engineering 1:35. Oct. 1957.

53. Survey of solar furnace installations in the United States, supplement. Journal of Solar Energy Science and Engineering 2:55. July-Oct. 1958.

54. Trombe, Felix. Solar furnaces and their applications. Journal of Solar Energy Science and Engineering 1:9-15. April-July 1957.

55. Trombe, Felix and M. Foex. Traitements a haute temperature au moyen de fours centrifuges chauffes par l'energie solaire. In: International Conference on the Use of Solar Energy: the Scientific Basis. vol. 2 141-181. Tucson, University of Arizona Press, 1958. 5 vols.

56. Tuddenham, W. M. A solar furnace for research in non-ferrous metallurgy. Journal of Solar Energy Science and Engineering 1:48-51. April-July 1957.

57. Wight, Ralph H. Materials and surfaces for solar furnaces. Journal of Solar Energy Science and Engineering 1:108-114. April-July 1957.

58. Zone melting route to larger and purer crystals. Chemical Engineering 66:40. Dec. 28, 1959.

APPENDIX

OPTICAL AND RADIANT ENERGY CALCULATIONS FOR THE OREGON STATE COLLEGE SOLAR FURNACE

These calculations are based upon the equations and charts developed in the section, Optical and Radiant Energy Considerations for a Solar Furnace. The equation and figure numbers to be used refer to that section.

The diameter of the hot spot or central zone of constant (nearly) intensity, d:

$$d = a\alpha = 26(0.00931) = 0.242 \text{ inch} \tag{1}$$

The diameter of the hot spot fringe is equal to the length of a major axis of an ellipse, b_2, where:

$$b_2 = \frac{\rho\alpha}{\text{Cos } \theta_1} \tag{2}$$

Where θ_1 is the rim angle, 60^o. The radius of the paraboloid, ρ , corresponding to $\theta_1 = 60^o$ is determined from a consideration of the rim angle, θ_1, and the rim diameter, 60 inches, from Fig. 10:

$$\frac{60}{2\sin \theta_1} = \frac{60}{2(0.866)} = 34.6 \text{ inches}$$

Now from equation 2:

$$b_2 = \frac{\rho\alpha}{\text{Cos } \theta_1} = \frac{34.6(0.00931)}{0.500} = 0.645 \text{ inches}$$

Thus the perfect solar image at the focal plane of the furnace would have a central constant intensity zone of 0.242 inch diameter and a fringe of decreasing intensity having a diameter of 0.645 inches, see Fig. 11.

The concentration ratio of a perfect paraboloid having the same geometry as that in the furnace would be:

$$C = \frac{4}{\alpha^2} \sin^2 \theta_{,} = 34{,}000 \qquad (8)$$

The fraction of the energy reflected from the concentrator which goes into the central hot spot is equal to the ratio of the projected area of the concentrator and the area of the hot spot divided into the concentration ratio, i.e. 34,000. This is equal to:

$$\frac{(0.242)^2\ (34{,}000)}{60^2} = 0.552$$

Thus only 55% of the solar radiation reflected from the concentrator goes to the hottest zone of the focal image.

In tests the solar furnace attained a temperature of 2996°C in the melting of a tantalum foil. From Fig. 16 it is seen that a non-conductive, non-convective, black body temperature of 3000°C corresponds to a concentration ratio of 8,000. However, a tantalum foil is not a non-conductive, non-convective, black body. If the heat losses by convection and radial conduction along the foil are neglected, and the fact that the back side of the foil is almost as hot as the face is considered, then a more realistic concentration ratio is obtained. Since two faces are losing heat by radiation, rather than just one, the concentration ratio is determined from Fig. 16 to be 16,000 where the emissivities of the tantalum foil faces are assumed to be equal to black body emissivities.

The furnace factor, F, corresponding to a concentration ratio of 16,000 is:

$$F = \frac{16,000}{34,000} = 0.47$$

STAGES OF DEVELOPMENT OF THE OREGON STATE COLLEGE SOLAR FURNACE

Naturally, due to the developmental nature of this project, some revisions of the original design were necessary to optimize the performance of the solar furnace. The present form of the solar furnace has been described previously in the text of this paper. Features which have been revised from their original forms are subsequently briefly described.

HELIOSTAT AND STATIONARY REFLECTORS

Initial Designs:

The heliostat and stationary reflectors were originally each 7 feet square. Their surfaces were each composed of 16 mirrors, 21 inches square. The stationary reflector was made the same size as the heliostat so the same mirrors could be made interchangeable.

The individual mirror segments were mounted upon rubber pads with stainless steel bolts at each corner. The edges of the mirror segments were adjusted to co-planarity by placing shims between the mirror corners and the mounting pads. It became apparent that the non-planar character of the large mirror segments was limiting the performance of the solar furnace.

The maximum temperature attained during this stage was only about 1500°C.

First Interim Stage:

In this stage an attempt to deform the non-planar mirror segments into approximately planar shapes was made. The mirrors were mounted upon carefully leveled plywood panels attached to the basic framework. Inward bowed mirror segments were forced out by the solid plywood backing and the outward bowed mirrors were drawn in by means of bolts placed through holes drilled in the center of each mirror segment. This led to disastrous mirror breakage from point strains as dimensional changes in the plywood backing resulted from changes in temperature and humidity.

Second Interim Stage:

The large mirrors were cut into quarters to minimize the effects of non-planarity of the individual segments (Fig. 44). These segments were then temporarily mounted on the plywood from the previous stage of development. Only half the mirrors were mounted but temperatures as high as 1800°C were noted, indicating that a significant improvement over earlier designs had been achieved. With this stage serving as a model the present, successful, forms of the heliostat and stationary mirrors were designed and constructed.

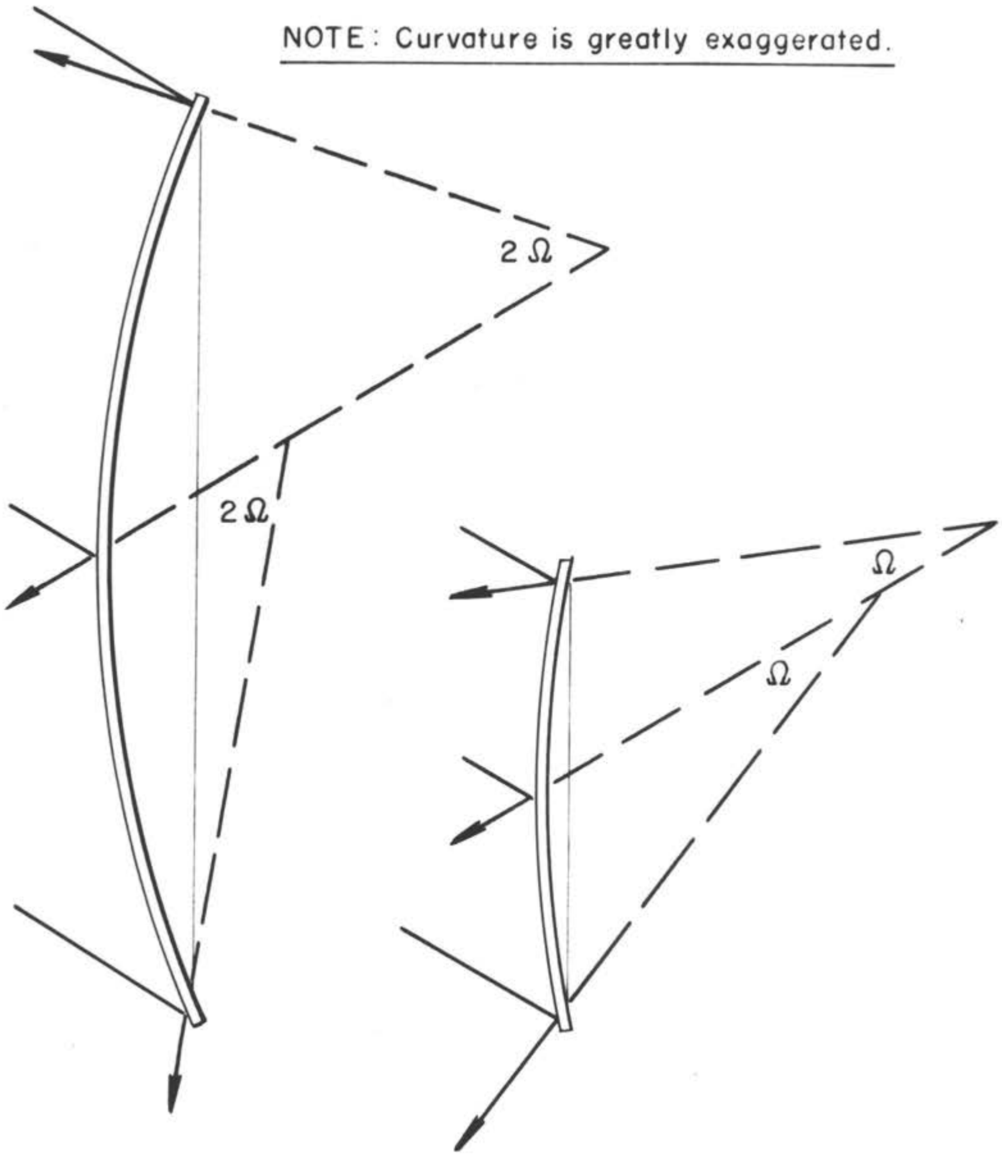

FIGURE 44
EFFECT OF HALVING SIZE OF NON-PLANAR MIRROR SEGMENTS

AZIMUTHAL TRACKING PHOTOCELL

The original design of the azimuthal tracking photocell optical system was exactly analagous to that of the altitude tracking photocell. The light-dark interface was provided by a black overlay on the heliostat mirror, (Fig. 45). This system required a prohibitively large shaded area for reliable operation, and was discarded in favor of the present system which provides increased sensitivity along with reduction of critical center shading.

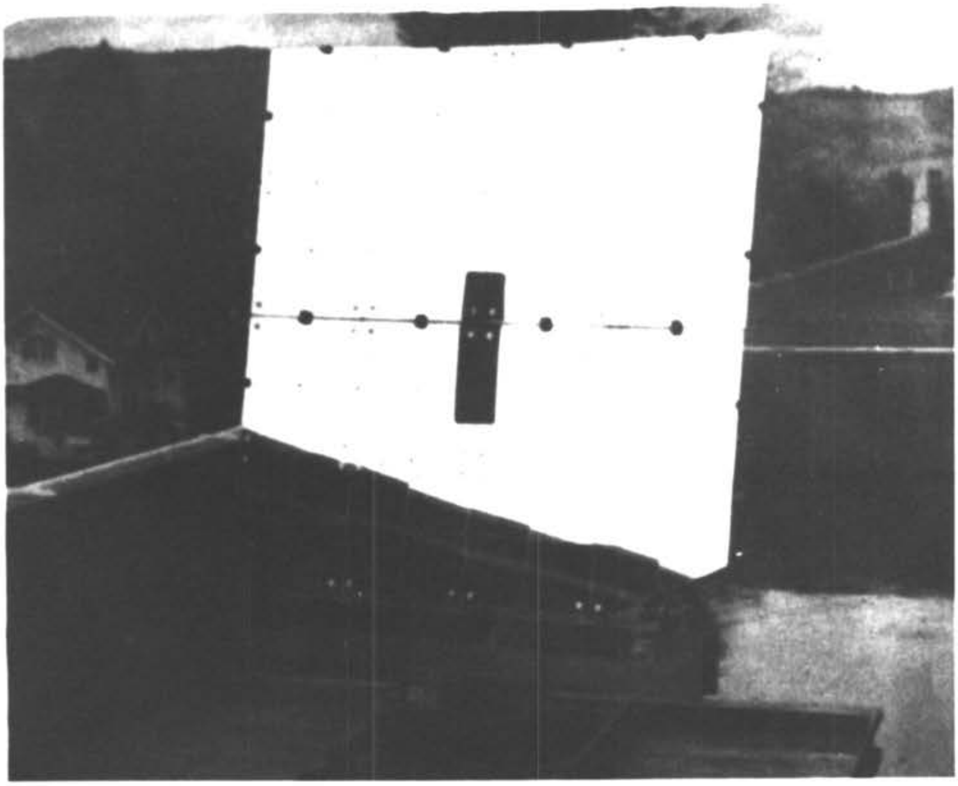

FIGURE 45

EARLY AZIMUTHAL CONTROL PATCH